Interfacial tension and finite-size effects of some exactly solved models in statistical mechanics

A thesis submitted for the degree
of Doctor of Philosophy of
the Australian National University

Michael J. O'Rourke

March 1996

The work contained in this thesis is my own original research, and any material taken from other references is explicitly acknowledged as such. I certify that the work contained in this thesis has not been submitted for any other degree.

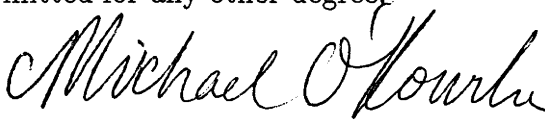

Michael O'Rourke

Abstract

We consider the two-dimensional six-vertex, Potts and chiral Potts models in lattice statistical mechanics.

Functional relations for the transfer matrices of the six-vertex model have been derived previously for both periodic and anti-periodic boundary conditions. We solve these functional relations to determine the largest eigenvalue(s) of the transfer matrices for both of these boundary conditions, on lattices with both an even and an odd number of columns. For lattices with an interface in the ordered anti-ferroelectric phase, we calculate the interfacial tension.

This method reproduces the known result for the interfacial tension. However, it is much simpler than other methods that have been used, and can be generalised in a straightforward manner to other models.

We then consider the chiral Potts model with skewed boundary conditions (the generalisation of anti-periodic boundary conditions to higher state spins). The functional relations for the transfer matrices of this model have been derived recently, and we solve them for a band of largest eigenvalues, from which we calculate the interfacial tension. We confirm that the interfacial tension of the chiral Potts model in its physical regime is the same as that of the non-physical superintegrable chiral Potts model when appropriate boundary conditions are applied, and that it is non-wetting. Our band of largest eigenvalues of the transfer matrix agrees with an earlier calculation of excitations by McCoy and Roan.

We also consider the critical three-state Potts model, and calculate exact partition functions of this model on finite rectangular lattices with a variety of boundary conditions. We study linear combinations of these partition functions for the patterns of zeros which will give us the structure of the general solution on finite lattices. The partition functions are then used to test the finite-size scaling predictions of conformal and modular invariance.

Acknowledgements

I would like to thank my supervisory panel Rodney Baxter, Murray Batchelor and Vladimir Bazhanov, for their excellent assistance and advice during the course of my doctorate, and also my sister Carolyn for her able assistance in the final proof-reading.

Contents

CHAPTER 1

Introduction—statistical mechanics and solvable lattice models

That matter can exist in a variety of different phases has been known since early times; indeed, it has been remarked that the ancient classification of the "elements" into earth, fire, air and water is really a classification of matter into commonly occurring phases.

Phase changes are induced by altering various state variables such as pressure P or applied magnetic field H, or by changing the temperature T. A phase transition is marked by some non-analyticity of the free energy F which describes the equilibrium state of the system.

Phase transitions are divided into two classes depending on the nature of the non-analyticity of F. A phase transition is said to be "first order" if the first temperature derivative of F is discontinuous; this is reflected as a discontinuity in the internal energy

$$U = -T^2 \left(\frac{\partial}{\partial T} \frac{F}{T} \right)_V .$$

Classic examples of first order phase transitions are steam condensing into water or sublimating into ice. The discontinuity in the internal energy corresponds to the emission or absorption of a latent heat.

When a system is at a first-order phase transition, the two homogeneous phases can co-exist in equilibrium with one another. The phases are in contact along a surface, the presence of which gives rise to a measurable surface (interfacial) tension s; this is equal to the energy required to increase the surface of contact by unit area.

Alternatively, the first derivative of the free energy may be continuous through the phase transition, and the non-analyticity of F will manifest itself in some other

way, usually as a discontinuity in or divergence of a higher order derivative of the free energy, such as the specific heat $C = \partial U/\partial T$. Such a phase transition is said to be "second order" or "continuous."

Archetypal examples of continuous phase transitions are the Curie point of a ferromagnet and the critical point of a fluid.

The former was apparently first observed by Gilbert in his treatise on magnetism published in 1600 [47,59]. Quantitative studies only began in the nineteenth century when Thomas Andrews described in his famous Bakerian lecture of 1869 his studies of how the liquid and gaseous phases continuously merge into a single homogeneous fluid phase at a certain critical temperature and pressure [103].

The similarities between the critical behaviour of these two systems was noted as long ago as 1895 in Curie's classic work on magnetism [43].

Critical points often correspond to order-disorder transitions, with the ordered phase occurring at sufficiently low temperatures, and the disordered phase occurring beyond the critical point.

A convenient characterisation of a phase transition is the "order parameter" R; this differentiates between the equilibrium phases in the ordered (subcritical) regime, and is identically equal to zero when the system is disordered. The order parameter usually has a jump discontinuity through a first order transition, and vanishes continuously as a critical point is approached.

In a magnetic system, the order parameter is the spontaneous (zero-field) magnetisation, which vanishes in the paramagnetic phase. For a fluid, one uses the difference between the densities of the liquid and the gaseous phases; this is identically zero beyond the critical point.

Low temperature phases are generally more ordered; there are of course exceptions, with the ferroelectric transition of the Rochelle salt being a notable one.

Beyond the critical point, the two phases are indistinguishable, and as the critical point is approached along the co-existence curve of the two phases, the interfacial tension between the phases vanishes.

The critical point is usually accompanied by other anomalous behaviour, such as critical opalescence in fluids, and vanishing or divergence of various thermodynamic quantities such as the specific heat, compressibility, and magnetic susceptibility over a narrow range of temperatures.

1.1 Statistical mechanics

The theory of statistical mechanics, which was first formally expounded by Gibbs in 1901 [56], has proven admirable for describing systems in which phase transitions occur. Given the description of a system on the microscopic scale, statistical mechanics describes the macroscopic state by averaging over Gibbs' canonical ensemble of identical systems.

The microscopic interactions of a system are described by a Hamiltonian $\mathcal{H}(s)$ (where s describes the microscopic state of the system), and the thermodynamics of a system follow from a knowledge of the system's partition function Z,

$$Z = e^{-F/k_BT} = \sum_{\text{states}} \exp(-\mathcal{H}(s)/k_BT) \tag{1.1}$$

where T is the absolute temperature and k_B is Boltzmann's constant. The average of a quantity $A(s)$ (for example, the internal energy, pressure, magnetisation, et cetera) which depends on the microscopic state of the system is given by

$$\langle A \rangle = Z^{-1} \sum_{\text{states}} A(s) \exp(-\mathcal{H}(s)/k_BT)$$

where the summation is over all microscopic states.

In order to predict thermodynamics correctly, the "thermodynamic limit" must be taken; this process can be complicated to describe in general, but basically involves taking the number of interacting degrees of freedom in the system to infinity in a certain way. For a system with $\mathcal{N}$ degrees of freedom, the free energy per site in the thermodynamic limit is defined as

$$-f/k_BT = \lim_{\mathcal{N}\to\infty} \mathcal{N}^{-1} \ln Z$$

(other limits may be needed as well, such as taking the volume V to infinity while keeping the density $\mathcal{N}/V$ fixed). Only in the thermodynamic limit can the non-analyticities in the free energy which herald a phase transition or critical point appear.

It is now well known that the partition function contains all of the information needed to describe both phases in a phase transition. What was not at all obvious to researchers at first is the converse; that all of the information contained in the partition function is needed in order to describe accurately the singular nature of the continuous phase transition. At the critical point, the interacting degrees of freedom in the system are very strongly correlated, and the correlations are very

long-ranged. As a result, most approximate theories break down around the critical point. It took the exact computation of Z for a simple model of an interacting system, the Ising model, to render this fact apparent.

1.2 Scaling, universality, and the renormalisation group

Over the last few decades, an understanding of exactly how different critical phenomena can be classified has been evolving. A (very) brief survey of the status quo is included here.

The anomalous behaviour of a physical quantity in the vicinity of the critical point (the "scaling region") is characterised by a critical exponent and a scaling function.

This introduces a large number of critical exponents; however making certain assumptions on the analytic nature of the scaling functions (namely, that they are generalised homogeneous functions of all of their arguments) implies simple relations between the critical exponents of the system.

For the simple critical points that we consider, the scaling relations reduce the total number of independent exponents to only two ("two-exponent scaling"), which are usually expressed in terms of the "scaling dimensions."

Systems are assumed to be divided into "universality classes" which exhibit the same critical behaviour (i.e. have the same critical exponents and scaling functions). The universality class is expected to be largely independent of the "details" of the Hamiltonian, so a wide variety of very different physical systems could be in the same universality class.

The universality class depends on only the spatial dimensionality of the system and the symmetries of the Hamiltonian.

Examples of the scaling functions are as follows; we consider magnetic systems. The singular part of the free energy per site (the difference between f for $T < T_c$ and its analytic continuation from $T > T_c$) scales as

$$f_{\text{sing}} \sim |t|^{2-\alpha} Y(H/|t|^{\Delta})$$

where t is the dimensionless "reduced temperature"

$$t = (T - T_c)/T_c$$

and α is a critical exponent that describes how the specific heat diverges as $t \to 0$; it is usually positive, but $\alpha = 0$ can imply either a jump discontinuity or a logarithmic

divergence. The scaling function $Y(x)$ is undetermined by the theory; Δ is called the "gap exponent."

The order parameter (spontaneous magnetisation) vanishes as

$$R \sim |t|^{\beta} W(H/|t|^{\Delta})$$

as $t \to 0^{-}$, with scaling function $W(x)$ and critical exponent β. Scaling predicts that these exponents are related by

$$\alpha + \beta + \Delta = 1.$$

As the critical temperature is approached along the co-existence curve, the interfacial tension vanishes as $s \sim (-t)^{\mu}$, and the exponent μ satisfies the relation

$$d\mu = (d-1)(d-\alpha)$$

where d is the spatial dimensionality of the system. Exponent relations depending on d cannot be derived from scaling alone, and require the stronger "hyperscaling" hypothesis; there is some doubt as to how generally hyperscaling can be applied, but it is believed to hold for $d = 2$, which is the only case that we consider.

The concepts of universality and scaling can be "rigourised" to an extent using the approach of the renormalisation group. The underlying assumption is that at the critical point, the system is scale invariant. The concept of the renormalisation group was introduced into statistical mechanics in the early 1970s by Wilson [111, 112], and as well as providing a revealing insight into the concept of universality and a more rigorous means of justifying phenomenological scaling, it has also provided a framework for carrying out detailed calculations of critical behaviour.

The renormalisation group uses an iterative transformation of the Hamiltonian to account for correlations on all length scales, with a critical model corresponding to a fixed point of the transformation. Critical exponents can be calculated by considering the behaviour of the transformation in the vicinity of the fixed point. Universality classes are described as all Hamiltonians which map to the same fixed point under the iterated transformation, and Hamiltonians which are in the same universality class can differ only by so-called "irrelevant" operators. Hamiltonians differing by "relevant" operators have different critical behaviour, and perturbing a system by a relevant operator will cause it to "cross over" into a different universality class, with behaviour near the critical point being described by different critical exponents and scaling functions. Other "marginal" operators are found also, and

these are responsible for non-universal behaviour such as the continuously variable exponents in the eight-vertex model.

1.2.1 Exactly solvable models

That real physical systems have extremely complicated interactions goes virtually without saying. The evaluation of the partition function of a realistic system is clearly unfeasable, especially for a system with a very large number of degrees of freedom.

In order to describe the critical behaviour of such systems, simplified models must be introduced, which hope to capture the salient aspects of the physical reality. Even then, calculating the partition function of the simplified models is very complicated.

One must avoid using mean field approximations to describe critical behaviour, and the limitations of numerical techniques such as monte carlo are well known. Series expansions have proven very useful for predicting critical behaviour, although to derive accurate results can be computationally intensive. The renormalisation group, while at least in principal capable of predicting exactly the behaviour around critical points, can be difficult to apply, and usually involves some sort of approximation, such as expanding critical exponents in powers of the "small" parameter $\epsilon = 4 - d$.

The method we favour is to focus on simple models for which at least some interesting thermodynamic quantities can be calculated exactly. The critical behaviour of the model is then described accurately, and universality asserts that there is potentially a large class of complicated physical systems exhibiting the same critical behaviour. These systems can be identified by their dimensionality and symmetries.

There is a well known class of "integrable" models, and we restrict our attention to such models which reside on two-dimensional square lattices. This may seem somewhat restrictive, but there is any number of systems displaying interesting critical behaviour which takes place in two dimensions, and solutions in two dimensions can give important qualitative insights into critical behaviour in three dimensions.

The square lattice can be oriented in its "usual" way, Figure 1.1(a), or rotated through 45 degrees, Figure 1.1(b). For the lattice in Figure 1.1(a), there are L spins

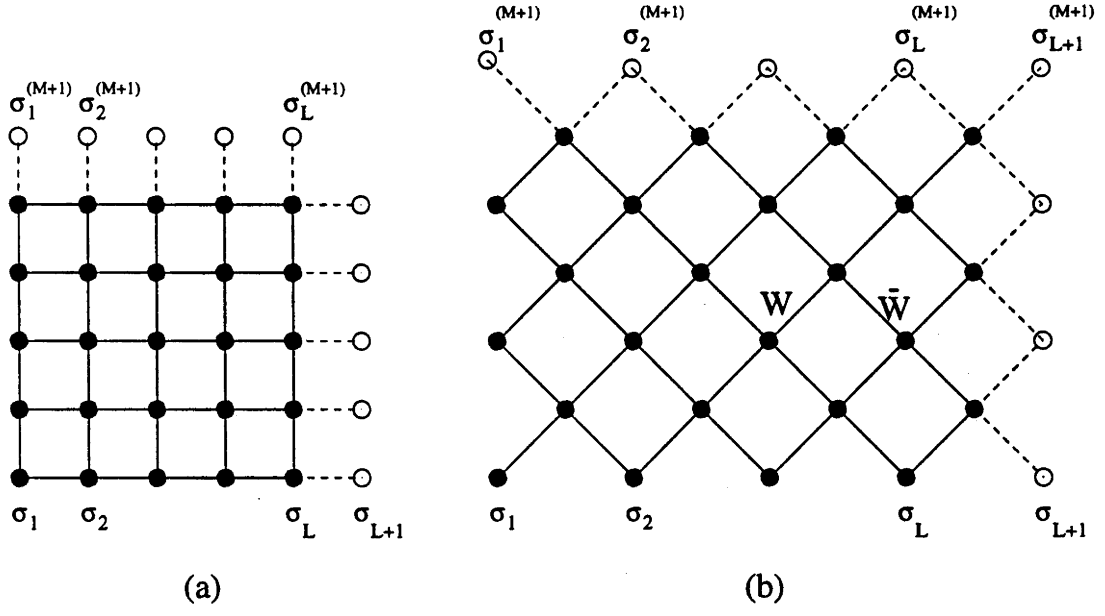

Figure 1.1: (a) The square $L \times M$ lattice in its "usual" orientation, shown here for $L = M = 5$. (b) The square $L \times M$ lattice rotated through 45 degrees, shown here for $L = 4$ and $M = 3$.

in a row of the lattice, and M such rows, for a total of LM spins on the lattice. For the lattice in Figure 1.1 (b), there are L spins in a row of the lattice, but $2M$ such rows, for a total of $2LM$ spins on the lattice. According to universality, the thermodynamics of the model should be largely independent of the choice of lattice, and so a particular lattice is chosen more for computational convenience.

The models we analyse are the six-vertex, self-dual Potts and chiral Potts models, which are defined later in this thesis. Before this, we review some aspects of the exact solution of the Ising model. Onsager's solution of this in 1944 is a true watershed in the theory of statistical mechanics, and is by some touted as the starting point for the modern theory of critical phenomena.

1.3 The Ising model

The Ising model was proposed as a model of the ferromagnetic-paramagnetic phase transition, and is now known as a reasonably good description of the order-disorder transition in binary alloys and of the liquid-gas phase transition and critical point.

It is a lattice spin model; the Ising spins can be in one of two states, which are usually taken to be $+1$ and -1. Nearest-neighbour spins interact along the edges of the lattice with an anisotropic homogeneous interaction, with energy $E\sigma\sigma'$ for two nearest-neighbour spins interacting along a horizontal edge of the lattice, and $\bar{E}\sigma\sigma'$ for two nearest-neighbour spins interacting along a vertical edge. The spins can also interact with a uniform external magnetic field H, with an energy $H\sigma$. Appropriate choices of E and $\bar{E}$ give either a ferromagnetic or an anti-ferromagnetic interaction.

The energy of the system is given simply by addition;

$$\mathcal{H}(s) = -E \sum_{\text{horiz.}} \sigma\sigma' - \bar{E} \sum_{\text{vert.}} \sigma\sigma' - H \sum_{\text{all spins}} \sigma,$$

where the first sum is over all nearest-neighbour pairs of spins σ and σ' connected by a horizontal edge, the second is over all pairs connected by a vertical edge, and the third sum describes the interaction between the spins and the external magnetic field. The variable s represents the state of the system, i.e. the value of all of the spins on the lattice.

To fully specify the model, we must also specify the conditions at the boundary of the lattice. Again, the boundary conditions are usually chosen for computational convenience, and provided that the model is "physical" (the interaction energies must be real), the boundary conditions of the lattice cannot possibly affect the bulk thermodynamics of the system.

We often consider periodic boundary conditions; this corresponds to setting $\sigma_{L+1} = \sigma_1$ in each row of the lattice in Figure 1.1(a). The spin σ_1 then interacts with the spin σ_L along the bond indicated by the broken line, and this is equivalent to wrapping the lattice onto a cylinder. When we impose the periodic boundary condition in the vertical direction also, setting $\sigma_1 = \sigma_1^{(M+1)}$ in each column of the lattice, we effectively wrap the lattice onto a torus; these are toroidal boundary conditions. We also consider anti-periodic boundary conditions, which corresponds to setting $\sigma_{L+1} = -\sigma_1$, so that the spin σ_L is interacting with the spin $-\sigma_1$. (Other

boundary conditions which are sometimes considered are the fixed and free boundaries, but we do not use these.)

For a ferromagnet, the order parameter is the spontaneous magnetisation; this can be defined as the average magnetic moment per site, and is given by

$$m(0,T) = -\lim_{H\to 0^+} \frac{\partial}{\partial H} f(H,T).$$

1.3.1 Partition function and free energy

For his Ph.D. thesis in 1925 [64], Ising considered this model on a one dimensional lattice, and obtained the exact partition function of the model with a non-zero magnetic field. He found that there was no spontaneous magnetisation away from absolute zero, and argued that this would remain the case in higher dimensions.

In 1936, Peierls [101] demonstrated that in two dimensions the model has a finite critical temperature, and in 1941, Kramers and Wannier [78] introduced the idea of transfer matrices, and using these and a powerful duality relation, which relates high temperatures to low temperatures, exactly located the critical temperature of the model.

The transfer matrix formalism expresses the partition function (1.1) as the trace of a product of the matrices $\mathbf{T}$ and $\hat{\mathbf{T}}$, where multiplication by the matrix $\mathbf{T}$ or $\hat{\mathbf{T}}$ corresponds to adding a row of horizontal or vertical edges to the lattice. These matrices have dimension 2^L, and elements of the transfer matrices correspond to the energy of possible configurations of spins in a row of the lattice. When periodic boundaries are applied in both directions, the partition function can be expressed as

$$Z = \text{trace}\,\left(\mathbf{T}\hat{\mathbf{T}}\right)^M = \sum_{j=1}^{2^L} \Lambda_j^M$$

where the Λ_j are the eigenvalues of the matrix $\mathbf{T}\hat{\mathbf{T}}$. For a physical model, the elements of the transfer matrices are positive, so the Perron-Frobenius theorem asserts that there exists a unique non-degenerate largest eigenvalue, $\Lambda_{\max}$, and hence for large L and M, $Z \sim \Lambda_{\max}^M$, and the free energy per site is

$$-f/k_BT = \lim_{L,M\to\infty} L^{-1} \ln \Lambda_{\max}.$$

In his monumental paper of 1944 [93], Onsager computed the thermodynamic properties of the zero-field model exactly, diagonalising the transfer matrix and

calculating the partition function for a lattice wrapped onto a cylinder which is infinite in one direction. The free energy per site in the thermodynamic limit is given by

$$-f/k_BT = \frac{1}{2\pi}\int_0^\pi d\theta \ln 2\left[\cosh 2K \cosh 2\bar{K} + k^{-1}\left(1 - 2k\cos 2\theta + k^2\right)^{1/2}\right]$$

where

$$k^{-1} = \sinh 2K \sinh 2\bar{K} \tag{1.2}$$

and $K = E/k_BT$ and $\bar{K} = \bar{E}/k_BT$ are the dimensionless interaction parameters. The free energy has a singularity when $k = 1$, which corresponds to the critical point of the model; this confirmed the prediction of Kramers and Wannier exactly. Around this point, the singular part of the free energy scales as $f_s \sim t^2 \ln|t|$, which implies the specific heat critical exponent $\alpha = 0$. Onsager calculated other thermodynamic quantities of the model, including the interfacial tension and order parameter, and with his student Kaufman considered the correlations.

1.3.2 Correlation function and correlation length

The critical point is heralded on the microscopic scale by long-range correlations throughout the system; the classical approximations ignore these, and hence erroneously predict behaviour about the critical point. Kaufman and Onsager [73] calculated exactly the degree of correlation in the Ising model.

The degree of correlation between the spins is measured through the two-point correlation function $g(\mathbf{r})$, defined as

$$g(\mathbf{r}_{ij}) = \langle\sigma_i\sigma_j\rangle - \langle\sigma_i\rangle\langle\sigma_j\rangle.$$

This depends on the distance $r = |\mathbf{r}_{ij}|$ between the spins σ_i and σ_j. For a translationally invariant system, $\langle\sigma_j\rangle$ is the same for all sites j, and is equal to the spontaneous magnetisation. The correlation function is related to the probability that the spins σ_i and σ_j are in the same state.

In the ordered (low temperature) region, the spins are strongly correlated over both long and short distances; the spins have a preference for a particular orientation, so there is a correlation between the spins which is virtually independent of their spatial separation. This long-range order disappears beyond T_c, and in the

high temperature disordered phase, the spins are weakly correlated over long distances. However short-range order persists, with small drops of spins in the same state, and so the correlation function is still finite.

The correlation function for the Ising model can be calculated exactly, and displays fairly simple behaviour for large $r = |\mathbf{r}|$. Away from the critical point, it decays as

$$g(\mathbf{r}) \sim r^{-\tau} e^{-r/\xi}$$

for r large compared to the lattice spacing, where τ is a positive number and ξ is a parameter of the system called the correlation length; this is a measure of the distance over which the spins are correlated. It is infinite at absolute zero temperature, and diverges as the temperature approaches T_c from either side with a power law

$$\xi \sim |t|^{-\nu} \quad \text{as } t \to 0^{\pm},$$

(scaling predicts that the exponent is the same from either side of the critical temperature) and this divergence is regarded as a hallmark of a critical point. At the critical point, the correlation function decays as

$$g(\mathbf{r}) \sim r^{-d+2-\eta}$$

for large r, where η is another critical exponent, the anomalous dimension, which classical theories predict to be zero.

For the Ising model, the diagonal correlations are [19]

$$g(r) \sim r^{-2} e^{-r/\xi_<} \quad \text{for } T < T_c, \quad \text{and} \quad g(r) \sim r^{-1/2} e^{-r/\xi_>} \quad \text{for } T > T_c$$

for large r, where $\xi_<^{-1} = -\ln k$ and $\xi_>^{-1} = \frac{1}{2}\ln k$, with k as defined in Equation (1.2). It is clear that the correlations are much longer-ranged for $T < T_c$.

Although the correlation length is itself dependent on direction, it becomes isotropic in the scaling limit [89], and hence the critical exponents are independent of the direction in which ξ is defined.

1.3.3 Order parameter

The spontaneous magnetisation has been calculated also, originally by Onsager, with a derivation published by Yang [119] and is $M(0,T) = (1-k^2)^{1/8}$; as $T \to T_c^-$, this vanishes as $\sim (-t)^{1/8}$, with critical exponent $\beta = 1/8$.

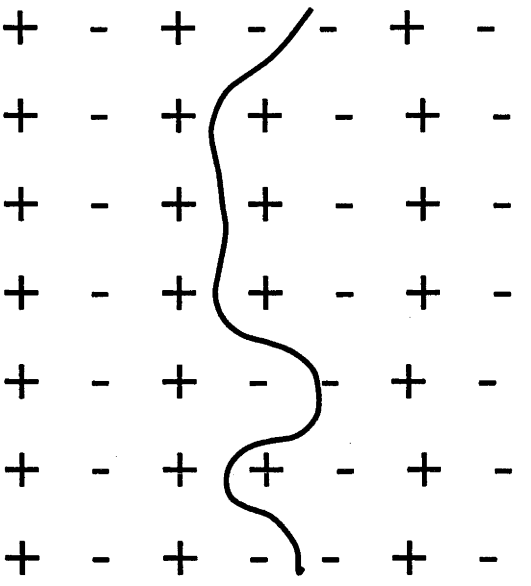

Figure 1.2: A configuration of the anti-ferromagnetic Ising model, with periodic boundary conditions and an odd number of columns. The interface, in bold, meanders down the lattice.

1.3.4 Interfacial tension

Along the co-existence curves in the phase diagram (for the Ising ferromagnet, this corresponds to $H = 0$ and $T < T_c$), it is possible for domains of both up and down spins to co-exist, the domains containing "mostly" spins of only the one phase. The two phases are in contact along an interface, and this gives rise to an interfacial tension, which produces an excess in the free energy equal to the length of the interface multiplied by s, the interfacial tension per unit length.

To calculate the interfacial tension for a lattice model, we have to introduce an interface into the lattice. Onsager accomplished this for the anti-ferromagnetic Ising model with periodic boundary conditions by allowing an odd number L of spins in each row. When L is even, a perfectly ordered anti-ferromagnetic ground state is possible, but when L is odd, this is no longer the case. There must be a site somewhere in each row of the lattice which separates two regions of opposite anti-ferromagnetic order. As rows are added together to form the lattice, the so-called "anti-ferromagnetic seam," or interface, is formed, separating these oppositely ordered regions. This is illustrated in Figure 1.2. For large M, the length of the interface is proportional to the height M of the lattice.

This interface persists until the temperature is increased to the critical temperature, $k = 1$, where the system has a transition to a completely disordered phase. For large L and M, the Ising model partition function on an $L \times M$ lattice with an interface grows as

$$\ln Z_{LM} = -LMf/k_BT - Ms/k_BT + \cdots$$

where f is the per-site free energy; Onsager found the interfacial tension per unit length s to be

$$-s/k_BT = 2(K - \tanh^{-1} e^{-2K})$$

in the horizontal direction. For the Ising model this vanishes as $s \sim (-t)^{\mu}$ as $T \to T_c^-$, with critical exponent $\mu = 1$.

Alternatively, the interface may be created by imposing anti-periodic boundary conditions. This works for a system with either ferromagnetic or anti-ferromagnetic interactions. For instance, imposing anti-periodic boundary conditions in the horizontal direction in the sub-critical phase of a ferromagnetic system, the spins on one side of the lattice will preferentially order into the state σ say, where $\sigma = +1$ or -1, as before, but because of the anti-periodic boundary, the spins on the other side of the lattice will prefer order into the contrary state, $-\sigma$.

At zero temperature, the lowest-energy configuration of the lattice is for the interface to run exactly vertically down, and there are L positions in each row to put the interface. As the temperature is increased, the interface will begin to meander, "overhangs" may appear, et cetera, along with the drops of overturned spins in the bulk of the lattice. The interface persists until the critical temperature is reached. Due to the periodic boundaries in the vertical direction, the interface will begin and end in the same column of the lattice.

An alternative formula for the interfacial tension is due to Fisher [53]. Onsager [93] noted that the transfer matrix has two asymptotically degenerate largest eigenvalues, $\Lambda_{\max}$ and Λ_1, corresponding to the two possible ordered ground states of the system related to one another by spin-reversal, but did not investigate this point any further. These eigenvalues are related by $\Lambda_{\max}/\Lambda_1 = 1+$ exponentially smaller terms, which vanish as $M \to \infty$. Fisher notes that "by general arguments" (given for example in Reference [19]) the two asymptotically degenerate largest eigenvalues $\Lambda_{\max}$ and Λ_1 are related by

$$\Lambda_{\max}/\Lambda_1 = 1 + O(e^{-sM/k_BT}) \quad \text{as} \quad M \to \infty \tag{1.3}$$

where s is the interfacial tension per unit length, given by

$$-s/k_BT = \lim_{M\to\infty} M^{-1} \ln(\Lambda_{\max}/\Lambda_1).$$

In Reference [53] Fisher calculates s for the Ising model using this definition, and re-derives Onsager's result.

The interface in the diagonal direction (which is the horizontal direction of the lattice in Figure 1.1(b)) can be calculated from the diagonal-to-diagonal transfer matrices (the row-to-row transfer matrices of the diagonally oriented lattice), which is done in Reference [19], with the result $-s/k_BT = \ln k$, and the same critical exponent $\mu = 1$.

The interfacial tension and correlation length of the Ising model are related by

$$s\,\xi = k_BT; \tag{1.4}$$

this relation seems to have been satisfied for every model for which both of these quantities have been calculated. This is interesting; it is unclear whether or not it can be assumed to be a general relation.

Other methods of calculating the interfacial tension have been used, for instance Fisher and Ferdinand proposed a method which allows calculation of surface free energies as well as interfacial tensions in [52], and there is a discussion of the interfacial tension of the Ising model by Gallavotti and Martin-Löf [55]. The calculations of these papers do not generalise to the models we consider in an obvious way.

Part I

The six-vertex model

CHAPTER 2

The six-vertex model

2.1 Origins

The six-vertex model was first proposed by Slater in 1941 [106] in an attempt to describe the ferroelectric-paraelectric transition of potassium dihydrogen phosphate, KH_2PO_4, or simply KDP. This is one of the simplest crystals which exhibits such a transition, with a single critical temperature at $\sim$ 122 K. Slater considered a three dimensional model, in which the phosphate ions occupy the sites of a tetrahedral lattice, and one hydrogen ion lies on each bond, creating a hydrogen bonded lattice. Rather than lying precisely in the middle of the bonds, the hydrogens tend to lie closer to one of the adjoining phosphate ions. The ice rule embodies the assumption that, on the four bonds associated with any one phosphate ion, there are precisely two hydrogens closer to the central phosphate ion, and two hydrogens closer to the adjoining phosphates. These assumptions had appeared earlier in the literature, in a calculation by Pauling of the residual entropy of ice [98]. Slater's model of KDP was a generalisation of Pauling's, in that the six vertices of the ice model possess equal energy, but that two of the allowed vertices of KDP have different energies from the other four, giving the crystal a preferred direction, along which a spontaneous electrical polarisation appears at a low enough temperature.

It was later suggested by Rys [105] that a model of an anti-ferroelectric based on the KDP model could be obtained by a suitable choice of vertex energies. The model proposed by Rys is known as the F model.

Exact solutions of these three-dimensional models have not yet been found.

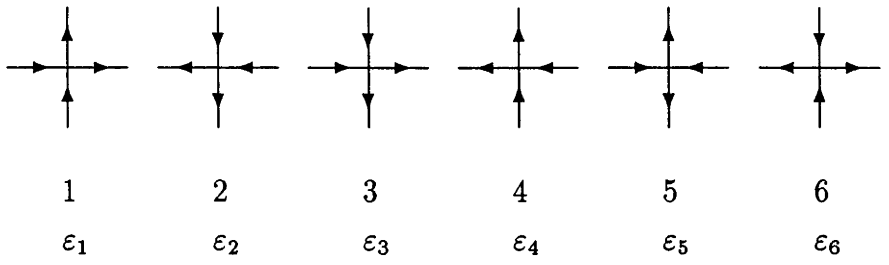

Figure 2.1: The six vertices allowed by the ice rule, with their associated vertex energies.

2.2 The two dimensional six-vertex model

Consider the square lattice with its usual orientation (as in Figure 1.1(a)), and place an arrow on each bond of the lattice, pointing either up or down on the vertical bonds, and either to the left or to the right on the horizontal bonds. There are a total of $2^4 = 16$ possible arrangements of arrows around each vertex. (The arrows represent the direction of the dipoles which arise as a result of the location of the electrons on the bonds of the lattice.) Imposing the ice rule implies that at each vertex there are two arrows pointing in and two arrows pointing out. This reduces the number of allowed vertices from sixteen to only six—the six-vertex model.

The vertices allowed by the ice rule are shown in Figure 2.1, along with their vertex energies $\varepsilon_1, \ldots, \varepsilon_6$. The energy of an allowed configuration of arrows on the lattice is assumed to be given simply by addition; if there are m_j vertices of type j, then the energy of a configuration is

$$E = \sum_{j=1}^{6} m_j \varepsilon_j.$$

The partition function of the model is given by equation (1.1) from Chapter 1.

Vertices 1 through 4 have a net polarisation in one of four directions, while vertices 5 and 6 have no net polarisation. As a result, the six-vertex model can be used to model a ferroelectrically or an anti-ferroelectrically ordered crystal, or a completely disordered crystal, depending on the assignments of energy given to each vertex.

2.2.1 The exact solution

In 1967, Lieb published an exact solution of three special but archetypal cases of the two-dimensional six-vertex model, which corresponded to particular choices of the vertex energies. The first was for the residual entropy of square ice [80,81]. For ice, the energy of each vertex, and hence of each configuration, is chosen to be zero; the partition function Z for square ice is simply the number of arrow configurations on the square lattice that satisfy the ice constraint. Lieb calculated Z in the thermodynamic limit after exactly diagonalising the transfer matrix using an ansatz for the eigenvectors known as the Bethe ansatz. The residual entropy is given by $S = k_B \ln Z$, and Lieb showed that for a square lattice with $\mathcal{N}$ vertices the partition function scales as $Z^{1/\mathcal{N}} \sim (4/3)^{3/2} \sim 1.54$ for large $\mathcal{N}$. It is interesting to compare this to the simple estimate of Pauling's [98], who by a simple approximation found $Z^{1/\mathcal{N}} \sim 3/2$. The two answers are remarkably close.

The next models Lieb solved were the two-dimensional versions of Rys's F model and Slater's KDP model, in References [82, 83]. In the F model, the vertices 1 through 4 have an energy $\epsilon > 0$, while vertices 5 and 6 have zero energy. Hence at low enough temperatures, vertices 5 and 6 will be favoured, discouraging a spontaneous polarisation, and producing an anti-ferroelectrically ordered configuration. Slater's KDP model of a ferroelectric ascribes to either the pair of vertices 1 and 2 or 3 and 4 a zero energy, while the remaining four vertices have energy $\epsilon > 0$. Hence at low enough temperatures, a net polarisation is encouraged, giving the model a ferroelectrically ordered ground state. (These solutions are special in statistical mechanics as they are an exact solution of a two dimensional physical model in the presence of an applied field, although we are only interested in the zero-field models.)

In the same year, Sutherland solved a more general model which contains the models solved by Lieb as special cases [107]. This was followed closely by joint work with Yang and Yang [108,120], in which the solution of the general six-vertex model, with $\varepsilon_1, \ldots, \varepsilon_6$ different from one another, was obtained.

2.2.2 Other ferroelectric models—the eight-vertex model

Lieb's work was generalised by other authors, see for example References [12, 19,49,84,109,113–117] and references contained therein. The most famous of these models is the eight-vertex model [49,109], which allows two new "doubly ionised"

vertices, one with four arrows pointing in and one with four pointing out. For this model, the Bethe ansatz fails, but Baxter managed to solve the model in zero field, introducing the "commuting transfer matrix method" and deriving a functional relation which defines all of the eigenvalues of the transfer matrix, and hence calculated the free energy [13,14]. The eight-vertex model contains the Ising and six-vertex models as special cases.

We mention some exact calculations that have been performed on the eight-vertex model. The interfacial tension was calculated by Baxter in 1973 [16] using the asymptotically degenerate largest eigenvalues of the transfer matrix, as mentioned in Chapter 1. The interfacial tension was found to be the same for both the six-vertex and the eight-vertex models.

The correlation length was calculated by Johnson et al. in References [67,68]. As well as the two asymptotically degenerate largest eigenvalues, the transfer matrix has a band of complex next-largest eigenvalues. Johnson et al. demonstrated that this entire band of eigenvalues is necessary in order to calculate the correlation length, and determined ξ; this is related to the interfacial tension of the eight-vertex model via equation (1.4).

We also mention the sixteen-vertex model first studied by Wu [116], in which all of the vertices have finite Boltzmann weights. Again, arrow conservation is lost, but for this model, the property of commuting transfer matrices is lost too, and exact results are sparse. The sixteen-vertex model reduces to the eight and six-vertex models in the appropriate limits, and is equivalent to an Ising model with two, three and four body interactions in a non-zero external magnetic field.

2.2.3 Zero-field six-vertex model

The Boltzmann weight for vertex j is

$$\omega_j = e^{-\varepsilon_j/k_BT}.$$

In general, the vertex weights can be distinct, but for a model in a zero applied external electric field, the vertex energies satisfy $\varepsilon_1 = \varepsilon_2$, $\varepsilon_3 = \varepsilon_4$, and $\varepsilon_5 = \varepsilon_6$, so in zero field we define the Boltzmann weights a, b and c as

$$a = \omega_1 = \omega_2, \quad b = \omega_3 = \omega_4 \quad \text{and} \quad c = \omega_5 = \omega_6.$$

This choice of vertex weights defines the symmetric (zero field) six-vertex model.

To calculate the interfacial tension, we consider the model with both the periodic and anti-periodic boundary conditions. For periodic boundary conditions in the horizontal direction, the first and the last arrow in each row of horizontal edges are identified, so that they point in the same direction; for anti-periodic boundary conditions they oppose one another. Likewise, periodic boundary conditions and anti-periodic boundary conditions can be imposed in the vertical direction, but we only consider the former. When anti-periodic boundary conditions are applied horizontally, arrow conservation from row to row is lost.

The partition function is a polynomial (multinomial) in a, b and c, which we denote $Z(a,b,c)$. Consider a rotation of the lattice through 90 degrees; this will change the vertices with weight a into vertices with weight b and vice versa, and merely change the vertices with weight c from vertex 5 into vertex 6 and vice versa. When periodic boundary conditions are applied, the partition function satisfies the symmetry relation

$$Z(a,b,c) = Z(b,a,c). \tag{2.1}$$

2.3 The transfer matrix and its eigenvalues

The transfer matrices with periodic and anti-periodic boundary conditions are defined as follows.

Consider a row of horizontal edges of the lattice, and the adjacent rows of vertical edges. The arrows can be represented by "spins" μ_i on the bonds of the lattice, with $\mu_i = +1$ if the corresponding arrow points up or to the right, and $\mu_i = -1$ if the arrow points down or to the left. The Boltzmann weight for the vertex can be written graphically as

$w(\mu, \alpha|\beta, \mu') =$ 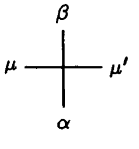

so that the six non-zero vertex weights are given by

$$w(+,+|+,+) = w(-,-|-,-) = a$$
$$w(+,-|-,+) = w(-,+|+,-) = b$$
$$w(+,-|+,-) = w(-,+|-,+) = c.$$

Denote the arrow or "spin" configuration on the lower row of vertical edges by $\boldsymbol{\alpha} = \{\alpha_1, \ldots, \alpha_L\}$ and on the upper row by $\boldsymbol{\beta} = \{\beta_1, \ldots, \beta_L\}$. The row-to-row transfer matrix $\mathbf{V}$ is a matrix with elements

$$\mathbf{V}_{\boldsymbol{\alpha}|\boldsymbol{\beta}} = \sum_{\mu_1} \cdots \sum_{\mu_L} w(\mu_1, \alpha_1|\beta_1, \mu_2) w(\mu_2, \alpha_2|\beta_2, \mu_3) \cdots w(\mu_L, \alpha_L|\beta_L, \mu_{L+1})$$

where we put $\mu_{L+1} = \mu_1$ in the case of periodic boundary conditions, and $\mu_{L+1} = -\mu_1$ for anti-periodic boundary conditions. For the anti-periodic boundary conditions, the transfer matrix satisfies $\mathbf{V}(v + 2\pi i) = -\mathbf{V}(v)$ [11].

All elements of $\mathbf{V}$ are multinomials in a, b and c. On a lattice with periodic boundary conditions in the vertical direction, which requires M be even, the partition function is written in terms of $\mathbf{V}$ in the usual way as

$$Z = \operatorname{trace}\left\{\mathbf{V}^M\right\} = \sum \Lambda_j^M$$

where Λ_j are the eigenvalues of $\mathbf{V}$; the problem is to determine these. This can be done in a number of ways. When the periodic boundary conditions are applied, the Bethe ansatz can be used, but for the anti-periodic boundary conditions the arrow conservation property is lost, and the Bethe ansatz does not work. In either case, a functional relation can be derived from which the eigenvalues of the transfer matrices can be calculated.

2.3.1 The Bethe ansatz

When horizontal periodic boundary conditions are applied, the number of down-pointing arrows is a conserved quantity from row to row. As a result, an element $\mathbf{V}_{\boldsymbol{\alpha}|\boldsymbol{\beta}}$ of the transfer matrix $\mathbf{V}$ will be zero unless $\boldsymbol{\alpha}$ and $\boldsymbol{\beta}$ contain the same number n of down arrows. Thus the elements of the transfer matrix can be arranged so that $\mathbf{V}$ is block-diagonal, with $L + 1$ blocks, each block corresponding to arrow configurations with a particular value of $n = 0, 1, \ldots, L$. One may restrict attention to a particular block of the matrix, and then choose the value of n which gives the maximum eigenvalue of $\mathbf{V}$.

The Bethe ansatz is based on a particular ansatz for the eigenvectors of the transfer matrix. It was originally introduced by Bethe to diagonalise the Heisenberg spin chain [37], and had been used to solve a number of related problems before Lieb used it on the ice model. The Heisenberg Hamiltonian can be exactly diagonalised by assuming the wave functions are a finite sum of plane waves, with coefficients determined by a set of transcendental equations. Lieb noted the eigenvectors of

the transfer matrix of the six-vertex model were exactly the same as those of the Heisenberg spin chain, and was thus able to borrow from Yang and Yang's analysis to identify and evaluate the maximum eigenvalue of the transfer matrix in the thermodynamic limit.

The method is complicated to apply, and a large number of equations are derived in a smaller number of unknowns; however, the method works beautifully, with all unwanted terms cancelling. The transcendental equations, known as the Bethe-ansatz equations, can be solved explicitly in the thermodynamic limit, and hence the large-lattice free energy can be calculated. Lieb accomplished this, and we reproduce the free energy shortly. The six-vertex model is even solvable in an applied electric field, which is rare for exactly solvable models.

The Bethe ansatz has proven to be a very powerful tool for solving statistical mechanical problems, and has also been used to solve a number of colouring problems in graph theory [19].

2.3.2 Commuting transfer matrices and the functional relations

The method known as the commuting transfer matrix method was introduced by Baxter in 1971 when he solved the zero-field eight-vertex model [13,14].

For a certain class of statistical mechanical models, specifically, models whose Boltzmann weights satisfy the star-triangle relations, the transfer matrices form commuting families. Onsager was aware that the diagonal-to-diagonal transfer matrices of the Ising model form commuting families [94], but did not use this in his solution [93].

However, Baxter capitalises on this observation in his solution of the eight-vertex model, and derives a functional relation which determines the eigenvalues of the transfer matrix, and hence enables calculation of the free energy.

Baxter relates how he came across the discovery in References [33]; the Bethe ansatz solution of the six-vertex model clearly pointed the way, demonstrating that the eigenvectors of the transfer matrix $\mathbf{V}$ of the six-vertex model depend on the vertex weights a, b, and c only via the parameter

$$\Delta = (a^2 + b^2 - c^2)/2ab.$$

Hence two transfer matrices with different Boltzmann weights but the same value of Δ commute. Fixing Δ still leaves one non-trivial degree of freedom, the "spectral

parameter" v; two six-vertex models with the same value of Δ but different values of v will have transfer matrices that satisfy the commutation relation

$$\mathbf{V}(v)\mathbf{V}(u) = \mathbf{V}(u)\mathbf{V}(v).$$

By considering a local "propagation through a vertex" property, it can be shown that there also exists a matrix function $\mathbf{Q}(v)$ such that

$$\mathbf{V}(u)\mathbf{Q}(v) = \mathbf{Q}(v)\mathbf{V}(u)$$

and that $\mathbf{Q}(v)$ and $\mathbf{V}(v)$ also satisfy a functional relation, which determines all of the eigenvalues of $\mathbf{V}(v)$ and $\mathbf{Q}(v)$; these can be solved explicitly in the thermodynamic limit, and quantities such as the free energy and interfacial tension can be calculated.

That the transfer matrix commutation could be established directly, with the condition for commuting transfer matrices being simply that the Boltzmann weights satisfy the star-triangle relations, pointed the way towards the solution of the eight-vertex model, and has been used for the solution of a great many models since.

The functional relations for the six-vertex model are different for the periodic and anti-periodic boundary conditions. We pre-empt our interest in the anti-ferroelectric model by parameterising the Boltzmann weights as

$$a = \rho \sinh \tfrac{1}{2}(\lambda - v), \quad b = \rho \sinh \tfrac{1}{2}(\lambda + v), \quad c = \rho \sinh \lambda \tag{2.2}$$

so that

$$\Delta = -\cosh \lambda. \tag{2.3}$$

Periodic boundary conditions

For the six-vertex model with periodic boundary conditions, a derivation of the functional relation is given in Chapter 9 of Reference [19]. The transfer matrix $\mathbf{V}(v)$ satisfies the functional relation

$$\mathbf{V}(v)\mathbf{Q}(v) = \phi(\lambda - v)\mathbf{Q}(v + 2\lambda') + \phi(\lambda + v)\mathbf{Q}(v - 2\lambda')$$

where $\phi(v)$ is an auxiliary (known) scalar function. As the matrices $\mathbf{V}(v)$ and $\mathbf{Q}(v)$ commute, they can be simultaneously diagonalised by a similarity transformation which depends on Δ but is independent of v. Hence the eigenvalues satisfy the functional relation

$$\Lambda(v)q(v) = \phi(\lambda - v)q(v + 2\lambda') + \phi(\lambda + v)q(v - 2\lambda'), \tag{2.4}$$

where $\Lambda(v)$ is an eigenvalue of $\mathbf{V}(v)$, $q(v)$ is an eigenvalue of $\mathbf{Q}(v)$, and the functions $\phi(v)$ and $q(v)$ are

$$\phi(v) = \rho^L \sinh^L \tfrac{1}{2}v \tag{2.5}$$

and

$$q(v) = \prod_{j=1}^{n} \sinh \tfrac{1}{2}(v - v_j). \tag{2.6}$$

The transfer matrix is block diagonal, and the integer n labels the sectors of the transfer matrix. The unknowns v_j satisfy the Bethe-ansatz equations

$$\frac{\phi(\lambda - v_j)}{\phi(\lambda + v_j)} = -\frac{q(v_j - 2\lambda')}{q(v_j + 2\lambda')}, \quad j = 1, \ldots, n \tag{2.7}$$

which follow from (2.4).

Anti-periodic boundary conditions

The six-vertex model with anti-periodic boundary conditions was solved in 1995 by Batchelor et al. [11]. The functional relation for the transfer matrices is derived following closely the working of Reference [19] for the periodic boundary conditions.

The transfer matrices satisfy the functional relation

$$\mathbf{V}(v)\mathbf{Q}(v) = \phi(\lambda - v)\mathbf{Q}(v + 2\lambda') - \phi(\lambda + v)\mathbf{Q}(v - 2\lambda')$$

and once again the matrices $\mathbf{V}(v)$ and $\mathbf{Q}(v)$ are simultaneously diagonalisable, so the functional relation can be written as a relation between the eigenvalues;

$$\Lambda(v)q(v) = \phi(\lambda - v)q(v + 2\lambda') - \phi(\lambda + v)q(v - 2\lambda') \tag{2.8}$$

where $\phi(v)$ is still given by equation (2.5), but now

$$q(v) = \prod_{j=1}^{L} \sinh \tfrac{1}{4}(v - v_j). \tag{2.9}$$

The variables v_j are the solutions to the Bethe-ansatz equations

$$\frac{\phi(\lambda - v_j)}{\phi(\lambda + v_j)} = \frac{q(v_j - 2\lambda')}{q(v_j + 2\lambda')}, \quad j = 1, \ldots, L \tag{2.10}$$

which follow from (2.8). In contrast to the periodic case, the number of roots is fixed at L.

2.4 Solution to the six-vertex model—free energy and interfacial tension

We solve the functional relations (2.4) and (2.8) for the eigenvalues of the transfer matrices of the six-vertex model with both periodic and anti-periodic boundary conditions, in order to calculate the free energy and interfacial tension of the model.

To determine the free energy of the model with periodic boundaries, one must determine in which block of $\mathbf{V}$ the maximum eigenvalue lies; it is usually assumed to lie in the subspace corresponding to $n = \frac{1}{2}L$ if L is even or $\frac{1}{2}(L \pm 1)$ if L is odd. This has been confirmed in numerical calculations for finite L, and although a proof is lacking, it shall be assumed here.

Once this is established, the maximum eigenvalue and hence the free energy can be calculated in the thermodynamic limit, after making certain analyticity assumptions. The model has three seperate phases, in each of which the free energy assumes a different analytical form. The phases are classified by the parameter Δ.

The ferroelectric model corresponds to $\Delta > 1$; in this phase, the system is "frozen" into its ground state configuration for all sub-critical temperatures, maintaining perfect, zero-temperature polarisation all the way up to the critical temperature, where it has first order phase transition into a disordered state. This was pointed out by Slater in his 1941 paper [106]. The interfacial tension between oppositely ferroelectrically-ordered regions is infinite, and so this phase of the six-vertex model is of little interest to us here.

The region $-1 < \Delta < 1$ is rather unusual; it corresponds to the disordered region (containing the infinite temperature point $a = b = c = 1$), but the correlation length is infinite for all a, b and c in this region, and hence the model is critical throughout the entire disordered phase. As the system is disordered, the interfacial tension is zero. Re-parameterising the Boltzmann weights in terms of circular trigonometric functions, $a = \rho \sin \frac{1}{2}(\mu - w)$, $b = \rho \sin \frac{1}{2}(\mu + w)$, $c = \rho \sin \mu$, so $\Delta = -\cos \mu$, where $-\mu < w < \mu$, $0 < \mu < \pi$, the free energy per site is

$$f/k_B T = \log \rho - \int_{-\infty}^{\infty} \frac{\sinh(\mu - w)x \sinh(\pi - \mu)x}{2x \sinh \pi x \cosh \mu x} dx.$$

2.4.1 Anti-ferroelectric phase

We are mainly interested in the six-vertex model in its anti-ferroelectric phase, with $c > a + b$, or $\Delta < -1$. The free energy is calculated in the following chapter,

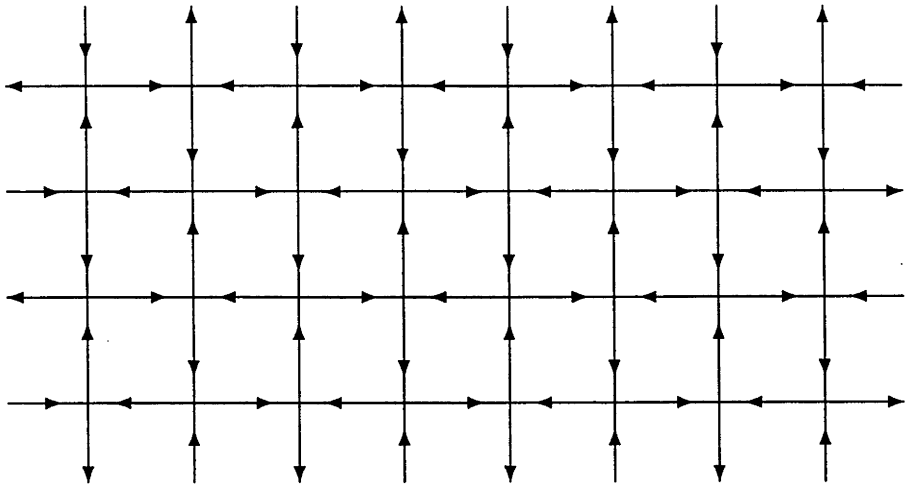

Figure 2.2: One of the two possible ground state configurations, with L even and periodic boundary conditions.

and can be written

$$f = \varepsilon_1 - k_B T \left\{ \tfrac{1}{2}(\lambda + v) + \sum_{m=1}^{\infty} \frac{\exp(-m\lambda)\sinh m(\lambda + v)}{m \cosh m\lambda} \right\} \tag{2.11}$$

for $-\lambda < v < \lambda$.

2.4.2 The interfacial tension

In the anti-ferroelectric phase the six-vertex model has a non-zero interfacial tension s, given by

$$e^{-s/k_B T} = 2x^{1/2} \prod_{m=1}^{\infty} \left(\frac{1 + x^{4m}}{1 + x^{4m-2}} \right)^2 \tag{2.12}$$

where

$$x = e^{\lambda}.$$

The interfacial tension of the six-vertex model was originally calculated by Baxter for the eight-vertex model, in Reference [16], from the two asymptotically degenerate numerically largest eigenvalues of the transfer matrix, for a lattice with periodic boundary conditions. This calculation was actually for the symmetric eight-vertex model, but the result is independent of the vertex weight $d = e^{-\varepsilon_7/k_B T} = e^{-\varepsilon_8/k_B T}$, so is the same for both the eight- and six-vertex models.

We do not calculate it this way; instead, we force an interface in the lattice, and calculate the interfacial tension from the asymptotic behaviour of the partition

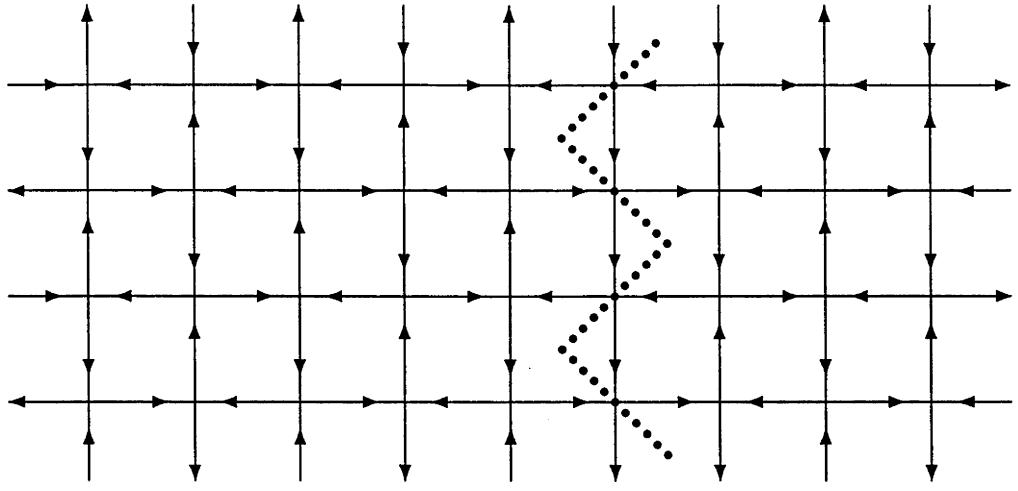

Figure 2.3: One of L possible lowest-energy configuration, with L odd and periodic boundary conditions.

function as the lattice size tends towards infinity. There are two ways we create the interface, which we describe here.

First consider the lattice with periodic boundary conditions in both the horizontal and vertical directions, and L and M both even. In the anti-ferroelectric phase, and at the absolute zero of temperature, vertices with weight c dominate; the ground state of this lattice is shown in Figure 2.2. The vertices all have Boltzmann weight c, and the lattice shows perfect anti-ferroelectric order.

If instead we take the number of columns L to be odd, then just as Onsager found that this produced an "anti-ferromagnetic seam" in his Ising lattice, so we find that an "anti-ferroelectric seam" is produced, on either side of which the lattice is ordered into a perfect anti-ferroelectric state. There must be an even number of vertices with weight c in each row to ensure the periodic boundary condition. In the zero temperature limit, a typical row will be composed of as many vertices with weight c as possible, but the requirement of an odd number of vertices in each row implies that the lowest-energy configuration of a row must contain a vertex with weight a or b. As rows are added together to form the lattice, these anomalous vertices form an interface running down the lattice. The interface may meander from left to right, but its mean direction will be downwards. The interfacial tension is the surplus free energy due to the presence of the interface. An example of the seam is shown in Figure 2.3. We take the number of rows, M, to be even to ensure periodic boundary conditions in the vertical direction, so that there will not also

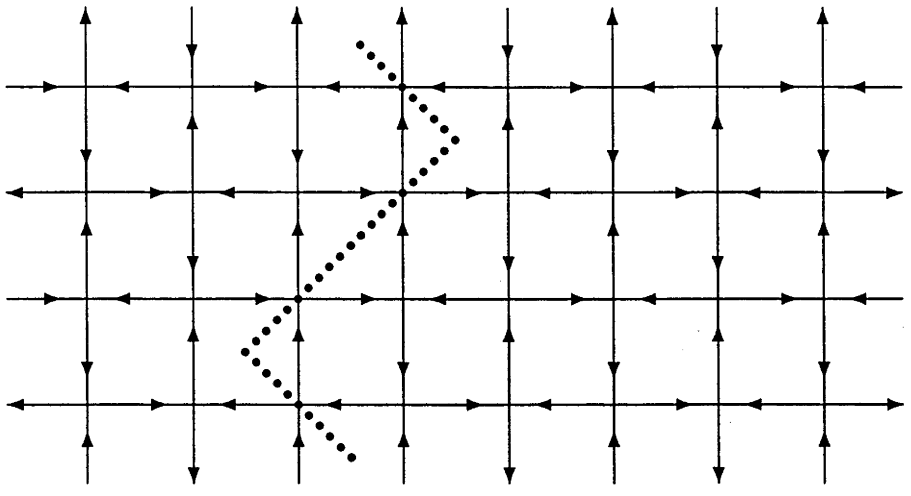

Figure 2.4: One of L possible lowest-energy configuration, with L even and anti-periodic boundary conditions.

be an interface running in the horizontal direction.

When we impose anti-periodic boundary conditions, and consider an even number L of columns, the ground state configuration in Figure 2.2 is again inconsistent. To ensure the anti-periodic boundary condition, vertices with Boltzmann weight c must occur an odd number of times in each row. Thus the lowest-energy configuration for the row, which is favoured at low temperatures, will consist of $L-1$ vertices with weight c, and one vertex with either weight a or b. This vertex can occur anywhere in the row. As we add rows to form the lattice, the a or b vertex in each row forms a "seam" running approximately vertically down the lattice; it can jump from left to right but the mean direction is downwards. A typical lowest-energy configuration is shown in Figure 2.4.

Finally, we consider the effect of having both anti-periodic boundary conditions from left to right, and an odd number of columns. Figure 2.5 shows a ground state of this lattice, which has perfect anti-ferroelectric order in the zero temperature limit. Hence there is no interface in this lattice.

For those lattices with vertical interfaces, the interfacial tension will grow as the length of the interface grows; this is proportional to the height M of the lattice, so we expect that for large L and M the partition function of the lattice will be of the form

$$Z \sim \exp\left[(-LMf - Ms)/k_BT\right] \tag{2.13}$$

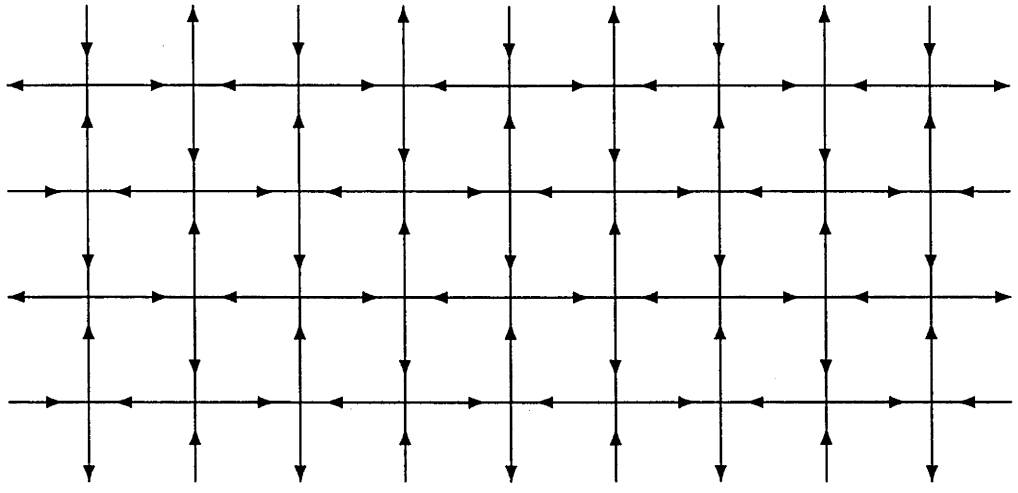

Figure 2.5: One of the two possible ground state configuration, with L odd and anti-periodic boundary conditions.

where f is the normal bulk free energy, and s is the interfacial tension per unit length.

2.4.3 Critical behaviour

We mention the critical behaviour of the anti-ferroelectric six-vertex model [19]. The phase transition occurs when $a + b - c = 1$, and near criticality we have $T - T_c \sim t = (a + b - c)/c$; the singular part of the free energy scales as $f_{\text{sing}} \sim \exp(-c/(-t)^{1/2})$, which has an essential singularity at $t = 0$. The free energy and all of its derivatives vanish as $t \to 0^-$, and the transition is "infinite order." The interfacial tension, correlation length and order parameter all have essential singularities at the critical point also, rather than vanishing or diverging as power laws, and so the corresponding critical exponents cannot be properly defined. This behaviour is interesting and rather unusual, and is due to the imposition of the ice rule; it does not persist in the eight-vertex model.

2.5 Results and discussion

We investigated the transfer matrices for the anti-ferroelectric six-vertex model with both periodic and anti-periodic boundary conditions, and considered the model on lattices with both an even and an odd number of columns.

The only such case that has been investigated previously is the model with

periodic boundary conditions and an even number of columns. In this case, the transfer matrix has a unique largest eigenvalue which gives the free energy, and an asymptotically degenerate next-largest eigenvalue from which the interfacial tension may be calculated. This maximum eigenvalue is given by equation (3.40) of Chapter 3.

For the model with periodic boundary conditions and an odd number L of columns, the lattice has an interface ("anti-ferroelectric seam") in its lowest-energy configuration, and a calculation of the partition function enables the calculation of the interfacial tension due to this seam. We find that the transfer matrix has a set of L largest eigenvalues, which are given by equations (3.71) and (3.72) of Chapter 3. The interfacial tension is derived by performing a saddle point integration, giving equation (2.12), as expected.

We also considered the model with anti-periodic boundary conditions, and some of this work has been published in Reference [11]. When this model has an even number of columns, once again there is an interface in the lowest-energy configuration. We find that the transfer matrix has a set of L largest eigenvalues, given by equations (3.106) and (3.72) of Chapter 3. From these, we re-derived equation (2.12) for the interfacial tension.

Finally, we considered the model with anti-periodic boundary conditions and an odd number of columns; the ground state of this lattice shows perfect anti-ferroelectric order, and we find that the transfer matrix has a unique positive largest eigenvalue.

The detailed working is included in the following chapter.

In conclusion, we have used the functional relations to calculate the largest eigenvalue or eigenvalues of the transfer matrices of the six-vertex model in its anti-ferroelectric phase. Using these results, we re-derived the known formula for the interfacial tension of the model, and we feel that this method is much simpler than that used in an earlier calculation [16].

In the next part of this thesis, we use a similar method to calculate the interfacial tension of the chiral Potts model. This is an N-state generalisation of the Ising model, and the generalisation of anti-periodic boundary conditions to N-state spins is the skew-periodic boundary conditions.

CHAPTER 3

Calculation of the interfacial tension of the six-vertex model

In this chapter we present the solution to the functional relations (2.4) and (2.8) for both L even and L odd, obtaining explicit results in the limit $L \to \infty$. We employ the Weiner-Hopf factorisation technique to solve the functional relations. While our working is not mathematically rigorous, we believe our assumptions to be justifiable, and hence claim that our results are exact.

To enhance readability of what is a rather technical chapter, we summarise each of the sections here.

In Section 3.1, we write the functional relation for the model with periodic boundary conditions, equation (2.4), as a relation between polynomials, equation (3.4). This is not essential to the solution, but we find it to be very convenient. In Subsection 3.1.1, we go on to solve this functional relation for L even, computing the largest eigenvalue of the transfer matrix $\mathbf{V}$ in the thermodynamic limit, equation (3.40), and hence calculate the free energy per site, deriving equation (2.11) from Chapter 2. Then in Subsection 3.1.2, we solve the same functional relation for L odd, computing a band of L largest eigenvalues, which are given by equations (3.71) and (3.72). From these we calculate the interfacial tension, deriving the expression (2.12) of the previous chapter.

In Section 3.2 we consider the model with anti-periodic boundary conditions, writing the functional relation for the transfer matrix, equation (2.8) of Chapter 2, as a relation between polynomials, equation (3.78) of this chapter. This is solved in Subsection 3.2.1 for even L, from which we calculate a band of L largest eigenvalues, which are given by equations (3.106) and (3.72). From these eigenvalues we again derive (2.12) for the interfacial tension.

Finally, in Subsection 3.2.2, we solve the functional relation (3.78), this time for

L odd, and find that there is a unique largest eigenvalue of the transfer matrix.

3.1 Periodic boundary conditions

We present the solution of the functional relations for periodic boundary conditions and an even number of columns first. This is the simplest case to solve, and the method generalises to the other cases we consider.

To facilitate the solution, we define a new variable z by

$$z = e^v, \tag{3.1}$$

so from the symmetry (2.1), the partition function is now invariant under $z \to 1/z$. All of the eigenvalues of $\mathbf{V}(v)$ and $\mathbf{Q}(v)$ are Laurent polynomials in z, and we rewrite the functional relation between the eigenvalues of $\mathbf{V}(v)$ and $\mathbf{Q}(v)$ in terms of polynomials in z as follows. Define the polynomials $Q(z)$ and $V(z)$ as

$$Q(z) = \prod_{j=1}^{n}(z - z_j) \tag{3.2}$$

and

$$V(z) = e^{-\pi i n} 2^L \rho^{-L} e^{Lv/2} \Lambda(v) x^{L/2-n}, \tag{3.3}$$

so the functional relation (2.4) becomes

$$V(z)Q(z) = (1 - zx)^L Q(zx^{-2}) + x^{L-2n}(zx^{-1} - 1)^L Q(zx^2). \tag{3.4}$$

The function $Q(z)$ is a polynomial in z of degree n, with zeros $z_1, \ldots, z_n$. The right hand side of (3.4) is a polynomial in z of degree $L+n$, and so $V(z)$ is a polynomial in z of degree L.

We will solve the functional relation (3.4) for the polynomial $V(z)$ corresponding to the maximum eigenvalue of $\mathbf{V}(v)$, for both the cases L even and L odd. From the last chapter, when L is even, we expect that the partition function will grow as

$$Z \sim e^{-LMf/k_BT}$$

as L and M tend to infinity, where f is the bulk free energy per site in the thermodynamic limit. Taking L odd will force an interface in the lattice, so the partition function will grow as in equation (2.13) as L and M tend to infinity, where s is the interfacial tension per unit length.

3.1.1 Even L

To calculate the maximum eigenvalue of $\mathbf{V}$, we find the maximum eigenvalue in the $n = L/2$ subspace, for finite n and L, and then take the limit $L \to \infty$ with $n = L/2$ fixed, remembering that L is even. With this value of n, the functional relation (3.4) becomes

$$V(z)Q(z) = (1 - zx)^L Q(zx^{-2}) + (zx^{-1} - 1)^L Q(zx^2). \tag{3.5}$$

Of the many possible solutions to the functional relations, we have to determine which of these corresponds to the maximum eigenvalue of $\mathbf{V}$. The relation contains solutions corresponding to all of the eigenvalues in the particular block, plus possibly others that do not correspond to any eigenvalues at all. Our approach is to identify the solutions corresponding to the largest eigenvalue in the zero-temperature limit. We describe the polynomials by determining the location of their zeros in the complex z plane. We then make assumptions based on this limiting behaviour to locate the zeros corresponding to the largest eigenvalue of $\mathbf{V}$ for non-zero temperatures. The temperature-like variable we use is x (or alternatively λ or Δ). When $x = 0$ ($\lambda = \infty$, $\Delta = -\infty$), the system is in one of two possible perfectly ordered anti-ferroelectric ground states, and undergoes an order to disorder transition as $x \to 1$ ($\Delta \to -1$ or $\lambda \to 0$).

We are considering the anti-ferroelectric model, with $c > a+b$. Hence as $\lambda \to \infty$, the maximum eigenvalue of the system will correspond to the state in which vertices with the vertex weight c appear most. The periodic boundary condition from left to right requires that the vertices with weight c occur an even number of times in each row, so as L is even, then in the limit $x \to 0$ the maximum eigenvalue will be, to leading order $\Lambda(v) \sim c^L$, and hence

$$V(z) \sim z^n x^{-L} \tag{3.6}$$

as $x \to 0$. We make the (self-consistent) assumption that the polynomial $Q(z)$ is bounded as $x \to 0$, and that its zeros are order unity. The right hand side of (3.5) is, up to a constant (order unity) multiple,

$$z^n x^{-L} (1 + (-z)^n z_1 z_2 \dots z_n) \tag{3.7}$$

where the z_j, $j = 1, \dots, n$ are the zeros of $Q(z)$. Substituting expression (3.6) for $V(z)$ into the relation (3.5), we find the following expression for $Q(z)$ which is valid in the limit $x \to 0$;

$$Q(z) = \text{constant} \cdot (1 + (-z)^n z_1 \cdots z_n) \tag{3.8}$$

where the constant is order unity. Equating (3.2) and (3.8) we find that the zeros of $Q(z)$ satisfy the following relation in this limit

$$(z_1 \cdots z_n)^2 = 1, \tag{3.9}$$

and hence that

$$Q(0) = (-)^n z_1 \cdots z_n = \pm 1. \tag{3.10}$$

Equations (3.8) and (3.9) imply that in this limit, the n zeros of $Q(z)$ lie on the unit circle, and are the solutions to the equation

$$z_j^n = \pm 1, \quad j = 1, \ldots, n. \tag{3.11}$$

The $\pm$ signs in equations (3.9)–(3.11) correspond to the two asymptotically degenerate largest eigenvalues of $\mathbf{V}$. This two-fold degeneracy is unimportant in our calculations.

For the zeros of the polynomial $V(z)$; from equation (3.6), n of these lie at the origin in the limit $x \to 0$, and by the $z \to 1/z$ symmetry of the partition function, a further n lie at infinity.

Thus we have located the zeros of the polynomials $Q(z)$ and $V(z)$ which correspond to the maximum eigenvalue of $\mathbf{V}$ in the limit $x \to 0$. We wish to solve the functional relation for x non-zero also, so we have to determine how the zeros behave as x increases.

At least some of the zeros will certainly move; some or all of the zeros of $V(z)$ will move from the origin and from infinity into the finite part of the z plane, and some or all of the zeros of $Q(z)$ may move. If x is sufficiently small, the zeros of $V(z)$ and $Q(z)$ should not move by "too much," by this we mean that the zeros of $V(z)$ will still lie in some neighbourhood of the origin and of infinity, and the zeros of $Q(z)$ will still lie in some neighbourhood of the unit circle. This distribution of zeros is indicated in Figure 3.1.

Based on these assumptions, we can factor $V(z)$ as

$$V(z) = A(z)B(z), \tag{3.12}$$

where $A(z)$ is a polynomial in z of degree n whose zeros are those of $V(z)$ that lie inside the unit circle, and $B(z)$ a polynomial of the same degree, whose zeros are

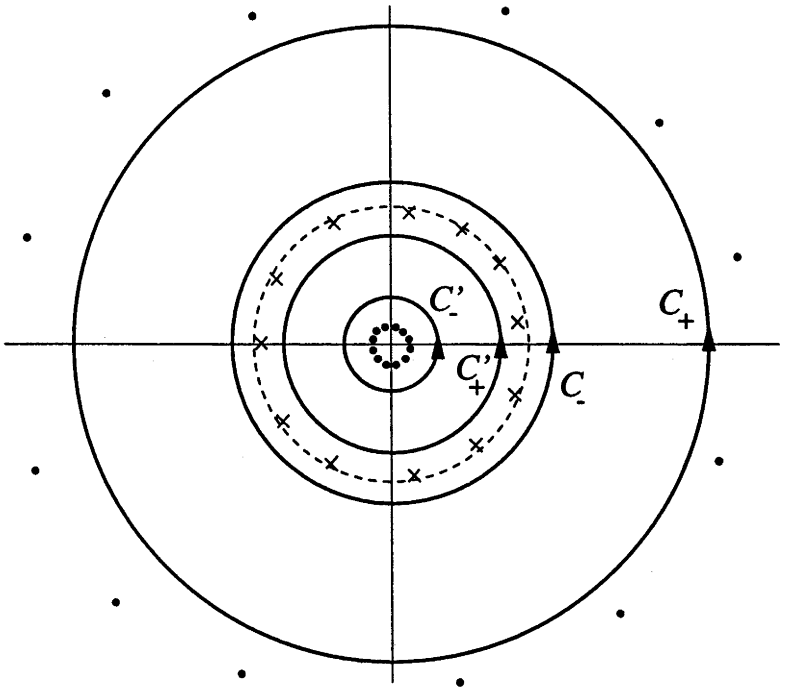

Figure 3.1: The zeros of $Q(z)$ (×) and $V(z)$ (•) in the complex z-plane, for periodic boundary conditions and an even number of columns L. The contours $\mathcal{C}_+$ and $\mathcal{C}_-$ lie outside the unit circle (broken line), and the contours $\mathcal{C}'_+$ and $\mathcal{C}'_-$ lie inside.

those of $V(z)$ that lie outside the unit circle. As $x \to 0$, all of the zeros of $A(z)$ move to the origin, and all of the zeros of $B(z)$ move to infinity.

The zeros of the functions $V(z)$ and $Q(z)$ as described lie clustered around the origin, the unit circle and the point at infinity (at least for x sufficiently small). Hence there will be two annular regions in the z-plane, inside which the polynomials $V(z)$ and $Q(z)$ are both non-zero. Draw the curves $\mathcal{C}_+$ and $\mathcal{C}_-$ as in Figure 3.1, both oriented in the positive direction and both outside the unit circle. Inside $\mathcal{C}_-$ lie the zeros of $Q(z)$ and $A(z)$, while outside $\mathcal{C}_+$ lie the zeros of $B(z)$. Let $\mathcal{C}$ be the curve $\mathcal{C}_+ - \mathcal{C}_-$. This is a curve oriented in the positive direction, the interior of which is the annular region between $\mathcal{C}_+$ and $\mathcal{C}_-$. Both $V(z)$ and $Q(z)$ are non-zero when z is inside $\mathcal{C}$.

Define a function $r(z)$ as the ratio of the first and second terms on the right hand side of the functional relation (3.5),

$$r(z) = \frac{(1 - zx)^L Q(zx^{-2})}{(zx^{-1} - 1)^L Q(zx^2)}. \tag{3.13}$$

We shall construct Weiner-Hopf factorisations of $1 + r(z)$ and $1 + 1/r(z)$ which are valid in appropriate regions of the complex z-plane, in order to factorise the polynomial $V(z)$. The function $r(z)$ is an analytic and non-zero function of z when z is inside $\mathcal{C}$.

When $|z| > 1$, then in the limit $x \to 0$ we see that $|r(z)| \sim |z|^{-n}$, so that $|r(z)| < 1$. Hence we can choose $\ln[1 + r(z)]$ to be a single-valued analytic function of z when z lies inside $\mathcal{C}$, and we assume that this can be done for non-zero values of x.

We then factorise $1 + r(z)$ by defining the functions $P_+(z)$ and $P_-(z)$ as

$$\ln P_\pm(z) = \pm \frac{1}{2\pi i} \oint_{\mathcal{C}_\pm} \ln[1 + r(w)] \frac{dw}{w - z}. \tag{3.14}$$

The function $P_+(z)$ is an analytic and non-zero function of z when z is inside $\mathcal{C}_+$ (see for example Reference [42], §5.5), and $P_-(z)$ is an analytic and non-zero function of z when z lies outside $\mathcal{C}_-$.

When z lies inside $\mathcal{C}$, Cauchy's integral formula implies

$$1 + r(z) = P_+(z)P_-(z) = \frac{V(z)Q(z)}{Q(zx^2)(zx^{-1} - 1)^L}. \tag{3.15}$$

The first of these equalities demonstrates the Weiner-Hopf factorisation of $1 + r(z)$ in terms of the functions $P_+(z)$ and $P_-(z)$. With the second we can make a Weiner-Hopf factorisation of $V(z)$ as follows. Let

$$V_+(z) = P_+(z)Q(zx^2) \tag{3.16}$$

$$V_-(z) = P_-(z)(1 - zx^{-1})^L / Q(z)\,. \tag{3.17}$$

The function $V_+(z)$ is an analytic and non-zero function of z for z inside $\mathcal{C}_+$, while $V_-(z)$ is an analytic and non-zero function of z for z outside $\mathcal{C}_-$. When z is inside $\mathcal{C}$, we have the equality

$$V(z) = V_+(z)V_-(z) \tag{3.18}$$

and thus we have Weiner-Hopf factorised $V(z)$ in terms of the functions $P_+(z)$ and $P_-(z)$. Equating the expressions (3.12) and (3.18) for $V(z)$, we can write

$$\frac{V_+(z)}{B(z)} = \frac{A(z)}{V_-(z)}, \tag{3.19}$$

which is valid when z is inside $\mathcal{C}$. Both sides of this equation are analytic functions in their respective domains, and agree identically when z is inside $\mathcal{C}$. Noting that

as $|z| \to \infty$, $P_-(z) \to 1$, Liouville's theorem implies that both sides of (3.19) are identically constant, c_1 say;

$$V_+(z) = c_1 B(z), \quad z \text{ inside } \mathcal{C}_+ \tag{3.20}$$

$$V_-(z) = c_1^{-1} A(z), \quad z \text{ outside } \mathcal{C}_-. \tag{3.21}$$

The constant c_1 is left undetermined for now.

We basically repeat this working to factorise $1 + 1/r(z)$. Draw the curves $\mathcal{C}'_+$ and $\mathcal{C}'_-$, both inside the unit circle, and both oriented in the positive direction. Inside $\mathcal{C}'_-$ lie the zeros of $A(z)$, while outside $\mathcal{C}'_+$ lie the zeros of $Q(z)$ and $B(z)$. Let $\mathcal{C}' = \mathcal{C}'_+ - \mathcal{C}'_-$ be a curve oriented in the positive direction; the interior of $\mathcal{C}'$ is the annulus between the contours $\mathcal{C}'_+$ and $\mathcal{C}'_-$, and inside $\mathcal{C}'$ the polynomials $V(z)$ and $Q(z)$ are both non-zero. These curves are also indicated in Figure 3.1.

When $|z| < 1$, in the limit $x \to 0$ we see that $|1/r(z)| < 1$, so we can choose $\ln[1 + 1/r(z)]$ to be analytic and single-valued when z is inside $\mathcal{C}'$. Again, we will assume that this can be done for all x.

Define the functions $P'_+(z)$ and $P'_-(z)$ as

$$\ln P'_\pm(z) = \pm \frac{1}{2\pi i} \oint_{\mathcal{C}_\pm} \ln\left[1 + \frac{1}{r(w)}\right] \frac{dw}{w - z}, \tag{3.22}$$

where $P'_+(z)$ is analytic and non-zero for z inside $\mathcal{C}'_+$, and $P'_-(z)$ is analytic and non-zero for z outside $\mathcal{C}'_-$. When z lies inside $\mathcal{C}'$, Cauchy's integral formula now implies that

$$1 + 1/r(z) = P'_+(z)P'_-(z) = \frac{V(z)Q(z)}{Q(zx^{-2})(1 - zx)^L}. \tag{3.23}$$

Thus we have split $1 + 1/r(z)$ into two factors, $P'_+(z)$ and $P'_-(z)$, where $P'_+(z)$ is an analytic and non-zero function of z for z inside $\mathcal{C}'_+$, and $P'_-(z)$ is an analytic and non-zero function of z for z outside $\mathcal{C}'_-$.

We use (3.23) to split $V(z)$ into two factors, $V'_+(z)$ and $V'_-(z)$, with the same analyticity properties, by defining

$$V'_+(z) = P'_+(z)(1 - zx)^L / Q(z) \tag{3.24}$$

$$V'_-(z) = P'_-(z)Q(zx^{-2}). \tag{3.25}$$

Then from previous comments, $V'_+(z)$ is an analytic and non-zero function of z when z is inside $\mathcal{C}'_+$, and $V'_-(z)$ is an analytic and non-zero function of z when z is outside $\mathcal{C}'_-$. When z is inside $\mathcal{C}'$, we have

$$V(z) = V'_+(z)V'_-(z). \tag{3.26}$$

Once more, equating (3.26) and (3.12), we have

$$\frac{V'_+(z)}{B(z)} = \frac{A(z)}{V'_-(z)} \tag{3.27}$$

which is valid for z inside $\mathcal{C}'$. By the same arguments preceding equations (3.20) and (3.21) we conclude that both sides of (3.27) are constant, say c_2. Thus

$$V'_+(z) = c_2 B(z), \quad z \text{ inside } \mathcal{C}'_+ \tag{3.28}$$

$$V'_-(z) = c_2^{-1} A(z), \quad z \text{ outside } \mathcal{C}'_-. \tag{3.29}$$

Equations (3.20),(3.21) and (3.28),(3.29) relate the functions $V_+(z)$, $V_-(z)$, and $V'_+(z)$, $V'_-(z)$ to the polynomials $A(z)$ and $B(z)$. Equating (3.20), (3.28) and (3.21), (3.29), we find

$$V'_+(z) = (c_2/c_1)V_+(z), \quad z \text{ inside } \mathcal{C}'_+ \tag{3.30}$$

$$V'_-(z) = (c_2/c_1)V_-(z), \quad z \text{ outside } \mathcal{C}_-, \tag{3.31}$$

which eliminates the functions $A(z)$ and $B(z)$. We evaluate the constant c_2/c_1 by considering the limit $|z| \to \infty$, then using equations (3.31), (3.25), (3.22), (3.17), (3.14) and (3.2), to find that $c_2/c_1 = 1$.

Equations (3.30) and (3.31) are used to derive expressions for the polynomials $Q(z)$ and $V(z)$ in appropriate domains of the z-plane as follows. When z is inside $\mathcal{C}'_+$, then equations (3.30), (3.24) and (3.16) imply that $Q(z)$ satisfies the recurrence relation

$$Q(z)Q(zx^2) = (1 - zx)^L \frac{P'_+(z)}{P'_-(z)}, \quad z \text{ inside } \mathcal{C}'_+. \tag{3.32}$$

Iterating this, $Q(z)$ can be written as the infinite product

$$Q(z) = Q(0) \prod_{m=1}^{\infty} \left(\frac{1 - zx^{4m-3}}{1 - zx^{4m-1}} \right)^L \frac{P'_+(zx^{4m})P_+(zx^{4m-2})}{P'_+(zx^{4m-2})P_+(zx^{4m})}, \quad z \text{ inside } \mathcal{C}'_+ \tag{3.33}$$

which is an exact expression for finite L. When L is large, the functions $P_+(z)$ and $P'_+(z)$ differ from unity by an exponentially small amount. In the thermodynamic limit $L \to \infty$, $P_+(z)$ and $P_-(z)$ both tend towards unity, and $Q(z)$ becomes

$$Q(z) = Q(0) \prod_{m=1}^{\infty} \left(\frac{1 - zx^{4m-3}}{1 - zx^{4m-1}} \right)^L, \quad z \text{ inside } \mathcal{C}'_+. \tag{3.34}$$

This is an exact expression in the limit $L \to \infty$.

We repeat this working for z outside $\mathcal{C}_-$. Then we use equations (3.31), (3.25) and (3.17) and get the recurrence relation

$$Q(z)Q(zx^{-2}) = (zx^{-1} - 1)^L \frac{P_-(z)}{P'_-(z)}, \quad z \text{ outside } \mathcal{C}_-, \tag{3.35}$$

which is an exact expression for finite L. We can solve (3.35) iteratively as before, exactly for finite L in terms of the functions $P_-(z)$ and $P'_-(z)$, which in the limit $L \to \infty$ becomes

$$Q(z) = z^n \prod_{m=1}^{\infty} \left(\frac{1 - z^{-1}x^{4m-3}}{1 - z^{-1}x^{4m-1}} \right)^L, \quad z \text{ outside } \mathcal{C}_-. \tag{3.36}$$

This is all the information needed to write down an expression for $V(z)$ from the functional relation (3.5), valid for z inside $\mathcal{C}$ or z inside $\mathcal{C}'$.

First consider the zeros of $Q(z)$; we shall show that these lie exactly on the unit circle for all x. Let $z = z_j$ be a zero of $Q(z)$, and substitute this into equation (3.5). The left hand side vanishes, and using equation (3.34) for $Q(zx^{-2})$ and equation (3.36) for $Q(zx^2)$, then in the thermodynamic limit the zeros of $Q(z)$ corresponding to the maximum eigenvalue of $\mathbf{V}$ satisfy

$$[\psi(z)]^L = \pm 1 \tag{3.37}$$

where

$$\psi(z) = z^{1/2} \prod_{m=1}^{\infty} \left(\frac{1 - zx^{4m-1}}{1 - zx^{4m-3}} \cdot \frac{1 - z^{-1}x^{4m-3}}{1 - z^{-1}x^{4m-1}} \right). \tag{3.38}$$

The $\pm$ sign corresponds to the asymptotically degenerate largest eigenvalues; the zeros of $Q(z)$ lie densely spaced on the unit circle for all x in th limit $L \to \infty$. Equation (3.37) reduces to (3.11) in the limit $x \to 0$, as expected.

As the zeros of $Q(z)$ lie exactly on the unit circle in the $L \to \infty$ limit, we can shift the contours $\mathcal{C}_-$ and $\mathcal{C}'_+$ and write equations (3.34) and (3.36) as

$$Q(z) = Q(0) \prod_{m=1}^{\infty} \left(\frac{1 - zx^{4m-3}}{1 - zx^{4m-1}} \right)^L, \quad |z| < 1$$

$$Q(z) = z^{L/2} \prod_{m=1}^{\infty} \left(\frac{1 - z^{-1}x^{4m-3}}{1 - z^{-1}x^{4m-1}} \right)^L, \quad |z| > 1.$$

We now calculate the function $V(z)$ as an infinite product. When z is inside $\mathcal{C}$, equation (3.18) implies that

$$V(z) = Q(0)z^n x^{-L} \prod_{m=1}^{\infty} \left(\frac{1 - zx^{4m-1}}{1 - zx^{4m+1}} \cdot \frac{1 - z^{-1}x^{4m-1}}{1 - z^{-1}x^{4m+1}} \right)^L \tag{3.39}$$

in the limit $L \to \infty$ with $n = L/2$. Similarly, when z is inside $\mathcal{C}'_-$, equation (3.26) gives the same expression for the function $V(z)$ in the $L \to \infty$, $n = L/2$ limit. Hence we can take this equation for $V(z)$ throughout the annulus between the contours $\mathcal{C}'_-$ and $\mathcal{C}_+$.

The eigenvalue $\Lambda(v)$ is related to $V(z)$ by equation (3.3), so we have, for the maximum eigenvalue of $\mathbf{V}(v)$,

$$\Lambda(v) = \pm(\rho/2x)^L \prod_{m=1}^{\infty} \left(\frac{1 - zx^{4m-1}}{1 - zx^{4m+1}} \cdot \frac{1 - z^{-1}x^{4m-1}}{1 - z^{-1}x^{4m+1}} \right)^L \tag{3.40}$$

which is valid for z inside $\mathcal{C}$ and z inside $\mathcal{C}'$, or inside the annulus between $\mathcal{C}'_-$ and $\mathcal{C}_+$. The $\pm$ signs are unimportant, and one derives equation (2.11) for the free energy.

3.1.2 Odd L

We now consider the functional relation for L odd, and calculate a set of L largest eigenvalues of the transfer matrix, from which we derive the interfacial tension via equation (2.13). We expect the maximum eigenvalues to occur in the $n = (L-1)/2$ or $(L+1)/2$ subspace of $\mathbf{V}$, the maximum eigenvalue in either subspace will lead to the same result through the symmetry under arrow reversal.

We take

$$n = (L-1)/2, \quad L = 2n+1$$

and the functional relation (3.4) now reads

$$V(z)Q(z) = (1 - zx)^L Q(zx^{-2}) + x(zx^{-1} - 1)^L Q(zx^2). \tag{3.41}$$

The right hand side of (3.41) is a polynomial in z of degree $3n+1$, and $Q(z)$ is a polynomial of degree n; therefore $V(z)$ is a polynomial in z with degree $L = 2n+1$.

We locate the zeros of $Q(z)$ and $V(z)$ in the $x \to 0$ limit and proceed as before. The largest eigenvalue will be dominated by the row configuration with the greatest number of vertices with the vertex weight c. Such vertices must still occur an even number of times in each row to ensure the periodic boundary conditions, but as L is now odd, there will be at least one vertex in each row with weight a or b. The maximum eigenvalue of $\mathbf{V}$ will correspond to a configuration with exactly one

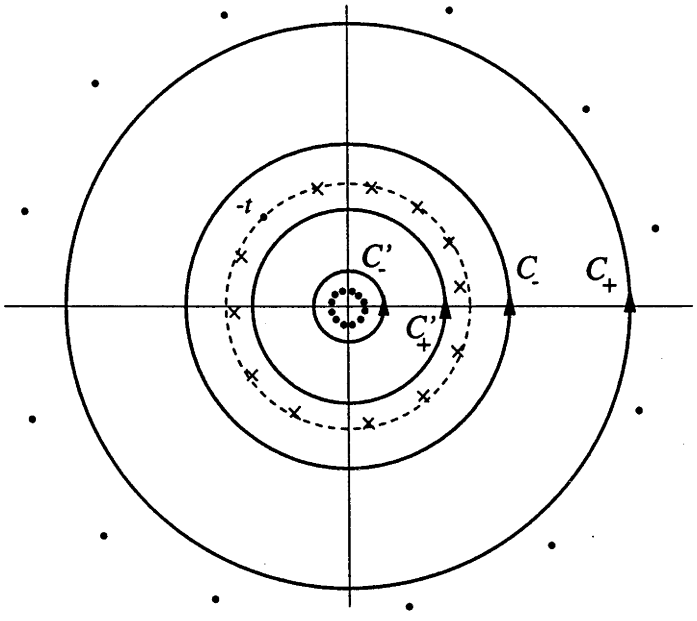

Figure 3.2: The zeros of $Q(z)$ ($\times$) and $V(z)$ ($\bullet$) in the complex z-plane for periodic boundary conditions and an odd number of columns L. The unit circle is indicated by the broken circle, and the contours $\mathcal{C}_+$ and $\mathcal{C}_-$ lie outside the unit circle, the contours $\mathcal{C}'_+$ and $\mathcal{C}'_-$ inside. The point $-t$, the extra zero of $V(z)$, is indicated.

vertex with weight a or b in each row. There are L places to put this vertex, which corresponds to the set of L largest eigenvalues of the transfer matrix (with one of these being positive and numerically larger than the others, by the Perron-Frobenius theorem).

Hence the largest eigenvalues are of the form (for $x \to 0$) $\Lambda(v) \sim c^{L-1}(d_1 a + d_2 b)$, where d_1 and d_2 are numbers which are order unity as $x \to 0$, and the corresponding polynomial $V(z)$ is

$$V(z) \sim z^n x^{-2n}(z+t) \tag{3.42}$$

where t, to be determined, is order unity. To find an expression for $Q(z)$ in this limit, we again assume that the zeros of $Q(z)$ are bounded as $x \to 0$. Then the right hand side of (3.41) is

$$z^n x^{-2n}\left(1-(-z)^{n+1}z_1\cdots z_n\right) \tag{3.43}$$

as $x \to 0$. Using (3.42) and (3.43), the functional relation (3.41) gives the low-temperature formula for $Q(z)$

$$Q(z)(z+t) = \text{constant} \cdot \left(1 - (-z)^{n+1} z_1 \cdots z_n\right) \tag{3.44}$$

where the constant is order unity. Both sides of (3.44) are polynomials of degree $n+1$, and using expression (3.2) for $Q(z)$ to equate coefficients of equal powers of z, we find

$$(z_1 \cdots z_n)^2 t = 1, \tag{3.45}$$

in contrast to equation (3.9) from the previous subsection. Hence

$$Q(0) = (-)^n z_1 \cdots z_n = \pm t^{-1/2}. \tag{3.46}$$

In particular, setting the right hand side of (3.44) to zero gives an equation for the $n+1$ zeros of the left hand side, that is, the zeros of $Q(z)$ $z_1, \ldots, z_n$ and the zero of $V(z)$, $z = -t$;

$$z^{n+1} = \pm (z_1 \cdots z_n)^{-1} = \pm t^{1/2}. \tag{3.47}$$

Of the $n+1$ solutions to this equation, n of them make up the zeros of $Q(z)$, $z_1, \ldots, z_n$, and one of them is the zero of $V(z)$, $z = -t$. The parameter t satisfies

$$t^L = 1, \tag{3.48}$$

which gives L possible values for t leading to L possible eigenvalues via equation (3.42), as expected. The $\pm$ sign corresponds to the unimportant two-fold degeneracy in each largest eigenvalue.

From (3.42), n of the zeros of $V(z)$ lie at the origin in this limit, and n of them lie at infinity, making up $2n+1 = L$ zeros for $V(z)$ including the zero on the unit circle.

We apply the same arguments as in the previous subsection regarding the behaviour of the zeros as x increases. We expect that the zeros will lie as indicated in Figure 3.2, with the n zeros of $Q(z)$ and one zero of $V(z)$, $-t$, lying in some neighbourhood of the unit circle, and n zeros of $V(z)$ lying in a neighbourhood of the origin, n in a neighbourhood of infinity.

Hence we can factor $V(z)$ as

$$V(z) = (z+t)A(z)B(z) \tag{3.49}$$

where once more $A(z)$ is a polynomial in z of degree n, whose zeros are those of $V(z)$ that lie inside the unit circle, and $B(z)$ is a polynomial of the same degree whose zeros are those of $V(z)$ that lie outside the unit circle.

We define the contours $\mathcal{C}_+$, $\mathcal{C}_-$, $\mathcal{C}$ and $\mathcal{C}'_+$, $\mathcal{C}'_-$, $\mathcal{C}'$ as before, with the zero $z = -t$ of $V(z)$ lying inside $\mathcal{C}_-$ and outside $\mathcal{C}'_+$. The contours are indicated in Figure 3.2.

Define $r(z)$ to be the ratio of the functions on the right hand side of (3.41),

$$r(z) = \frac{(1-zx)^L Q(zx^{-2})}{x(zx^{-1}-1)^L Q(zx^2)}. \tag{3.50}$$

We construct a Weiner-Hopf factorisation of $1 + r(z)$ and $1 + 1/r(z)$ as we did in the previous subsection. In the limit $x \to 0$, we see that $|r(z)| \sim |z|^{-n-1}$, so when $|z| > 1$ then $|r(z)| < 1$, and when $|z| < 1$ then $1/|r(z)| < 1$. Hence $\ln[1 + r(z)]$ can be chosen to be analytic for z inside $\mathcal{C}$, and $\ln[1 + 1/r(z)]$ can be chosen to be analytic for z inside $\mathcal{C}'$. We define the functions $P_+(z)$ and $P_-(z)$ as in equation (3.14) but with equation (3.50) for $r(z)$. Then $P_+(z)$ and $P_-(z)$ give a Weiner-Hopf splitting of $1 + r(z)$, ala the first equality of equation (3.15).

Using this we define a Weiner-Hopf splitting of $V(z)$ by defining the functions $V_+(z)$ and $V_-(z)$ as

$$V_+(z) = P_+(z) x Q(zx^2) \tag{3.51}$$

$$V_-(z) = P_-(z)(zx^{-1}-1)^L / Q(z), \tag{3.52}$$

where $V_+(z)$ is an analytic and non-zero function of z for z inside $\mathcal{C}_+$, and $V_-(z)$ is an analytic and non-zero function of z for z outside $\mathcal{C}_-$. We have the equality (3.18) when z is inside $\mathcal{C}$.

Equating (3.49) with the Weiner-Hopf factorisation (3.18), we have

$$\frac{V_+(z)}{B(z)} = \frac{A(z)}{V_-(z)}(z+t), \tag{3.53}$$

which is valid when z is inside $\mathcal{C}$, and Liouville's theorem again implies that both sides of (3.53) are identically constant, c_1 say, so (3.53) can be written

$$V_+(z) = c_1 B(z), \quad z \text{ inside } \mathcal{C}_+ \tag{3.54}$$

$$V_-(z) = c_1^{-1}(z+t)A(z), \quad z \text{ outside } \mathcal{C}_-. \tag{3.55}$$

Similarly, we factorise $V(z)$ for $|z| < 1$ by factorising $1 + 1/r(z)$. Define $P'_+(z)$ and $P'_-(z)$ as in (3.22), but with equation (3.50) for $r(z)$, and let

$$V'_+(z) = P'_+(z)(1-zx)^L / Q(z) \tag{3.56}$$

$$V'_-(z) = P'_-(z) Q(zx^{-2}) \tag{3.57}$$

where $V'_+(z)$ is analytic and non-zero when z is inside $\mathcal{C}'_+$, and $V'_-(z)$ is analytic and non-zero when z is outside $\mathcal{C}'_-$. When z is inside $\mathcal{C}'$, then $V(z) = V'_+(z)V'_-(z)$. We can equate expressions for $V(z)$ to write

$$\frac{V'_+(z)}{(z+t)B(z)} = \frac{A(z)}{V'_-(z)}, \tag{3.58}$$

when z is inside $\mathcal{C}'$. Again both sides of (3.58) are constant, say c_2, by Liouville's theorem. Hence we can write

$$V'_+(z) = c_2(z+t)B(z), \quad z \text{ outside } \mathcal{C}'_+ \tag{3.59}$$

$$V'_-(z) = c_2^{-1}A(z), \quad z \text{ inside } \mathcal{C}'_-. \tag{3.60}$$

Taking quotients of (3.20),(3.59) and (3.21), (3.60), we have

$$V'_+(z) = (c_1/c_2)(z+t)V_+(z), \quad z \text{ inside } \mathcal{C}'_+ \tag{3.61}$$

$$V_-(z) = (c_2/c_1)(z+t)V'_-(z), \quad z \text{ outside } \mathcal{C}_-. \tag{3.62}$$

The constant c_1/c_2 is unity (after considering (3.62) in the $|z| \to \infty$ limit). Equations (3.61) and (3.62) imply recursion relations for $Q(z)$ as before, and if we consider the $L \to \infty$ limit, so that $P_+(z)$, $P_-(z)$, $P'_+(z)$, $P'_-(z)$ are unity, the recursion relations are

$$Q(z)Q(zx^{-2}) = x(zx^{-1}-1)^L/(z+t), \quad z \text{ outside } \mathcal{C}_- \tag{3.63}$$

and

$$Q(z)Q(zx^2) = (1-zx)^L/(z+t), \quad z \text{ inside } \mathcal{C}'_+. \tag{3.64}$$

Iterating these, we have (in the limit $L \to \infty$)

$$Q(z) = z^n \prod_{m=1}^{\infty} \left(\frac{1-z^{-1}x^{4m-3}}{1-z^{-1}x^{4m-1}}\right)^L \left(\frac{1+z^{-1}tx^{4m-2}}{1+z^{-1}tx^{4m-4}}\right), \quad z \text{ outside } \mathcal{C}_- \tag{3.65}$$

and

$$Q(z) = Q(0) \prod_{m=1}^{\infty} \left(\frac{1-zx^{4m-3}}{1-zx^{4m-1}}\right)^L \left(\frac{1+zt^{-1}x^{4m-2}}{1+zt^{-1}x^{4m-4}}\right), \quad z \text{ inside } \mathcal{C}'_+. \tag{3.66}$$

From equation (3.64), we see that $[Q(0)]^2 = 1/t$, in agreement with equation (3.46).

The zeros of $Q(z)$ and $V(z)$ follow as in the previous subsection, from the functional relation (3.41). Using equation (3.65) for $Q(zx^{-2})$ and (3.66) for $Q(zx^2)$, the zeros of $Q(z)$ and $V(z)$ that lie in some neighbourhood of the unit circle satisfy

$$[\psi(z)]^L \, \phi(z/t) = \pm 1 \tag{3.67}$$

where $\psi(z)$ is given by (3.38) and

$$\phi(z) = z^{1/2} \prod_{m=1}^{\infty} \left(\frac{1 + zx^{4m}}{1 + zx^{4m-2}} \cdot \frac{1 + z^{-1}x^{4m-2}}{1 + z^{-1}x^{4m}} \right). \tag{3.68}$$

Equation (3.67) has $n + 1$ solutions (ignoring the $\pm$ sign, corresponding to the unimportant asymptotic degeneracy of the largest eigenvalues), which comprise the n zeros of $Q(z)$, and the zero $-t$ of $V(z)$. This satisfies the equation

$$[\psi(t)]^L = \pm 1. \tag{3.69}$$

In the limit $x \to 0$, this reduces to equation (3.48), as expected, and the different choices of t correspond to the L largest eigenvalues of $\mathbf{V}$.

All of the possible values of t are unimodular, as are the zeros of $Q(z)$, in the limit $L \to \infty$. Hence as in the previous subsection, we can move the contours $\mathcal{C}_-$ and $\mathcal{C}'_+$ onto the unit circle, and the expressions for $Q(z)$ are as follows:

$$Q(z) = Q(0) \prod_{m=1}^{\infty} \left(\frac{1 - zx^{4m-3}}{1 - zx^{4m-1}} \right)^L \left(\frac{1 + zt^{-1}x^{4m-2}}{1 + zt^{-1}x^{4m-4}} \right), \quad |z| < 1,$$

$$Q(z) = z^n \prod_{m=1}^{\infty} \left(\frac{1 - z^{-1}x^{4m-3}}{1 - z^{-1}x^{4m-1}} \right)^L \left(\frac{1 + z^{-1}tx^{4m-2}}{1 + z^{-1}tx^{4m-4}} \right), \quad |z| > 1.$$

Next we find the functions $V(z)$. When z is inside $\mathcal{C}$, then (considering L large, so $P_+(z)$ and $P_-(z)$ can be taken as unity) from (3.18)

$$V(z) = V_+(z)V_-(z) = xQ(zx^2)(1 - zx^{-1})^L / Q(z) \tag{3.70}$$

where we are again suppressing the correction terms, so

$$\Lambda(v) = \pm G(z/t)(\rho/2x)^L \prod_{m=1}^{\infty} \left(\frac{1 - zx^{4m-1}}{1 - zx^{4m+1}} \cdot \frac{1 - z^{-1}x^{4m-1}}{1 - z^{-1}x^{4m+1}} \right)^L \tag{3.71}$$

where

$$G(z) = x^{1/2}(z^{1/2} + z^{-1/2}) \prod_{m=1}^{\infty} \left(\frac{1 + zx^{4m}}{1 + zx^{4m-2}} \cdot \frac{1 + z^{-1}x^{4m}}{1 + z^{-1}x^{4m-2}} \right). \tag{3.72}$$

We arrive at exactly the same expression considering z inside $\mathcal{C}'$, so this expression for $\Lambda(v)$ is valid for z inside the annulus surrounded by the contours $\mathcal{C}_+$ and $\mathcal{C}'_-$.

Hence we have found L largest eigenvalues of the transfer matrix. By the Perron-Frobenius theorem, one of these should be real and positive, and this one should be the numerically largest of the set.

The two-fold degeneracy caused by the $\pm$ sign is irrelevant for calculating the free energy per site and the interfacial tension in the thermodynamic limit, but the L-fold degeneracy with the band of largest eigenvalues, while also unimportant to the free energy in the thermodynamic limit, is important when considering the interfacial tension in the limit $L \to \infty$. The partition function is given by

$$Z = \sum_{\text{all eigenvalues}} \Lambda(v)^M$$

where the sum is over all 2^L eigenvalues of $\mathbf{V}$. The sum is dominated by the band of L largest eigenvalues, given by equations (3.71), (3.72) and the solutions to (3.69). As $L \to \infty$, the sum over all values of t will become an integral around the unit circle,

$$Z = \oint R(t)\,[\Lambda(v)]^M\,dt \tag{3.73}$$

where $R(t)$ is some distribution function, independent of L and M. Substituting (3.71) into (3.73) then gives an integral expression for Z.

The eigenvalue (3.71) contains two distinct types of factors; those that are powers of L, and those that are not. The factors that increase exponentially with L contribute to the bulk part of the partition function, from which we calculate the free energy per site in the thermodynamic limit. This factor is also independent of t, so can be taken out of the integral (3.73). The integral is then independent of L, so we have, from equation (2.13)

$$e^{-f/k_BT} = (\rho/2x) \prod_{m=1}^{\infty} \left(\frac{1 - z^2x^{4m-1}}{1 - z^2x^{4m+1}} \cdot \frac{1 - z^{-2}x^{4m-1}}{1 - z^{-2}x^{4m+1}} \right)$$

for the free energy per site in the thermodynamic limit. This result agrees with the result for periodic boundary conditions, equation (2.11).

From equation (2.13), the other factors in (3.71) make up the interfacial tension, given by

$$e^{-Ms/k_BT} = \oint R(t)\,[G(z/t)]^M\,dt. \tag{3.74}$$

This integral is evaluated as $M \to \infty$ using the saddle point method. The function $G(z)$ satisfies the relation

$$G(z) = G(1/z)$$

and hence has saddle points at $z = 1$ and $z = -1$. The saddle point of the integrand is therefore

$$t = t_{\text{saddle}} = \pm z,$$

through which we may deform the contour of integration. Doing so, the saddle point method then gives equation (2.12) for the interfacial tension.

3.2 Anti-periodic boundary conditions

In this section we solve the functional relation (2.8) for the anti-periodic boundary conditions, to find the band of L largest eigenvalues for L even, and the single largest eigenvalue for L odd. To cast the eigenvalues of $\mathbf{Q}(v)$ and $\mathbf{V}(v)$ as polynomials in a variable z, we re-define z as

$$z = e^{v/2}. \tag{3.75}$$

Then let

$$Q(z) = \prod_{j=1}^{L}(z - z_j) \tag{3.76}$$

where $z_j = e^{v_j/2}$, $j = 1, \ldots, L$, and

$$V(z) = \Lambda(v)(2z\rho^{-1})^L e^{-\pi i L/2}. \tag{3.77}$$

We can re-write the functional relation (2.8) in terms of polynomials as

$$Q(z)V(z) = (1 - z^2x)^L Q(-zx^{-1}) - (1 - z^2x^{-1})^L Q(-zx). \tag{3.78}$$

Both terms on the right hand side of (3.78) are polynomials in z of degree $3L$, but the coefficients of 1 and z^{3L} vanish, so $z^{-1}V(z)$ is a polynomial in z of degree $2L-2$.

3.2.1 Even L

We need an idea of where the zeros of the polynomials $Q(z)$ and $V(z)$ which correspond to the L largest eigenvalues lie in order to construct the desired Wiener-Hopf factorisations. From the anti-periodicity of $\mathbf{V}(v)$ we see that $V(z)$ is an odd function of z,

$$V(-z) = -V(z) \tag{3.79}$$

so its zeros must occur in plus–minus pairs.

We first consider the limit $x \to 0$. In this limit the partition function will be dominated by the state with the greatest number of vertices with weight c, and there must be an odd number of such vertices in each row to ensure the anti-periodic boundary conditions. Hence as L, the number of columns in the lattice, is now even, a vertex of either type a or b will occur in the lowest energy configuration of each row. As $x \to 0$, the maximum eigenvalue will be, to leading order, $\Lambda(v) \sim c^{L-1}(d_1 a + d_2 b)$, where d_1 and d_2 are constants which are order unity as $x \to 0$. Hence

$$z^{-1}V(z) \sim z^{L-2}x^{-L+1/2}\left(z^2+t^2\right)$$

as $x \to 0$, where t^2 is order unity. Thus $z^{-1}V(z)$ has $L-2$ zeros at the origin and a corresponding set of $L-2$ at infinity, and two that are bounded as $x \to 0$. We also need to know where the zeros of $Q(z)$ lie; in the previous calculations, we assumed that they were all bounded as $x \to 0$, and found that they all moved on to the unit circle as $L \to \infty$. This assumption was self-consistent when periodic boundary conditions were applied. If we make the same assumption in the anti-periodic case, then as $x \to 0$, the right hand side of the functional relation (3.78) becomes

$$z^L x^{-L}\left(1 - z^L z_1 \cdots z_L\right) \tag{3.80}$$

and so

$$Q(z)(z^2 + \text{constant}) \sim z x^{-1/2}\left(z^L z_1 \cdots z_L - 1\right) \tag{3.81}$$

where the constant is order unity, which implies that $Q(z)$ has a zero at the origin, contradicting the assumption that the zeros are bounded as $x \to 0$. Instead, guided by the form of equation (3.81), we assume that all but two of the zeros of $Q(z)$ are bounded as $x \to 0$, the other two moving to the origin and to infinity as $x \to 0$. Let z_1 and z_2 be the two zeros that are not bounded, and put $z_1 = \alpha$, $z_2 = \beta^{-1}$, where $\alpha, \beta \to 0$ as $x \to 0$. We can find out how fast α and β approach zero, assuming first that as $x \to 0$, $Q(z)$ has the following behaviour

$$Q(-zx^{-1}) \sim z^L x^{-L}, \qquad Q(-zx) \sim z_1 \cdots z_L,$$

when $z = O(1)$ (which is the case with periodic boundary conditions). Then equations (3.80) and (3.81) are still true, and from equation (3.76) we have

$$Q(z) \sim -z\beta^{-1}\left(z^{L-2} + \cdots + z_3 \cdots z_L\right)$$

as $x \to 0$, so equating this and (3.81), we see that

$$z_1 \cdots z_L \beta = O(x^{1/2}) \quad \text{and} \quad z_3 \cdots z_L t^2 \beta^{-1} = O(x^{-1/2}),$$

but the numbers $z_3, \ldots, z_L$ and t are all order unity, so

$$\alpha,\ \beta = O(x^{1/2}) \quad \text{as} \quad x \to 0.$$

We can show, using the approach of the previous section, that the zeros of $Q(z)$ and $V(z)$ satisfy

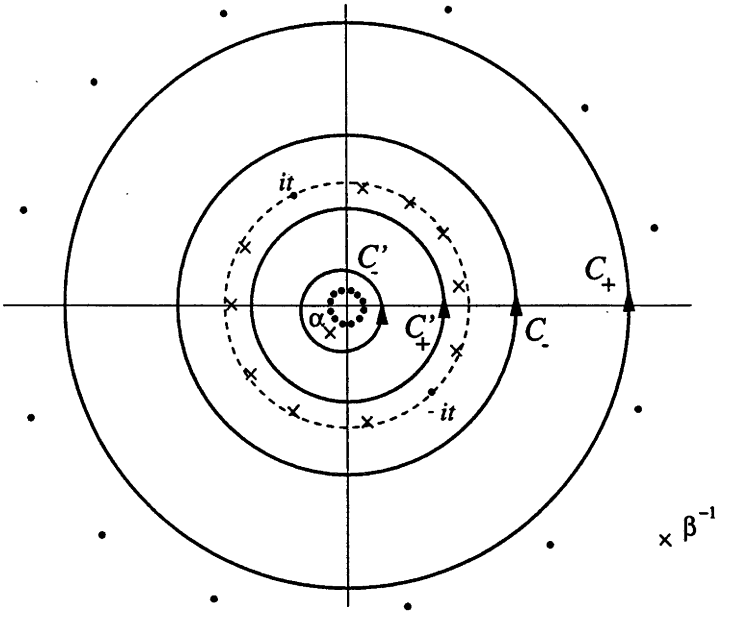

Figure 3.3: The zeros of $Q(z)$ (×) and $V(z)$ (•) in the complex z-plane, for anti-periodic boundary conditions and an even number of columns L. The contours C_+ and C_- lie outside the unit circle (broken line), the contours C'_+ and C'_- inside. The anomalous zeros of $V(z)$, $+it$ and $-it$, are indicated, as are the anomalous zeros of $Q(z)$, α and β^{-1}.

$$(z_1 \cdots z_L)^2 t^2 \alpha \beta^{-1} = 1$$

in contrast to the similar results for periodic boundary conditions, equations (3.45) and (3.9), and that

$$Q(0) = z_1 \cdots z_L = \pm t^{-1} \alpha^{1/2} \beta^{-1/2}. \tag{3.82}$$

The choice of sign corresponds to the two-fold degeneracy in the largest eigenvalues.

In summary, then, the zeros of $Q(z)$ and $V(z)$ are as follows. In the $x \to 0$ limit, $L-2$ of the L zeros of $Q(z)$ lie on the unit circle, the other two, α and β^{-1} lying at distances proportional to $x^{1/2}$ and $x^{-1/2}$ respectively. For $V(z)$, there is the simple zero at the origin, and two zeros, $+it$ and $-it$, on the unit circle. The remaining $2L-4$ zeros of $V(z)$ are divided into two sets, with $L-2$ of them that approach the origin and $L-2$ that approach infinity as $x \to 0$. The L zeros of the two polynomials that lie on the unit circle are spaced evenly around the circle.

As x is increased, the zeros of $Q(z)$ and $z^{-1}V(z)$ will all shift. The zeros at the origin and at infinity will move into the finite part of the z-plane, and the zeros

that lie on the unit circle in the $x \to 0$ limit will also move as x increases. Thus $Q(z)$ has $L-2$ zeros "near" the unit circle, and two others, one (α) inside and one (β^{-1}) outside. Both α and β are $O(x^{1/2})$ as $x \to 0$. Also, $V(z)$ has two zeros "near" the unit circle, which we call t_1 and t_2, one zero at the origin, and the final $2L-4$ zeros of $V(z)$ are made up of $L-2$ zeros inside and $L-2$ zeros outside the unit circle. This distribution of zeros is illustrated in Figure 3.3.

Hence we can factor $Q(z)$ as

$$Q(z) = (z-\alpha)(z-\beta^{-1})Q_1(z) \tag{3.83}$$

where $Q_1(z)$ is a polynomial of degree $L-2$ whose zeros are $O(1)$ as $x \to 0$, and $\alpha, \beta = O(x^{1/2})$, so α lies inside the unit circle, β^{-1} outside.

Also, let $V(z) = z(z-t_1)(z-t_2)A(z)B(z)$, where $A(z)$ and $B(z)$ are both polynomials of degree $L-2$, the zeros of $A(z)$ being all the zeros of $V(z)$ that lie inside the unit circle, the zeros of $B(z)$ being those of $V(z)$ that lie outside, and t_1 and t_2 are the zeros that lie on the unit circle. Since $V(z)$ is an odd function, we must have $t_1 = -t_2$; letting $t_1 = -t_2 = it$, we write

$$V(z) = z(z^2+t^2)A(z)B(z). \tag{3.84}$$

Draw the contours $\mathcal{C}_+$ and $\mathcal{C}_-$ in the complex z-plane, both oriented in the positive direction, with $\mathcal{C}_-$ outside the unit circle, $\mathcal{C}_+$ outside $\mathcal{C}_-$, and such that there are no zeros of $Q(z)$ or $V(z)$ on the boundary of or inside the annulus between $\mathcal{C}_-$ and $\mathcal{C}_+$. Then β^{-1} and all the zeros of $B(z)$ lie outside $\mathcal{C}_+$ (see Figure 3.3). Let $\mathcal{C} = \mathcal{C}_+ - \mathcal{C}_-$, a contour oriented in the positive direction, the interior of which is the annulus between the curves $\mathcal{C}_+$ and $\mathcal{C}_-$. The polynomials $V(z)$ and $Q(z)$ are both non-zero when z is inside $\mathcal{C}$.

Define $r(z)$ as the quotient of the two terms in the right hand side of the functional relation (3.78)

$$r(z) = -\frac{Q(-zx^{-1})(1-z^2x)^L}{Q(-zx)(1-z^2x^{-1})^L} \tag{3.85}$$

($r(z)$ has no zeros or poles on or between the curves $\mathcal{C}_+$ and $\mathcal{C}_-$). Then in the $x \to 0$ limit, we see that $|r(z)| \sim 1/|z|^L$, so when $|z| > 1$, $|r(z)| < 1$. Thus $\ln[1+r(z)]$ can be chosen to be single-valued and analytic when z lies in the annulus between $\mathcal{C}_-$ and $\mathcal{C}_+$. Assuming that this is so for all x, we make a Wiener-Hopf factorisation of $1+r(z)$ by defining the functions $P_+(z)$ and $P_-(z)$ as in (3.14), but with (3.85) for $r(z)$. Then $P_+(z)$ is an analytic and non-zero function of z for z inside $\mathcal{C}_+$, and

$P_-(z)$ is an analytic and non-zero function of z for z outside $\mathcal{C}_-$. As $|z| \to \infty$, $P_-(z) \to 1$. When z is inside $\mathcal{C}$, we have, by Cauchy's integral formula

$$1 + r(z) = P_+(z)\, P_-(z) = \frac{V(z)Q(z)}{Q(-zx)(1 - z^2x^{-1})^L}. \tag{3.86}$$

We use (3.86) to make a Weiner-Hopf factorisation of $V(z)$, defining the functions $V_+(z)$ and $V_-(z)$

$$V_+(z) = P_+(z)Q(-zx)/(z - \beta^{-1}) \tag{3.87}$$

$$V_-(z) = P_-(z)(1 - z^2x^{-1})^L\,/[Q_1(z)(z - \alpha)] \tag{3.88}$$

where $V_+(z)$ is an analytic and non-zero function of z for z inside $\mathcal{C}_+$, and $V_-(z)$ is an analytic and non-zero function of z for z outside $\mathcal{C}_-$. We have split $V(z)$ into two factors, $V_+(z)$ and $V_-(z)$, with $V(z) = V_+(z)V_-(z)$ when z is inside $\mathcal{C}$.

From (3.84) we have

$$\frac{V_+(z)}{B(z)} = \frac{A(z)}{V_-(z)} z(z^2 + t^2), \tag{3.89}$$

when z is inside $\mathcal{C}$. The left hand side (right hand side) is an analytic and non-zero function of z inside $\mathcal{C}_+$ (outside $\mathcal{C}_-$), which is bounded as $|z| \to \infty$ and so the function must be a constant, c_1 say. Thus

$$V_+(z) = c_1 B(z), \quad z \text{ inside } \mathcal{C}_+ \tag{3.90}$$

$$V_-(z) = c_1^{-1} z(z^2 + t^2)A(z), \quad z \text{ outside } \mathcal{C}_-. \tag{3.91}$$

When $|z| < 1$, we proceed in the same way to factorise $1 + 1/r(z)$. Draw the curves $\mathcal{C}'_+$ and $\mathcal{C}'_-$, $\mathcal{C}'_+$ inside the unit circle, $\mathcal{C}'_-$ inside $\mathcal{C}'_+$, and with α and all the zeros of $A(z)$ inside $\mathcal{C}'_-$. Let $\mathcal{C}'_+ = \mathcal{C}'_+ - \mathcal{C}'_-$ be a contour oriented in the positive direction, the interior of which is the annulus between $\mathcal{C}'_+$ and $\mathcal{C}'_-$, and inside of which both $V(z)$ and $Q(z)$ are non-zero.

In the limit $x \to 0$, $|1/r(z)| \sim |z|^L$, so $|1/r(z)| < 1$ when $|z| < 1$. Thus $\ln[1 + 1/r(z)]$ can be chosen to be single-valued and analytic when z is inside $\mathcal{C}'$, and we assume that this is the case for x non-zero. We can then Wiener-Hopf factorise $1 + 1/r(z)$ by defining the functions $P'_+(z)$ and $P'_-(z)$ as in equation (3.22) but with (3.85) for $r(z)$, so that $P'_+(z)$ is an analytic and non-zero function of z for z inside $\mathcal{C}'_+$, and $P'_-(z)$ is an analytic and non-zero of z for z outside $\mathcal{C}'_-$. As $|z| \to \infty$, $P'_-(z) \to 1$. When z is inside $\mathcal{C}'$, Cauchy's integral formula now implies

$$1 + \frac{1}{r(z)} = P'_+(z)\, P'_-(z) = -\frac{V(z)Q(z)}{Q(-zx^{-1})(1 - z^2x)^L}. \tag{3.92}$$

Using (3.92), we can Weiner-Hopf factorise $V(z)$ by defining the functions $V'_+(z)$ and $V'_-(z)$ as

$$V'_+(z) = P'_+(z)(1-z^2x)^L \Big/ \left[Q_1(z)(z-\beta^{-1})\right] \tag{3.93}$$

$$V'_-(z) = P'_-(z)Q(-zx^{-1})/(z-\alpha). \tag{3.94}$$

We have split $V(z)$ into two factors, $V'_+(z)$ which is an analytic and non-zero function of z for z inside $\mathcal{C}'_+$, and $V'_-(z)$ which is an analytic and non-zero function of z for z outside $\mathcal{C}'_-$. When z is inside $\mathcal{C}'$, we can write $V(z) = V'_+(z)V'_-(z)$, and using (3.84), we have

$$\frac{V'_+(z)}{B(z)(z^2+t^2)} = \frac{zA(z)}{V'_-(z)} \tag{3.95}$$

where now the left hand side (right hand side) is an analytic and non-zero function of z for z inside $\mathcal{C}'_+$ (outside $\mathcal{C}'_-$). The right hand side is bounded as $|z| \to \infty$, so by Liouville's theorem, both sides of the (3.95) are constant, c_2 say, and we have

$$V'_+(z) = c_2(z^2+t^2)B(z), \quad z \text{ inside } \mathcal{C}'_+ \tag{3.96}$$

$$V'_-(z) = c_2^{-1}zA(z), \quad z \text{ outside } \mathcal{C}'_-. \tag{3.97}$$

From equations (3.90), (3.96) and (3.91), (3.97), we have

$$V'_+(z) = (c_2/c_1)V_+(z)(z^2+t^2), \quad z \text{ inside } \mathcal{C}'_+ \tag{3.98}$$

$$V_-(z) = (c_1/c_2)V'_-(z)(z^2+t^2), \quad z \text{ outside } \mathcal{C}'_-. \tag{3.99}$$

To evaluate the constant c_1/c_2, consider (3.99) in the limit $|z| \to \infty$; we noted earlier that $P_-(z)$, $P'_-(z) \to 1$ as $|z| \to \infty$, so $c_1/c_2 = 1$.

We use equations (3.98) and (3.99) to derive recurrence relations satisfied by $Q(z)$, which we can solve explicitly in the $L \to \infty$ limit.

From equations (3.98), (3.93) and (3.87), we deduce

$$Q(z)\,Q(-zx) = (1-z^2x)^L \frac{(z-\alpha)(z-\beta^{-1})}{(z^2+t^2)} \frac{P'_+(z)}{P_+(z)}, \tag{3.100}$$

which is valid when z is inside $\mathcal{C}'_+$. In the limit $L \to \infty$, the P_+ and P'_+ functions $\to 1$, so we find that $Q(z)$ is given by

$$\begin{aligned} Q(z) \;=\; & Q(0) \prod_{m=1}^{\infty} \left(\frac{1-z^2x^{4m-3}}{1-z^2x^{4m-1}} \right)^L \frac{(1+z^2t^{-2}x^{4m-2})}{(1+z^2t^{-2}x^{4m-4})} \\ & \times \frac{(1-z\alpha^{-1}x^{2m-2})}{(1+z\alpha^{-1}x^{2m-1})} \frac{(1-z\beta x^{2m-2})}{(1+z\beta x^{2m-1})} \end{aligned} \tag{3.101}$$

up to correction terms that vanish exponentially as $L \to \infty$. This expression contains the still undetermined parameters t, α and β. From (3.100) in the $L \to \infty$ limit, setting $z = 0$ implies

$$[Q(0)]^2 = t^{-2}\alpha\beta^{-1} \tag{3.102}$$

in agreement with (3.82).

From equations (3.99), (3.94) and (3.88), we get the recurrence relation

$$Q(z)\,Q(-zx^{-1}) = (1 - z^2x^{-1})^L \frac{(z-\alpha)(z-\beta^{-1})}{(z^2+t^2)} \frac{P_-(z)}{P'_-(z)} \tag{3.103}$$

which is valid for z outside $\mathcal{C}_-$. Taking the limit $L \to \infty$ once more, so that the functions $P_-(z)$ and $P'_-(z) \to 1$, and iterating, we get

$$\begin{aligned} Q(z) \;=\; & z^L \prod_{m=1}^{\infty} \left(\frac{1 - z^{-2}x^{4m-3}}{1 - z^{-2}x^{4m-1}}\right)^L \frac{(1 + z^{-2}t^2x^{4m-2})}{(1 + z^{-2}t^2x^{4m-4})} \\ & \times \frac{(1 - z^{-1}\alpha x^{2m-2})}{(1 + z^{-1}\alpha x^{2m-1})} \frac{(1 - z^{-1}\beta^{-1}x^{2m-2})}{(1 + z^{-1}\beta^{-1}x^{2m-1})}. \end{aligned} \tag{3.104}$$

Following the working of the two previous calculations, we can now determine formulae for the zeros of $Q(z)$ and $V(z)$ from the functional relation (3.78) by setting the right hand side to zero, and substituting the formulae just derived for $Q(z)$. We defer this step, and proceed to find an expression for the set of largest eigenvalues of the transfer matrix, and find a relation between the parameters α, β and x.

When z is inside $\mathcal{C}$, from Equations (3.87) and (3.88),

$$V(z) = V_+(z)V_-(z) = Q(-zx)(1 - z^2x^{-1})^L/Q(z)$$

whereupon

$$\begin{aligned} V(z) \;=\; & \pm Q(0) z^L x^{-L} (1 - t^2/z^2) \prod_{m=1}^{\infty} \left(\frac{1 - z^2x^{4m-1}}{1 - z^2x^{4m+1}} \cdot \frac{1 - z^{-2}x^{4m-1}}{1 - z^{-2}x^{4m+1}}\right)^L \\ & \times \frac{1 + z\alpha^{-1}x^{2m-1}}{1 - z\alpha^{-1}x^{2m}} \cdot \frac{1 + z\beta x^{2m-1}}{1 - z\beta x^{2m}} \cdot \frac{1 + z^{-1}\alpha x^{2m-1}}{1 - z^{-1}\alpha x^{2m-2}} \\ & \times \frac{1 + z^{-1}\beta^{-1}x^{2m-1}}{1 - z^{-1}\beta^{-1}x^{2m-2}} \cdot \frac{1 + z^2t^{-2}x^{4m}}{1 + z^2t^{-2}x^{4m-2}} \cdot \frac{1 + z^{-2}t^2x^{4m}}{1 + z^{-2}t^2x^{4m-2}} \end{aligned}$$

using (3.101) for $Q(-zx)$ and (3.104) for $Q(z)$.

This rather cumbersome expression simplifies when we remember that $V(z)$ is an odd function of z. Thus all the poles and zeros of $V(z)$ must occur in plus–minus pairs. This is the case for the factors in this expression that depend on z through

z^2; those that contain z only linearly must cancel in some way. On closer inspection of the product, we see that the single poles and single zeros do in fact cancel if α and β are related by

$$\alpha\beta = -x. \tag{3.105}$$

Using this, Equations (3.77) and (3.102) imply that the eigenvalues are given by

$$\Lambda(v) = \pm G(z^2/t^2)(\rho/2x)^L \prod_{m=1}^{\infty} \left(\frac{1 - z^2x^{4m-1}}{1 - z^2x^{4m+1}} \cdot \frac{1 - z^{-2}x^{4m-1}}{1 - z^{-2}x^{4m+1}} \right)^L \tag{3.106}$$

where $G(z)$ is given by (3.72). Equation (3.106) is valid for z inside $\mathcal{C}$.

With relation (3.105) between α, β and x, the expression for $V(z)$ for z inside $\mathcal{C}'$ simplifies also, producing exactly the same expression for $\Lambda(v)$.

Using (3.105), the expressions for $Q(z)$ become

$$Q(z) = Q(0)(1 - z\alpha^{-1}) \prod_{m=1}^{\infty} \left(\frac{1 - z^2x^{4m-3}}{1 - z^2x^{4m-1}} \right)^L \frac{(1 + z^2t^{-2}x^{4m-2})}{(1 + z^2t^{-2}x^{4m-4})}, \tag{3.107}$$

$$Q(z) = z^{L/2}(1 - z^{-1}\beta^{-1}) \prod_{m=1}^{\infty} \left(\frac{1 - z^{-2}x^{4m-3}}{1 - z^{-2}x^{4m-1}} \right)^L \frac{(1 + z^{-2}t^2x^{4m-2})}{(1 + z^{-2}t^2x^{4m-4})}, \tag{3.108}$$

where the first expression is valid for z inside $\mathcal{C}'$, the second for z inside $\mathcal{C}$.

We now derive an expression for the zeros of $Q(z)$, following the method used in the previous two calculations, and assert that the free energy is once again analytic across the unit circle. Consider the functional relation (3.78); when z is a zero of either $V(z)$ or $Q(z)$, then the left hand side vanishes. In particular, we can substitute $z = it$ or $-it$, and hence derive an equation which describes the possible values of t. As t is order unity, $|tx| < 1$ and $|tx^{-1}| > 1$, so we use (3.107) for $Q(-zx)$, and (3.108) for $Q(-zx^{-1})$. We then derive an equation for the variable t, which still contains the unknown α. Demanding that this equation be valid for both $z = it$ and $z = -it$ gives the following relation between t and α

$$\alpha^2 = t^2x \tag{3.109}$$

whereupon t must satisfy

$$[\psi(t)]^L = \pm 1$$

where $\psi(z)$ is given by equation (3.38). Hence t lies on the unit circle for all x, and we have L eigenvalues of the transfer matrix. The right hand side of (3.78) also vanishes when z is a zero of $Q_1(z)$ so in the same way we show that the zeros of

$Q_1(z)$ lie exactly on the unit circle for all x. As the zeros lie exactly on the unit circle, we may shift the curves $\mathcal{C}_-$ and $\mathcal{C}'_+$ so that they just surround the unit circle. Hence equation (3.107) is valid for $|z| < 1$, and (3.108) is valid for $|z| > 1$.

The rest of the working is now exactly the same as at the end of Subsection 3.1.2; we have the same function $G(z)$, and are integrating over the same contour (the unit circle), and so arrive at the same expression for the interfacial tension, equation (2.12).

3.2.2 Odd L

Finally, we consider L odd. We expect that there will be a unique maximum eigenvalue of $\mathbf{V}$, and that this will give us the same free energy per site as the calculation in Subsection 3.1.

The right hand side of the functional relation (3.78) is a polynomial of degree $3L$, but the first and last terms cancel, as they did in the previous subsection, so $z^{-1}V(z)$ must be a polynomial of degree $2L-2$.

We have to locate the zeros of $Q(z)$ and $V(z)$ corresponding to the maximum eigenvalue of $\mathbf{V}$ in the limit $x \to 0$ once more. The maximum eigenvalue again corresponds to the state with the greatest number of vertices with weight c, which once more has to be odd to preserve the anti-periodic boundary conditions, but this time the odd number of columns is consistent with the fully anti-ferroelectrically ordered ground state. Thus in this limit, the maximum eigenvalue corresponds to $\Lambda(v) \sim c^L$ and so $V(z) \sim z^L x^{-L}$ as $x \to 0$, which is the same form as the periodic boundary conditions with even L, equation (3.6). We again assume that the zeros of $Q(z)$ are bounded as $x \to 0$, so in this limit the right hand side of the functional relation is proportional to $z^L x^{-L}\left(z^L z_1 \cdots z_L + 1\right)$. Hence $Q(z)$ is

$$Q(z) = \text{constant} \cdot \left(z^L z_1 \cdots z_L + 1\right)$$

where the constant is a number which is order unity as $x \to 0$, and carrying out the working as before, the $z_1, \ldots, z_L$ satisfy $(z_1 \cdots z_L)^2 = -1$, whereupon

$$Q(0) = -z_1 \cdots z_L = \pm i.$$

Hence $Q(z)$ has L zeros that lie on the unit circle as $x \to 0$, and $z^{-1}V(z)$ has $L-1$ zeros which lie at the origin and the same number which lie at the point at infinity.

As x increases, we make the usual assumptions regarding the behaviour of the zeros as a function of x. The zeros at the origin and at infinity will move into the

finite part of the z-plane, and the zeros on the unit circle might move slightly away from the unit circle.

We draw the contours $\mathcal{C}_+$, $\mathcal{C}_-$, $\mathcal{C}'_+$, $\mathcal{C}'_-$ and define $\mathcal{C}$ and $\mathcal{C}'$ as usual, so that inside $\mathcal{C}$ and $\mathcal{C}'$ the polynomials $V(z)$ and $Q(z)$ are non-zero. We can factor $V(z)$ as

$$V(z) = zA(z)B(z)$$

where both $A(z)$ and $B(z)$ are polynomials in z of degree $L-1$, the zeros of $A(z)$ are the zeros of $z^{-1}V(z)$ that lie inside the unit circle, and the zeros of $B(z)$ are those of $V(z)$ that lie outside.

Define

$$r(z) = -\frac{(1-z^2x)^L Q(-zx^{-1})}{(1-z^2x^{-1})^L Q(-zx)},$$

the ratio of the terms on the right hand side of the functional relation (3.78). As in the earlier calculations, $|r(z)| \sim |z|^{-L}$ as $x \to 0$, so for $|z| > 1$ we can choose $\ln[1+r(z)]$ to be analytic and single-valued, and for $|z| < 1$ we can choose $\ln[1+1/r(z)]$ likewise. We construct a Weiner-Hopf factorisation of $1+r(z)$ and of $1+1/r(z)$ as in the previous calculations. Define the functions $P_+(z)$, $P_-(z)$, $P'_+(z)$, and $P'_-(z)$ as in equations (3.14) and (3.22), where they have the usual analyticity properties. Then we can define a Weiner-Hopf splitting of $V(z)$ as follows; for z inside $\mathcal{C}$, then $V(z) = V_+(z)V_-(z)$ where

$$V_+(z) = -P_+(z)Q(-zx), \quad V_-(z) = P_-(z)(1-z^2x^{-1})^L/Q(z)$$

and for z inside $\mathcal{C}'$, $V(z) = V'_+(z)V'_-(z)$, where

$$V'_+(z) = P'_+(z)(1-z^2x)^L/Q(z), \quad V'_-(z) = P'_-(z)Q(-zx^{-1}).$$

Equating expressions for $V(z)$ in their respective domains, we can write

$$V_+(z)/B(z) = zA(z)/V_-(z), \quad V'_+(z)/B(z) = zA(z)/V'_-(z)$$

when z is inside $\mathcal{C}$ and $\mathcal{C}'$ respectively, which, using Liouville's theorem as in the previous subsections, implies that

$$V_+(z) = c_1 B(z), \quad V_-(z) = c_1^{-1}A(z)$$

when z is inside $\mathcal{C}$, and

$$V'_+(z) = c_2 B(z), \quad V'_-(z) = c_2^{-1}A(z)$$

when z is inside $\mathcal{C}'$, with c_1 and c_2 constants. Taking ratios of these equations, we find

$$V_+(z) = (c_1/c_2)V'_+(z), \quad \text{and} \quad V_-(z) = (c_2/c_1)V'_-(z)$$

when z is inside $\mathcal{C}'_+$ and outside $\mathcal{C}'_-$ respectively, and we see that $c_2/c_1 = 1$ by considering the limit $|z| \to \infty$. We can almost quote the working in Subsection 3.1; considering L large, we find recurrence relations for $Q(z)$;

$$Q(z)Q(-zx) = (1 - z^2x)^L \quad \text{when } z \text{ is inside } \mathcal{C}'$$

and

$$Q(z)Q(-zx^{-1}) = (1 - z^2x^{-1})^L \quad \text{when } z \text{ is inside } \mathcal{C}$$

and thus

$$Q(z) = Q(0) \prod_{m=1}^{\infty} \left(\frac{1 - z^2x^{4m-3}}{1 - z^2x^{4m-1}} \right)^L \quad \text{when } z \text{ is inside } \mathcal{C}' \tag{3.110}$$

and

$$Q(z) = z^L \prod_{m=1}^{\infty} \left(\frac{1 - z^{-2}x^{4m-3}}{1 - z^{-2}x^{4m-1}} \right)^L \quad \text{when } z \text{ is inside } \mathcal{C}. \tag{3.111}$$

We can then check that in the limit $L \to \infty$ the zeros of $Q(z)$ lie exactly on the unit circle, and thus that these expressions are valid all the way up to the unit circle, that is, (3.110) is valid for $|z| < 1$, and (3.111) for $|z| > 1$. Then the polynomial $V(z)$ and the eigenvalue $\Lambda(v)$ are calculated as before, giving equation (3.40) for the unique maximum eigenvalue of $\mathbf{V}$ in the thermodynamic limit, and equation (2.11) for the free energy, as expected.

Part II

The chiral Potts model

CHAPTER 4

The chiral Potts model

4.1 Origins

The chirally asymmetric clock model was introduced into statistical mechanics in 1981 by Ostlund [97] where it was proposed as a simple nearest-neighbour model with a spatially modulated ground state and a commensurate-incommensurate transition. Ostlund, and later that year Huse [61], considered a special case which we refer to as the Ostlund-Huse model, using a variety of approximation techniques [61] and a renormalisation group analysis [97] to determine the model's phase diagram, especially for the case $N = 3$.

In 1982 and 1983, Huse et al [62, 63] further considered the three-state chiral clock model, concentrating on the universality class of the order-disorder transition along the chiral melting line and the nature of the wetting curve. This subject was taken up by a number of authors in the following years, and we mention some of the resulting controversey shortly.

Also in 1983, Howes et al [60] considered the closely related three-state chiral Potts quantum spin chain, concentrating on what we now call the superintegrable model. Using series expansion techniques, they computed mass gaps and the order parameter, finding that these seem to have an extremely simple form.

Intrigued by these results, von Gehlen and Rittenberg [58] considered the self-dual $\mathbf{Z}_N$ symmetric quantum spin chains, which are an N-state generalisation of the Ising model spin chain and the model considered in [60]. They find that these models satisfy the Dolan-Grady criterion [46], and that the simple result for the mass gap persists in these higher-state models, and conclude that their models are "probably integrable."

The study of the integrable lattice model was initiated in 1987 by the authors Au-Yang, McCoy, Perk, Tang, Yan, and Sah in References [7, 8, 90, 100], when the

star-triangle relation for a chirally asymmetric, $\mathbf{Z}_N$-symmetric model was considered. This is an integrable chiral clock model whose transfer matrix commutes with the aforementioned spin chains. Solutions to the star-triangle relation were found for particular values of N for both the self-dual and non-self-dual models. The edge Boltzmann weights thus determined were found to depend on two "rapidity" variables, but had the unusual property that they do not depend simply on the differences between the rapidity variables, so the weights cannot be uniformised by elementary functions. This behaviour had been observed in some non-integrable models, but was in contrast to all previously known exactly solved models, for which this "difference property" plays an important part in the solution.

The most general solution to the star-triangle relation for a chirally asymmetric $\mathbf{Z}_N$ model was discovered by Baxter, Perk and Au-Yang in 1988 [22], when the Boltzmann weights for the integrable non-self-dual classical lattice model were derived for general N, and the function R which enters into the star-triangle relations was conjectured. The proof that the Boltzmann weights satisfy the star-triangle relations is presented by Au-Yang and Perk in Reference [9].

Work progressed rapidly in the following years on both the physical classical lattice model and on the non-physical superintegrable model (a much simpler case of the model, but with complex Boltzmann weights) as well as the associated quantum spin chain.

Baxter calculated the free energy of the model in 1988 [24], using the "399th" method he and Enting had introduced to solve the Ising model [17]. This solution relies only on the star-triangle relation, and the result is very complicated, but simplifies significantly in the scaling region, enabling the calculation of the specific heat critical exponent, $\alpha = 1 - 2/N$.

Functional relations for the transfer matrices of the model were conjectured and derived in 1989 and 1990 [2,27,35], and Baxter used these to calculate the free energy again in 1990 [28,29], producing a much simpler result. It has recently been shown that these results agree exactly in the scaling region and at criticality [34], but otherwise, the expressions have yet to be reconciled. The functional relation determines all of the eigenvalues of the transfer matrices, and also enables the calculation of other large-lattice quantities, such as the interfacial tension and the correlation length.

The interfacial tensions were considered in later publications by Baxter. In References [30, 31], the functional relations were re-derived for the model with

skewed boundary conditions; these were found to be only slight modifications of the functional relations for the periodic boundary conditions. The interfacial tensions were then calculated for the model in the zero-temperature limit as a first step towards a calculation valid for arbitrary temperatures. The interfacial tension was found to be independent of the vertical rapidity variables, as expected from Z-invariance.

This independence implies an alternative method of calculating the interfacial tension of the physical model at arbitrary temperatures. The vertical rapidities can be chosen so as to make the model superintegrable. This is a non-physical case of the model, for which the functional relations and transfer matrices take on a simpler form, rendering the model easier to solve. This should then give the interfacial tension of the model in its physical regime. In Reference [32], the interfacial tension was calculated for the superintegrable chiral Potts model. It was then argued using Z-invariance that this is the interfacial tension of the physical chiral Potts model. However, there is a potential problem with this argument, as the results of Z-invariance do not necessarily apply to a model whose Boltzmann weights are not positive [18].

We directly calculate the interfacial tensions of the physical chiral Potts model, without reference to the superintegrable model. We consider the functional relations of the model with skewed boundary conditions at sub-critical temperatures. We find that the method of solving the functional relations in [28] and [29] for the model with periodic boundary conditions generalises with only minor modifications to the skewed case. We solve the functional relations for a band of L complex largest eigenvalues, and from these we calculate the free energy and interfacial tension. We find that this is the same as the result calculated for the superintegrable model in [32] and hence that the Z-invariance arguments must hold.

In References [28] and [29], the free energy was calculated for the homogeneous model (with all vertical rapidities equal) and for $|\lambda_q| < 1$. Here we consider an alternating model (with the vertical rapidities alternately p and p' along the row), and with $|\lambda_q| > 1$. We find our result to be the analytical continuation of the $|\lambda_q| < 1$ result, and that the free energy of the alternating model is simply the arithmetic mean of the free energy of the homogeneous model with vertical rapidities p and p', as we expect from Z-invariance [19].

As well as this, our result seems to agree with a calculation by McCoy and Roan regarding some of the excitations in the spectrum of the chiral Potts transfer

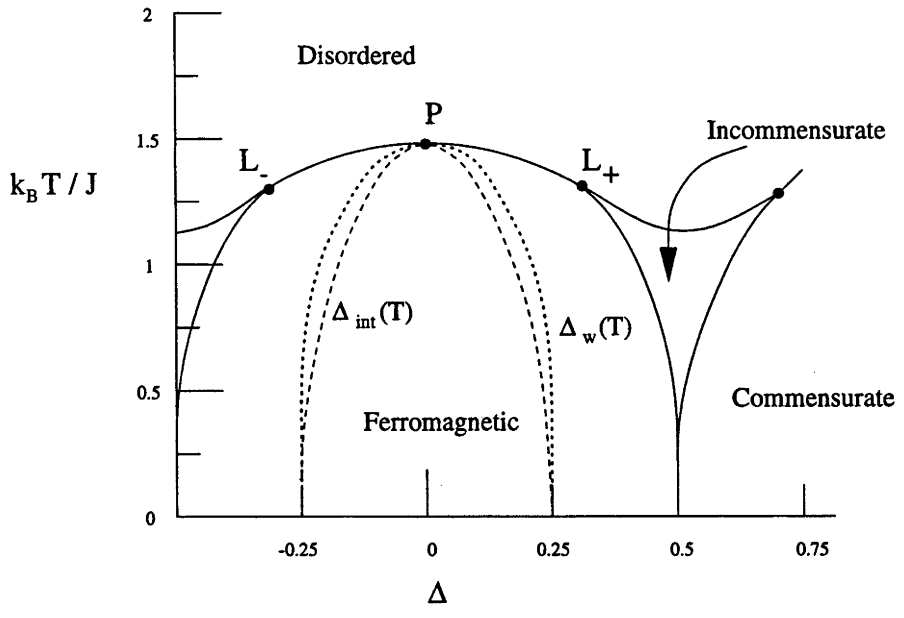

Figure 4.1: The phase diagram of the three-state Ostlund-Huse model, showing the ferromagnetic, disordered, commensurate and incommensurate phases. The Potts model critical point P is indicated, as well as the Lifshitz points L_+ and L_-. We indicate the wetting line $\Delta_w(T)$, along which the model has a wetting transition; and just below it, the integrable line, $\Delta_{int}(T)$, along which the model is exactly solvable. These two lines are very close, but not identical.

matrix [91,92].

4.2 The three-state chiral clock model

The chiral clock models describe a two-dimensional system in which an adsorbed commensurate surface phase melts continuously into an incommensurate or disordered phase. Real physical systems can be chirally asymmetric on the microscopic scale, so that the interfacial tension $s_{A,B}$ due to an A phase on the left of a B phase is in general not equal to $s_{B,A}$. This chiral asymmetry is described by the parameters Δ and $\bar{\Delta}$ in the three-state model.

The anisotropic three-state chiral clock model has Hamiltonian

$$\mathcal{H} = -K \sum \cos \frac{2\pi}{3}(\sigma_j - \sigma_{j+1} + \Delta) - \bar{K} \sum \cos \frac{2\pi}{3}(\sigma_i - \sigma_{i+1} + \bar{\Delta})$$

where the sums are over all nearest neighbour sites, the first in the SW→NE direction, and the second in the SE→NW direction. This model is equivalent to the three-state Potts and clock models when the chirality Δ and $\bar{\Delta}$ vanishes.

Two cases of this model have received much attention; the symmetric model, with $\mathcal{E}(n) = \bar{\mathcal{E}}(n)$, i.e. $K = \bar{K}$ and $\Delta = \bar{\Delta}$; and the Ostlund-Huse asymmetric model, for which $K = \bar{K}$ once more, but now $\bar{\Delta} = 0$, while Δ is a free variable.

We reproduce the phase diagram in Figure 4.2, for the Ostlund-Huse model. This model has been quite widely studied in the literature, [63] and references contained therein, and there is still some uncertainty about its exact structure. There has been some controversey surrounding the relevance of the chiral symmetry-breaking operator Δ at the pure Potts point ($\Delta = \bar{\Delta} = 0$), and the relation between the wetting curve of the Ostlund-Huse model and the integrable chiral Potts model.

4.2.1 The crossover phenomenon

At vanishing chirality, $\Delta = \bar{\Delta} = 0$, the ferromagnetic-to-paramagnetic phase transition is that of the three-state Potts model, and the critical point, labelled P in Figure 4.2, occurs at the Potts model critical temperature T_c^0.

It is not clear a priori whether the chiral symmetry breaking field Δ is relevant, irrelevant, or marginal at the pure Potts critical point. If irrelevant, the phase transition along the boundary between the ferromagnetic and paramagnetic regions is simply that of the three-state Potts model. If the field is relevant at the pure Potts point, the phase transition will have different critical exponents along this boundary, producing a new chiral universality class. A discussion of this is presented in [63], citing a number of analyses, which had predicted all three possible types of behaviour.

By scaling theory, near P, the interfacial tension $\varepsilon_r(T, \Delta)$ is expected to scale as

$$\varepsilon_r(T, \Delta) \sim |t|^{\mu} S(\Delta/|t|^{\phi}) \tag{4.1}$$

where μ is the pure $\Delta = 0$ Potts exponent, i.e. the critical exponent for the $N = 3$ Potts model interfacial tension, $S(z)$ is the corresponding scaling function, and t is the reduced temperature $t = (T - T_c^0)/T_c^0$. The chiral field is relevant if and only if ϕ is positive.

In [63], Huse et al. analyse high temperature expansions of the susceptibility and low temperature expansions of the surface tensions, and conclude that the chiral field is relevant, with $\phi = 0.19 \pm 0.06$. Our exact results confirm this, with $\phi = 1/2 - 1/N$ [10].

4.2.2 The wetting transition

Huse et al. also discuss the wetting line for both the symmetric and Ostlund-Huse models. The wetting line is the locus on the phase diagram at which wetting becomes favourable, and this line is indicated by the broken line marked $\Delta_w(T)$, which begins at zero temperature at $\Delta = 1/4$, and ends at the pure Potts critical point. The wetting transition occurs when [104]

$$\varepsilon_2(T, \Delta) = 2\,\varepsilon_1(T, \Delta).$$

Huse and Fisher calculate this locus to leading order in T, valid around $T = 0$, finding that for the symmetric case, the wetting line is given by

$$\Delta_w(T) = \frac{1}{4} - \frac{3}{2\pi} \sin^{-1} \frac{\ln 3/2}{3K} + \cdots$$

and that for the Ostlund-Huse case, the wetting line is

$$\Delta_w(T) = \frac{1}{4} - \frac{3z^2}{2\pi K} + \cdots$$

where $z = e^{-3K/2}$. These results are only approximate, and valid for very low temperatures, ignoring "overhangs" in the interfaces and "drops" of overturned spins in the bulk phases.

Also, in Reference [9], Au-Yang and Perk consider the integrable chiral Potts model, calculating (exactly) the integrable line for both the symmetric and the Ostlund-Huse model, finding the integrable lines to be

$$\Delta_{\text{int}}(T) = \frac{1}{4} - \frac{3}{2\pi} \sin^{-1} \frac{\ln 2}{3K} + \cdots$$

and

$$\Delta_{\text{int}}(T) = \frac{1}{4} - \frac{z}{\pi K} + \cdots$$

respectively. The wetting and integrable lines begin and end at the same points, and seem to have roughly the same shape. Au-Yang and Perk speculated that these two very special lines were in fact one and the same (so the approximations used in [63] were not as accurate as previously assumed).

As a result of the exact calculations of Baxter and O'Rourke, References [32,96], we can conclude that all of these results are accurate, and that the integrable chiral Potts model lies in the non-wetted region. The lines are, however, very close to one another, and are indicated in Figure 4.2. The integrable line lies just inside the wetting line. Further detail is included in the review by Au-Yang and Perk, Reference [10].

4.3 The chiral Potts model

The chiral Potts model is an N-state spin model, with spins living on the sites of the "$L \times M$" lattice shown in Figure 4.2. The spins take on the values $0, 1, \ldots, N-1$, and at sufficiently low temperatures the system is ordered into one of N possible equi-likely ferromagnetic ground states, and the system has an order-disorder transition at a critical temperature T_c. We use a temperature-like parameter k, similar to the Ising model (1.2); the phase transition occurs when $k = 1$.

The Boltzmann weights of this integrable model depend on a set of "rapidity" variables lying on the medial lattice, each carrying a variable $p, q, \ldots$ chosen from some manifold. The weights do not have the usual difference property, i.e. they do not depend on the rapidity variables simply as the differences of the two rapidities. The Boltzmann weights satisfy the star-triangle (Yang-Baxter) equations

$$\sum_{d=1}^{N} \bar{W}_{qr}(b-d)\, W_{pr}(a-d)\, \bar{W}_{pq}(d-c) = R_{pqr}\, W_{pq}(a-b)\, \bar{W}_{pr}(b-c)\, W_{qr}(a-c), \tag{4.2}$$

which holds for all values of the spins a, b, c and all rapidities p, q, r; that this is the case is proven in Reference [9]. As a result, the model is exactly solvable, and one should be able to calculate such thermodynamic quantities as the free energy per site, interfacial tensions, correlation lengths, and spontaneous magnetisation in the large lattice limit. The function R_{pqr} which enters into the star-triangle relation is defined shortly.

The medial lattice is indicated by the broken lines in Figure 4.2. The vertices of the medial lattice lie on the mid-point of the edges of the original lattice, and the vertices of the original lattice lie inside the faces of the medial lattice. In general, the vertical rapidities are allowed to be different on each row and column of the medial lattice, and we denote the rapidity variables associated with the columns $p_1, p_2, \ldots, p_L$, and those associated with the rows $q_1, q_2, \ldots, q_{2M}$; such a model is completely inhomogeneous. However, we find that a "sufficient level of generality" is to consider the "alternating" model, in which the vertical rapidities are alternately p and p', and the row variables are all the same value q. We sometimes consider the fully homogeneous case, in which all the vertical rapidities have the same value p.

The Boltzmann weights of the chiral Potts model are

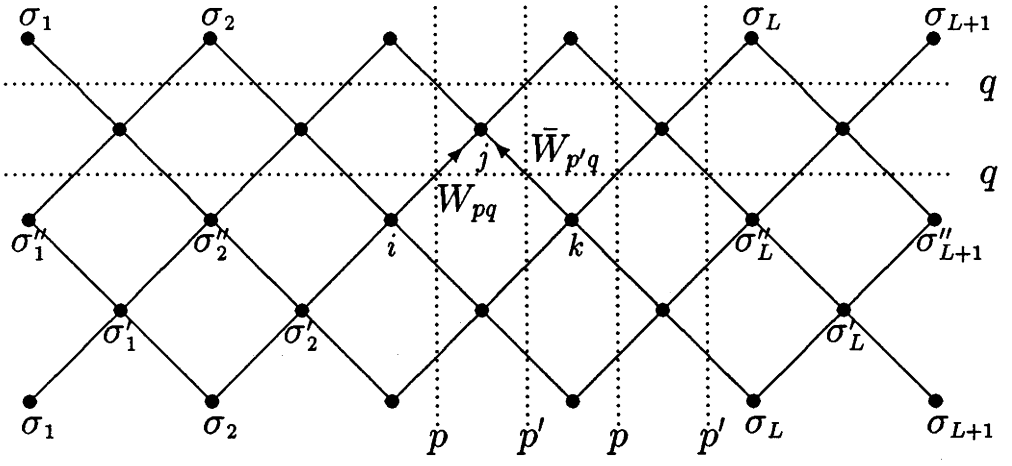

Figure 4.2: The square lattice with L sites per row and M=2. The Boltzmann weights W_{pq} and $\bar{W}_{p'q}$ in the SW $\rightarrow$ NE and SE $\rightarrow$ NW directions respectively are indicated. Also shown is the horizontal rapidity variable q, and the alternating vertical rapidities p and p'.

$$W_{pq}(n) = \left(\frac{\mu_p}{\mu_q}\right)^n \prod_{j=1}^{n} \frac{y_q - \omega^j x_p}{y_p - \omega^j x_q}, \quad \bar{W}_{pq}(n) = (\mu_p \mu_q)^n \prod_{j=1}^{n} \frac{\omega x_p - \omega^j x_q}{y_q - \omega^j y_p} \tag{4.3}$$

which satisfy the periodicity restriction

$$W_{pq}(n) = W_{pq}(N+n), \qquad \bar{W}_{pq}(n) = \bar{W}_{pq}(N+n) \tag{4.4}$$

and we specialise to the normalisation

$$W_{pq}(0) = \bar{W}_{pq}(0) = 1.$$

The variables x_q, y_q, μ_q are collectively known as the "q-variables," and similarly x_p, y_p, μ_p are known as the "p-variables." These are complex numbers which can be thought of as representing points on the algebraic curve described by the equations

$$x_q^N + y_q^N = k(1 + x_q^N y_q^N), \quad k x_q^N = 1 - k' \mu_q^{-N}, \quad \text{and} \quad k y_q^N = 1 - k' \mu_q^N \tag{4.5}$$

(with the p variables satisfying analogous relations). Here, k and k' are real positive numbers which are related by

$$k^2 + k'^2 = 1 \tag{4.6}$$

with $0 \leq k, k' \leq 1$. Fixing any one of these q-variables determines the other two up to choices of N-th roots of unity, so there is only one free parameter in each set.

Let η be the real solution to

$$\eta^N = (1-k')/(1+k'), \tag{4.7}$$

which is another temperature-like variable. We also define two other variables, t_q and λ_q, which prove to be particularly useful in our calculations,

$$t_q = x_q\, y_q, \quad \lambda_q = \mu_q^N$$

which are related to one another by

$$\lambda_q + 1/\lambda_q = \left(1 + k'^2 - k^2 t_q^N\right)/k', \quad \left(\frac{\lambda_q - 1}{\lambda_q + 1}\right)^2 = \frac{\eta^N - t_q^N}{\eta^{-N} - t_q^N}. \tag{4.8}$$

The periodicity requirements (4.4) imply that

$$\frac{y_p^N - x_q^N}{y_q^N - x_p^N} = \lambda_p/\lambda_q \quad \text{and} \quad \frac{y_q^N - y_p^N}{x_p^N - x_q^N} = \lambda_p\lambda_q,$$

and we also have the identities

$$k'(t_p^N - t_q^N) = \mu_q^N(x_p^N - x_q^N)(y_p^N - x_q^N) = \mu_q^{-N}(x_p^N - y_q^N)(y_p^N - y_q^N).$$

There are many automorphisms of the rapidity variables, which are listed in Reference [27]; we make use of the automorphism R,

$$R : \{x_q, y_q, \mu_q\} \to \left\{y_q, \omega x_q, \mu_q^{-1}\right\}, \tag{4.9}$$

and also the the automorphisms q and $\bar{q}$

$$q(k,l) : q \to \{\omega^k x_q, \omega^l y_q, \mu_q\}$$
$$\bar{q}(k,l) : q \to \{\omega^k x_q, \omega^l y_q, \mu_q^{-1}\}$$

with $R = \bar{q}(0,1)$. When the meaning is clear, we will write $q(k,l)$ and $\bar{q}(k,l)$ as qkl and $\bar{q}kl$. Also

$$t_{qkl} = t_{\bar{q}kl} = \omega^{k+l} t_q.$$

The function R_{pqr} from equation (4.2) was conjectured in [22] and the conjecture was proven by Matveev and Smirnov in [85], being

$$R_{pqr} = \frac{f_{pq} f_{qr}}{f_{pr}}$$

where f_{pq} is a complex-valued function of the p and q variables, with its Nth power being

$$f_{pq}^N = \det{}_N\left[\bar{W}_{pq}(i-j)\right] \Big/ \prod_{n=0}^{N-1} W_{pq}(n)\,,$$

where $\det_N\left[\bar{W}_{pq}(i-j)\right]$ is the determinant of the cyclic $N \times N$ matrix whose (i,j) element is $\bar{W}_{pq}(i-j)$; explicitly

$$\det_N\left[\bar{W}_{pq}(i-j)\right] = \left[\bar{W}_{pq}(0)\right]^N N^{N/2} e^{\pi i(N-1)(N-1)/12} \prod_{j=1}^{N-1} \frac{(t_p - \omega^j t_q)^j}{(x_p - \omega^j x_q)^j (y_p - \omega^j y_q)^j}.$$

We also define a related function, g_{pq}, with Nth power

$$g_{pq}^N = \det_N\left[\bar{W}_{pq}(i-j)\right] \prod_{n=0}^{N-1} W_{pq}(n).$$

Both of these functions are independent of the state of the system (i.e. the spin configuration of the lattice). We have the following identities for the function f_{pq}

$$f_{pp} = g_{pp} = 1, \qquad f_{p,Rq} f_{qp} = N k'^{(1-N)/N} w_{p,Rq} w_{qp}$$
$$g_{pq} g_{qp} = f_{pq} f_{qp} = N w_{pq} w_{qp} \frac{(x_p - x_q)(y_p - y_q)(t_p^N - t_q^N)}{(x_p^N - x_q^N)(y_p^N - y_q^N)(t_p - t_q)}.$$

4.3.1 Transfer matrices

As ever, we can choose the boundary spins of the lattice in a number of ways. If we identify the ith spin in the first (bottom) row of the lattice, $\sigma_i^{(1)}$, with the ith spin in the $2M+1$th (top) row of the lattice, $\sigma_i^{(2M+1)}$, for all columns i of the lattice, we have periodic boundary conditions in the vertical direction. Doing the same in the horizontal direction, imposing periodic boundary conditions from left to right, will give us toroidal boundary conditions on the lattice, which were the boundary conditions originally used to solve the model [24].

To calculate the interfacial tension, we are interested in imposing the skewed boundary conditions in the horizontal direction. In each row, the first and last spins, σ_1 and σ_{L+1}, are related by

$$\sigma_{L+1} = \sigma_1 - r, \tag{4.10}$$

where r, the "skew parameter," is an integer which we can without loss of generality restrict to the set $0, 1, \ldots, N-1$. With the choice $r = 0$, one regains normal periodic boundary conditions in the horizontal direction. We retain the periodic boundary conditions in the vertical direction.

The transfer matrices $\mathbf{T}$ and $\hat{\mathbf{T}}$ are defined in the usual way. Consider three consecutive rows of spins in the lattice, as indicated in the bottom three rows in

Figure 4.2. The spins in the lowest row are $\boldsymbol{\sigma} = \{\sigma_1, \sigma_2, \ldots, \sigma_{L+1}\}$, in the row above $\boldsymbol{\sigma}' = \{\sigma_1', \sigma_2', \ldots, \sigma_L'\}$, and in the third row, $\boldsymbol{\sigma}'' = \{\sigma_1'', \sigma_2'', \ldots, \sigma_{L+1}''\}$. The row-to-row transfer matrices $\mathbf{T}$ and $\hat{\mathbf{T}}$ are the $N^L \times N^L$ matrices with elements

$$\mathbf{T}_{\boldsymbol{\sigma}\boldsymbol{\sigma}'} = \prod_{j=1}^{L} W_{pq}(\sigma_j - \sigma_j')\bar{W}_{p'q}(\sigma_{j+1} - \sigma_j')$$

$$\hat{\mathbf{T}}_{\boldsymbol{\sigma}'\boldsymbol{\sigma}''} = \prod_{j=1}^{L} \bar{W}_{pq}(\sigma_j' - \sigma_j'')W_{p'q}(\sigma_j' - \sigma_{j+1}'') \tag{4.11}$$

where the spins σ_{L+1} and σ_{L+1}'' are given by (4.10). We will generally regard both p and p' as fixed, so the transfer matrices are matrix functions of the single variable q; this dependence is exhibited by the subscripts $\mathbf{T}_q$ and $\hat{\mathbf{T}}_q$. Indicating the dependence of the partition function on the skew parameter r, we have

$$Z_r = \text{trace}\left(\mathbf{T}_q\hat{\mathbf{T}}_q\right)^M. \tag{4.12}$$

The star-triangle relation (4.2) ensures the existence of a family of commuting transfer matrices, and the following commutation relations are derived in Reference [27],

$$\mathbf{T}_q\hat{\mathbf{T}}_s = (f_{p'q}f_{ps}/f_{pq}f_{p's})^L\,\mathbf{T}_s\hat{\mathbf{T}}_q \tag{4.13}$$

and

$$\hat{\mathbf{T}}_q\mathbf{T}_s = (f_{pq}f_{p's}/f_{p'q}f_{ps})^L\,\hat{\mathbf{T}}_s\mathbf{T}_q. \tag{4.14}$$

The spin-shift operator $\mathbf{X}$ is the $N^L \times N^L$ matrix with entries

$$\mathbf{X}_{\boldsymbol{\sigma},\boldsymbol{\sigma}'} = \prod_{j=1}^{L} \delta(\sigma_j, \sigma_{j+1}')$$

where the Kronecker-delta function is

$$\delta(a,b) = \begin{cases} 1 & \text{if } a = b \text{ modulo } N \\ 0 & \text{otherwise,} \end{cases}$$

and this commutes with the transfer matrices $\mathbf{T}_q$ and $\hat{\mathbf{T}}_q$,

$$\mathbf{X}\mathbf{T}_q = \mathbf{T}_q\mathbf{X} \quad \text{and} \quad \mathbf{X}\hat{\mathbf{T}}_q = \hat{\mathbf{T}}_q\mathbf{X}.$$

There are many identities satisfied by the transfer matrices which are derived and listed in [27], but we do not use any of these directly and so do not reproduce them here.

4.3.2 Diagonal representation

A consequence of the commutation relations (4.13) and (4.14) is that the matrices $\mathbf{T}_q$ and $\hat{\mathbf{T}}_q$ can be simultaneously diagonalised by the coupled similarity transformations

$$\mathbf{T}_q \to \mathbf{P}^{-1}\mathbf{T}_q\mathbf{Q}, \quad \hat{\mathbf{T}}_q \to \mathbf{Q}^{-1}\hat{\mathbf{T}}_q\mathbf{P}$$

where $\mathbf{P}$ and $\mathbf{Q}$ are "constant" matrices, independent of the vertical rapidity q. The "eigenvalues" and "eigenvectors" of $\mathbf{T}_q$ and $\hat{\mathbf{T}}_q$ are the solutions of the coupled vector equations

$$\mathbf{T}_q\mathbf{y} = T_q\mathbf{x}, \quad \hat{\mathbf{T}}_q\mathbf{x} = \hat{T}_q\mathbf{y}$$

where $\mathbf{x}$ and $\mathbf{y}$ are the eigenvectors, which are independent of q, and T_q and $\hat{T}_q$ are the corresponding eigenvalues.

The commutation property (4.13) also implies that the diagonalised transfer matrices are related by

$$\hat{\mathbf{T}}_q^{\mathrm{diag}} = (f_{pq}/f_{p'q})^L \, \mathbf{D}\, \mathbf{T}_q^{\mathrm{diag}} \tag{4.15}$$

where $\mathbf{D}$ is a diagonal matrix which is independent of q. For the homogeneous model, $p = p'$, this reduces to

$$\hat{\mathbf{T}}_q = \mathbf{T}_q\mathbf{S}_R = \mathbf{S}_R\mathbf{T}_q$$

where $\mathbf{S}_R$ is the spatial translation operator, with eigenvalues $2\pi i\ell_R/L$, $\ell_R = 0, 1, \ldots, L-1$ [1].

4.3.3 Physical model

The Boltzmann weights (4.3) of the integrable chiral Potts model are in general complex. For the lattice model to be physical, they must be real and positive; this is possible when we restrict the variables to a certain manifold. For the homogeneous model, if we choose the p and q variables x_p, y_p, x_q, y_q so they lie on the unit circle, and are arranged in the following order,

$$\arg(x_p) \le \arg(x_q) \le \arg(y_p) \le \arg(y_q) \le \arg(\omega x_p) \tag{4.16}$$

and

$$\arg(t_p) \le \arg(t_q) \le \arg(\omega t_p), \tag{4.17}$$

then the Boltzmann weights are real and positive, as required. This is particularly convenient for analysis as the Perron-Frobenius theorem can be applied to the transfer matrices.

For the spin chain, one is instead interested in the Hermitian case. This does not correspond to positive Boltzmann weights so the Perron-Frobenius theorem does not apply, and there is the possibility of ground state level crossing. The model is Hermitian when $u_p, u_{p'}, u_q - \pi/2N$ and $u_q - \pi/2N$ are all pure imaginary, $v_p, v_{p'}$ and μ_q are real, and $|\mu_p| = |\mu_{p'}| = 1$. Then $x_q, \omega^{-1/2} y_q, \omega^{1/2} t_q$ and λ_q are all real and positive, $\lambda_q > 1/k'$, $y_p = x_p^*$ and $\bar{W}_{pq}(-n) = W_{pq}(n)^*$ (similarly with $p \to p'$). Hence $\mathbf{T}_q$ is the Hermitian conjugate of $\hat{\mathbf{T}}_q$, so the transfer matrix $\mathbf{T}_q \hat{\mathbf{T}}_q$ is Hermitian, and its eigenvalues $T_q \hat{T}_q$ are real.

This Hermitian case intersects with the real one at the symmetric point $u_p = u_{p'} = 0$, $u_q = v_q = \pi/2N$.

The superintegrable model is discussed later in this chapter; analysis of this model is particularly simple for a number of reasons, but unfortunately the superintegrable model does not have a physical sub-case.

4.3.4 The interfacial tension

The interfacial tension has been defined earlier; we use the skewed boundary conditions to force an interface, but for an N-state model we also have to consider the possibility of interfacial wetting occurring [104], which we describe here.

For a lattice with toroidal (un-skewed) boundaries in each direction, at zero temperature, the system will order into one of N possible equi-likely ferromagnetic ground states, in which every spin in the lattice takes on the same value σ, for some $0 \leq \sigma \leq N-1$. This ferromagnetic ordering is completely consistent with the periodic boundaries, with the left-most and right-most spins in each row being related by $\sigma_1 = \sigma_{L+1}$.

However, when the skew parameter r is non-zero, the boundary conditions cease to be compatible with the completely ordered ferromagnetic ground state persisting throughout the system. Instead, the spins near the left-hand boundary of the lattice will all be in a state σ, while those near the other boundary will be in the state $\sigma - r$. Clearly there is a jump or a series of jumps in the values of the spins from left to right along the lattice, breaking the ferromagnetic ground state configuration.

Consider $r = 1$ first, so that down the left-hand boundary of the lattice the

spins take on some value σ, while down the right-hand boundary they take on the value $\sigma - 1$. Hence a completely ordered ferromagnetic ground state is no longer possible, and the favoured lowest-energy state consists of the system settling into two juxtaposed ferromagnetically ordered states, one adjoined to the left-hand boundary, in a phase σ, and the other adjoined to the right-hand boundary, in phase $\sigma - 1$. These are separated by an interface, across which the spins jump from σ to $\sigma - 1$. The interface may meander from left to right, especially as temperature is increased, but its mean direction will be approximately vertically down the lattice, as a result of the periodic boundary conditions in the vertical direction. There are L positions in each row of the lattice where the interface may occur.

We denote the resulting interfacial tension between phases σ and $\sigma - 1$, as ε_1. (Note that as a result of the chirality of the model, this is not equal to $\varepsilon_{-1} \equiv \varepsilon_{N-1}$, the interfacial tension due to an ordered $\sigma - 1$ phase on the left, and an ordered σ phase on the right of the interface.)

When $r = 2$, we have near the left-hand boundary of the lattice a ferromagnetically ordered phase in a state σ, and near the right-hand boundary of the lattice a similarly ordered phase, but in a state $\sigma - 2$. In between, there are a priori two possibilities. Either there is a single interface running down the lattice, across which the spins jump from σ to $\sigma - 2$, or else this interface breaks into two interfaces, with a phase $\sigma - 1$ interposed between the phases σ and $\sigma - 2$. In the former case, the interface will once again run approximately vertically down the lattice, and the corresponding interfacial tension is denoted as ε_2, corresponding to a jump from phase σ to phase $\sigma - 2$. In the latter case, the two interfaces will also run approximately vertically down the lattice, and as they meander from left to right, they can merge into a single interface, but not cross one another. The interface between the σ and the $\sigma - 1$ phases has interfacial tension ε_1, as does that of the interface between the $\sigma - 1$ and $\sigma - 2$ phases, and so the total interfacial tension of the two interfaces is $2\varepsilon_1$. In this case, the phase $\sigma - 1$ wets the $\sigma, \sigma - 2$ phases.

Whichever interfacial structure has lowest energy will preferentially occur, so the system will be in a wetting phase if $2\varepsilon_1 < \varepsilon_2$, and a non-wetting phase if $\varepsilon_2 < 2\varepsilon_1$. The special case $\varepsilon_2 = 2\varepsilon_1$ is called "superwetting," when either interface structure could occur with equal probability.

For $r > 2$, we have the obvious generalisation of the $r = 2$ case. There are spins in phase σ on the left-hand side of the lattice, in phase $\sigma - r$ to the right, but in between there are now a priori many possibilities.

The discussion for r non-zero has assumed thus far that the system is at zero temperature. We are most interested in the critical behaviour of the interfacial tensions, so have to consider what happens as k' increases. At non-zero temperatures, the phase we call σ will contain "mostly" spins with the value σ. Drops of overturned spins will typically begin to form, and the interfaces begin to meander more, form overhangs, and begin to widen and start to blur. The interfacial structure persists until the order-disorder transition at $k' = 1$. The system has a phase transition to a completely disordered state, in which the different phases are no longer distinguishable from one another, and the interfacial tension vanishes.

Below the critical temperature, the interfacial tensions are defined as usual. For large L and M, the partition function (4.12) grows as

$$Z_r \sim \exp\left[(-2LM\psi - M\varepsilon_r)/k_BT\right] \tag{4.18}$$

where ψ is the free energy per site in the thermodynamic limit, defined as

$$-\psi/k_BT = \lim_{L,M\to\infty} (2LM)^{-1} \ln Z_r \tag{4.19}$$

and the interfacial tension per unit length between phases σ and $\sigma - r$ is defined as

$$-\varepsilon_r/k_BT = \lim_{L,M\to\infty} M^{-1} \ln (Z_r/Z_0). \tag{4.20}$$

We only calculate the interfacial tensions in the horizontal direction (or the diagonal direction for the lattice oriented as in Figure 1.1). In Reference [10], Au-Yang and Perk note the anisotropy of the interfacial tensions of the chiral clock models. In particular, the diagonal interfaces will wet at zero temperature, whereas the horizontal interface will only wet at zero temperature for the symmetric model.

The interfacial tension is usually expected to become isotropic in the scaling region, which implies that the critical exponent μ is independent of direction. This is in contrast to the non-physical superintegrable model, which Baxter found to violate critical isotropy [26], producing different critical exponents for the interfacial tension in the horizontal and vertical directions.

4.3.5 The functional relations

The transfer matrices satisfy a set of functional relations, which define the matrices' eigenvalues, and hence the partition function, completely. The functional relations involve a family of associated matrices, denoted $\tau_j(t_q)$, $j = 0, 1, \ldots, N$,

the elements of which are polynomials in the single variable t_q with degree at most $(j-1)L$.

We use the following notation; for m and n integers, and x and y complex numbers,

$$(x,\, y)_{m,n} = \begin{cases} \prod_{j=m+1}^{n} (x - \omega^j y), & n \geq m \\ \prod_{j=n+1}^{m} (x - \omega^j y)^{-1}, & n \leq m, \end{cases}$$

and define the following functions, for all integers j, k and l, where $j = k + l$,

$$\Lambda_q^{(k,l)} = \left[\frac{(y_p,\, x_q)_{0,l-1} (y_q,\, x_p)_{-k,0} (y_q,\, y_{p'})_{0,N-k-1}}{N \mu_p^{-k} \mu_{p'}^{l} (x_{p'},\, x_q)_{-1,l-1}} \right]^L \tag{4.21}$$

$$H_{pq}^{(j)} = \left[\omega^j \mu_p^j (t_p,\, t_q)_{-1,j-1} / (y_p^N - x_q^N) \right]^L \tag{4.22}$$

$$\bar{H}_{p'q}^{(j)} = \left[\mu_{p'}^{-j} (t_{p'},\, t_q)_{j-1,N-1} / (x_{p'}^N - x_q^N) \right]^L. \tag{4.23}$$

Define the matrix $\boldsymbol{\Xi}_q^{(j)}$ as

$$\boldsymbol{\Xi}_q^{(j)} = \omega^{rk} \Lambda_q^{(k,l)} \mathbf{X}^k \hat{\mathbf{T}}_{\bar{q}kl} \tag{4.24}$$

where $\hat{\mathbf{T}}_{\bar{q}kl} = \hat{\mathbf{T}}(\omega^k y_q, \omega^j x_q, \mu_q^{-1})$. It is shown in [30] that $\boldsymbol{\Xi}_q^{(j)}$ depends on the integers k and l only through the sum $j = k + l$. We then have the functional relation

$$\mathbf{T}_q \boldsymbol{\Xi}_q^{(j)} = \bar{H}_{p'q}^{(j)} \boldsymbol{\tau}_j(t_q) + \omega^{jr} \mathbf{X}^j H_{pq}^{(j)} \boldsymbol{\tau}_{N-j}(\omega^j t_q). \tag{4.25}$$

The matrices $\boldsymbol{\tau}_j(t_q)$ in this equation are defined iteratively as follows. First, define the functions

$$z(t_q) = [\omega \mu_p \mu_{p'} (t_p - t_q)(t_{p'} - t_q)]^L \tag{4.26}$$

$$\alpha_q = [\lambda_q (y_p^N - x_q^N)(y_{p'}^N - x_q^N)/k']^L \tag{4.27}$$

$$\bar{\alpha}_q = [\lambda_q^{-1} (y_p^N - y_q^N)(y_{p'}^N - y_q^N)/k']^L \tag{4.28}$$

where we can write

$$\alpha_q = \left[k'(1 - \lambda_p \lambda_q)(1 - \lambda_{p'} \lambda_q) \,/\, k^2 \lambda_q \right]^L$$

$$\bar{\alpha}_q = \left[k'(\lambda_q - \lambda_p)(\lambda_q - \lambda_{p'}) \,/\, k^2 \lambda_q \right]^L,$$

so if we write $\alpha_q = \alpha(\lambda_q)$, then $\bar{\alpha}_q = \alpha(1/\lambda_q)$. We also have the relation

$$z(t_q) z(\omega t_q) \cdots z(\omega^{N-1} t_q) = \alpha_q \bar{\alpha}_q. \tag{4.29}$$

The matrices $\boldsymbol{\tau}_j(t_q)$ satisfy the recurrence relations

$$\boldsymbol{\tau}_0(t_q) = 0, \quad \boldsymbol{\tau}_1(t_q) = \mathbf{I}$$

$$\boldsymbol{\tau}_j(t_q)\,\boldsymbol{\tau}_2(\omega^{j-1}t_q) = z(\omega^{j-1}t_q)\,\omega^r\,\mathbf{X}\,\boldsymbol{\tau}_{j-1}(t_q) + \boldsymbol{\tau}_{j+1}(t_q) \tag{4.30}$$

$$\boldsymbol{\tau}_j(\omega t_q)\,\boldsymbol{\tau}_2(t_q) = z(\omega t_q)\,\omega^r\,\mathbf{X}\,\boldsymbol{\tau}_{j-1}(\omega^2 t_q) + \boldsymbol{\tau}_{j+1}(t_q) \tag{4.31}$$

$$\boldsymbol{\tau}_{N+1}(t_q) = z(t_q)\,\omega^r\,\mathbf{X}\,\boldsymbol{\tau}_{N-1}(\omega t_q) + (\alpha_q + \bar{\alpha}_q)\mathbf{I} \tag{4.32}$$

where (4.30) and (4.31) are equivalent. Finally, we have the following relation between the matrices $\mathbf{T}(x_q, y_q, \mu_q)$ and $\boldsymbol{\tau}_2(t_q)$;

$$\begin{aligned}\boldsymbol{\tau}_2(t_q)\mathbf{T}(x_q,\,\omega y_q,\,\mu_q) \;&=\; \omega^r\mathbf{X}\left[\frac{\omega\mu_p\mu_{p'}(x_p - y_q)(t_{p'} - t_q)}{y_{p'} - y_q}\right]^L \mathbf{T}(x_q,\,y_q,\,\mu_q)\\ &+\; \left[\frac{(y_{p'} - \omega y_q)(t_p - \omega t_q)}{x_p - \omega y_q}\right]^L \mathbf{T}(x_q,\,\omega^2 y_q,\,\mu_q).\end{aligned} \tag{4.33}$$

In Reference [30], the Boltzmann weights are re-parameterised for the real manifold, and these functional relations are put into an explicitly real form. We do not make use of this, but it demonstrates that when the Boltzmann weights are real, i.e. when the p and q variables lie on the unit circle and are arranged as in (4.16) and (4.17), the functional relations and transfer matrices are explicitly real also.

Finally, we have the matrix $\mathbf{S}(x_q, y_q, \mu_q)$

$$\mathbf{S}(x_q, y_q, \mu_q) = c\left(x_p^N - y_q^N\right)^{(N-1)L} \prod_{j=1}^{N-1}\left(\frac{y_{p'} - \omega^j y_q}{x_p - \omega^j y_q}\right)^{jL} \prod_{j=0}^{N-1} \mathbf{T}(\omega^j x_q,\, y_q) \tag{4.34}$$

where c is the q-independent constant $c = N^{-NL/2}(\lambda_p\lambda_{p'})^{(N-1)L/4}$. In References [28] and [29] it is shown that the matrix elements of $\mathbf{S}(x_q, y_q)$ are polynomials in the single variable λ_q with degree at most $(N-1)L$, so one can write $\mathbf{S}(\lambda_q) = \mathbf{S}(x_q, y_q, \mu_q)$. Hence the elements of the matrix $\hat{\mathbf{S}}(\lambda_q)$, defined by

$$\hat{\mathbf{S}}(\lambda_q) = \lambda_q^{(N-1)L}\mathbf{S}(1/\lambda_q) \tag{4.35}$$

will be polynomials in the single variable λ_q of degree at most $(N-1)L$. Explicitly, we have

$$\hat{\mathbf{S}}(\lambda_q) = c\,\lambda_q^{(N-1)L}\left(x_{p'}^N - x_q^N\right)^{(N-1)L} \prod_{j=1}^{N-1}\left(\frac{y_p - \omega^j x_q}{x_{p'} - \omega^j x_q}\right)^{jL} \prod_{j=0}^{N-1} \hat{\mathbf{T}}(\omega^j y_q,\, x_q). \tag{4.36}$$

The matrix $\hat{\mathbf{S}}(\lambda_q)$ commutes with $\mathbf{T}_q$, and hence the eigenvalues of $\hat{\mathbf{S}}(\lambda_q)$ are also polynomials in λ_q with degree at most $(N-1)L$.

The matrices $\boldsymbol{\tau}_j(t_q)$, $j = 2, \ldots, N$, and the matrices $\mathbf{S}(\lambda_q)$ and $\hat{\mathbf{S}}(\lambda_q)$ are diagonalised by the same similarity transformation which diagonalises the transfer matrices. This leads us to a notational simplification. If we let $\tau_j(t_q)$ represent an eigenvalue of the matrix $\boldsymbol{\tau}_j(t_q)$, then post-multiplying the functional relations of the previous subsection by the appropriate eigenvectors $\mathbf{x}$ or $\mathbf{y}$ will effectively replace the matrices by their corresponding eigenvalues. Hence we can re-write all of these equations in terms of the corresponding eigenvalues, and it is the relations between the eigenvalues which we will solve, in particular for the numerically largest eigenvalue(s) of $\mathbf{T}_q\hat{\mathbf{T}}_q$.

The functional relations for the model with skewed boundary conditions are very closely related to the relations for the model with toroidal boundaries. The only difference is to replace the spin-shift operator X everywhere by $\omega^r X$. Thus the functional relations have the same set of solutions, but a different set are chosen for the model with skewed boundaries.

We now summarise the exact results for the free energy of the model.

4.3.6 Free energy

The free energy of the chiral Potts model was first derived by Baxter in Reference [24], and is given by equations (5.37), (5.10), (5.18), (5.5), (4.13), (4.12), (3.45), (3.46), (3.44), (3.41) and (3.42) of this reference. The final result is too complicated to include in full. The derivation does not depend on the functional relations of Section 4.3.5, but rather adapted the "399th" solution of the Ising model [17]. Basically, the star-triangle relation implies certain functional relations for the free energy and correlations of the chiral Potts model, which can be solved, although the results can be extremely complicated. We include the free energy of the model in the scaling region, i.e. the limit $k \to 0$ ($k' \to 1$); in this limit, the difference property is restored, and the inversion relation [20] can be used to calculate the free energy. Letting $u = u_q - u_p$, the free energy per site on a square lattice is

$$-\Psi_{pq} = \int_0^\infty \frac{\text{sh } ux \text{ sh } (\pi - u)x \text{ sh } (N-1)\pi x}{x \text{ ch}^2 \pi x \text{ ch } N\pi x}\, dx \\ -\frac{N-1}{2N\pi} k^2 (u_q - u_p)\cos(u_p + u_q) + O(k^{2+4/N}),$$

and, as the reduced temperature is proportional to k^2 for small k, we have as the specific heat critical exponent $\alpha = 1 - 2/N$. At criticality, $k \to 0$, this is exactly the free energy of the Fateev-Zamolodchikov model [50].

A more compact way of writing the free energy can be found by solving the functional relations of the transfer matrices. Exactly how this is done will be the subject of the following chapter. The results will be stated here.

The free energy is defined terms of the following functions [29]. Let $|\lambda_p|,|\lambda_q| < 1$ and $-2\pi/N < \arg(t_p), \arg(t_q) < 0$. We define

$$A_{pq} = \frac{1}{2\pi}\int_0^{2\pi} \frac{1+\lambda_p e^{i\theta}}{1-\lambda_p e^{i\theta}} \sum_{j=1}^{N-1} (N-j) \ln\left[\omega^{-j/2}\Delta(\theta) - \omega^{j/2} t_q\right] d\theta, \tag{4.37}$$

$$\begin{aligned} B_{pq} &= \frac{1}{8\pi^2}\int_0^{2\pi}\int_0^{2\pi} \frac{1+\lambda_p e^{i\theta}}{1-\lambda_p e^{i\theta}} \frac{1+\lambda_q e^{i\phi}}{1-\lambda_q e^{i\phi}} \\ &\times \sum_{j=1}^{N-1} (N-2j) \ln\left[\omega^{-j/2}\Delta(\theta) - \omega^{j/2}\Delta(\phi)\right] d\theta d\phi, \end{aligned} \tag{4.38}$$

and

$$C_{pq} = \frac{1}{2\pi}\int_0^{2\pi} \frac{1+\lambda_p e^{i\theta}}{1-\lambda_p e^{i\theta}} \sum_{j=1}^{N-1} j \ln\left[\omega^{-j/2}\Delta(\theta) - \omega^{j/2} t_q\right] d\theta,$$

where the function $\Delta(\theta)$ is

$$\Delta(\theta) = \left[(1+k'^2 - 2k'\cos\theta)/k^2\right]^{1/N}$$

and we choose $\Delta(\theta)$ real when θ is real.

These functions can be analytically continued outside the stated domains, and we are especially interested in the continuation to $|\lambda_q| > 1$ and $0 < \arg(t_q) < 2\pi/N$. (This is equivalent to applying the automorphism R of equation (4.9).) The function A_{pq} does not depend explicitly on λ_q, and can trivially be analytically continued as t_q passes through unity. The function A_{qp} is slightly more complex, as it depends explicitly on λ_q. We derive the analytical continuation formula for A_{qp} by substituting $\lambda = e^{i\theta}$ and writing the integral as a contour integral around the unit circle in the λ-plane. Deforming the contours as λ_q crosses the unit circle, we can write the analytical continuation formula

$$A_{ac}(\lambda_q, t_p) = -A(1/\lambda_q, t_p) + 2\sum_{j=1}^{N-1} (N-j) \ln\left(\omega^{-j/2} t_q - \omega^{j/2} t_p\right). \tag{4.39}$$

Doing the same for $B_{pq} = B(\lambda_p, \lambda_q)$, we find

$$B_{ac}(\lambda_p, \lambda_q) = -B(\lambda_p, 1/\lambda_q) + A(\lambda_p, t_q) - C(\lambda_p, t_q). \tag{4.40}$$

In [29], Baxter calculates the maximum eigenvalue of $\mathbf{T}_q\hat{\mathbf{T}}_q$ when $r = 0$, i.e. when toroidal boundary conditions are applied to the lattice. The expression there derived for the homogeneous model, $p = p'$, is valid for $|\lambda_p|, |\lambda_q| < 1$ and $-2\pi/N < \arg(t_p), \arg(t_q) < 0$, the maximum eigenvalue being

$$N \ln(T_q\hat{T}_q) = 2L\left(N \ln g_{pq} + \tfrac{1}{2}(N-1)\ln(\lambda_q/\lambda_p) + A_{pq} - A_{qp} - B_{pq}\right) \quad (4.41)$$

which implies that the free energy per site ψ is

$$-N\psi/k_BT = N \ln g_{pq} + \tfrac{1}{2}(N-1)\ln(\lambda_q/\lambda_p) + A_{pq} - A_{qp} - B_{pq}.$$

When $|\lambda_q| > 1$, the eigenvalue $T_q\hat{T}_q$ will be given by (4.41), but with the integrals A and B replaced by their analytic continuations; we have for $|\lambda_q| > 1$

$$N \ln(T_q\hat{T}_q) = 2LE_{pq} \quad (4.42)$$

where

$$\begin{aligned} E_{pq} &= N \ln g_{pq} + \tfrac{1}{2}(N-1)\ln(\lambda_q/\lambda_p) + A(\lambda_q^{-1}, t_p) + C(\lambda_p, t_q) + B(\lambda_p, \lambda_q^{-1}) \\ &- 2\sum_{j=1}^{N-1}(N-j)\ln\left[\omega^{-j/2}t_q - \omega^{j/2}t_p\right], \end{aligned} \quad (4.43)$$

so the free energy is

$$-N\psi/k_BT = E_{pq}. \quad (4.44)$$

For the alternating model, which we consider in the following chapter, we find the free energy to be simply $\frac{1}{2}(E_{pq} + E_{p'q})$, as expected from Z-invariance. We derive these results directly for $|\lambda_q| > 1$ in the following chapter, and our results agree with the analytical continuation of Baxter's earlier calculation.

Calculating the free energy using the functional relations is much simpler than the method used in the original calculation. In References [28,29] the free energy above is put into a form which is more useful in the scaling region; one finds the same specific heat critical exponent, and the ensuing expression for the free energy reduces to that of the Fateev-Zamolodchikov model once more [34].

4.3.7 Z-invariance and the interfacial tensions

Consider a fully inhomogeneous model, with the column rapidity variables taking the values $p_1, p_2, \ldots, p_{2L}$. It follows from equation (4.20) that the interfacial

tension is invariant under any permutation of these rapidity variables, being a ratio of two Z-invariant partition functions.

Provided L is large enough, a single interface, separating spins in the two different phases, is not expected to pass through every column of the lattice; the vertical periodic boundary conditions ensure that the interface begins and ends in the same column of the lattice, and energetic considerations will suppress it from wandering too far to the left or to the right. Using Z-invariance arguments almost identical to those used in Section 5 of Reference [18], one can show that the interfacial tension can depend only on the rapidity variables of the rapidity lines through which the interface passes, and is completely independent of the other rapidity variables.

Hence the interfacial tension must be independent of all of the vertical rapidity variables $p_1, p_2, \ldots, p_{2L}$. Thus the interfacial tension of the fully inhomogeneous model must be the same as that of the alternating model, with rapidities $p, p', p, p', \ldots$, and also the same as that of the fully homogeneous model, with all vertical rapidities equal to the common value p.

Also, the interfacial tension of the physical chiral Potts model should be the same as the interfacial tension of the superintegrable model, which corresponds to a particular choice of the alternating vertical rapidities. This observation, pointed out in [30], simplifies the calculation of the interfacial tension. At the superintegrable point, the functional relations for the transfer matrices simplify, greatly facilitating their solution. An ansatz for the eigenvalues T_q is proposed in References [3] and [44], which is shown to follow directly from the functional relations in Reference [30]. The ansatz is then generalised to the alternating model with skewed boundary conditions. As a result, the simplest method of calculating the interfacial tension of the physical chiral Potts model should be to calculate the interfacial tension of the superintegrable chiral Potts, and to use Z-invariance to argue that the quantity is the same for the two models.

There is however a potential flaw in this argument. The superintegrable chiral Potts model is a non-physical model, in that its Boltzmann weights are in general complex. The Z-invariance argument may not hold for a system with non-positive Boltzmann weights; for such models, the interfacial tension (as well as other quantities such as local correlation functions) may be sensitive to the boundary conditions imposed on the lattice. This is demonstrated explicitly for the chiral Potts model in References [26, 32], where the interfacial tensions are calculated for the model with two different kinds of boundary condition; this yields different expressions,

and different critical exponents. These calculations are summarised in the next section. For a physical model, the interfacial tension should be independent of the boundary conditions, and the discrepancy can only be due to the non-positivity of the Boltzmann weights. Due to this unphysical behaviour, it is not clear that the results of the superintegrable model can be reliably applied to the physical case; a direct calculation of the interfacial tension is certainly desirable.

4.4 The superintegrable chiral Potts model

The most extensively studied case of the chiral Potts model is the so-called superintegrable model. This corresponds to the alternating column rapidity variables satisfying

$$x_{p'} = y_p, \quad y_{p'} = x_p, \quad \text{and} \quad \mu_{p'} = \mu_p^{-1}. \tag{4.45}$$

This choice of variables simplifies the functional relations. It has a Hermitian subcase, and so is important in the theory of the chiral Potts quantum spin chain. Unfortunately, the choice of vertical rapidities excludes the possibility of positive Boltzmann weights, so the lattice model is not of direct physical interest.

We summarise the two calculations of the interfacial tension of the superintegrable model.

4.4.1 Cylindrical boundary conditions

We summarise the work of References [1, 23, 26]. For the homogeneous superintegrable model, $x_p = y_p = x_{p'} = y_{p'} = 1$, it was shown in References [1, 23] that the row-to-row transfer matrix has a set S of eigenvalues which have a particularly simple form; if the largest eigenvalue of $\mathbf{T}$ is contained in S the bulk free energy is easily calculated. In [2] it is shown that for toroidal boundary conditions the largest eigenvalue is not contained in S, but in [23, 26] it was commented that if fixed spin boundary conditions are placed at the top and bottom rows of the lattice, and periodic boundary conditions are imposed from left to right, then only eigenvalues in S can contribute to the partition function. Such a lattice is illustrated in Figure 4.3. In [26], the partition function on such a lattice, with finite but arbitrary size, is calculated exactly, and from its asymptotic behaviour is calculated the bulk free energy per site, surface free energy per unit length due to the fixed and free bound-

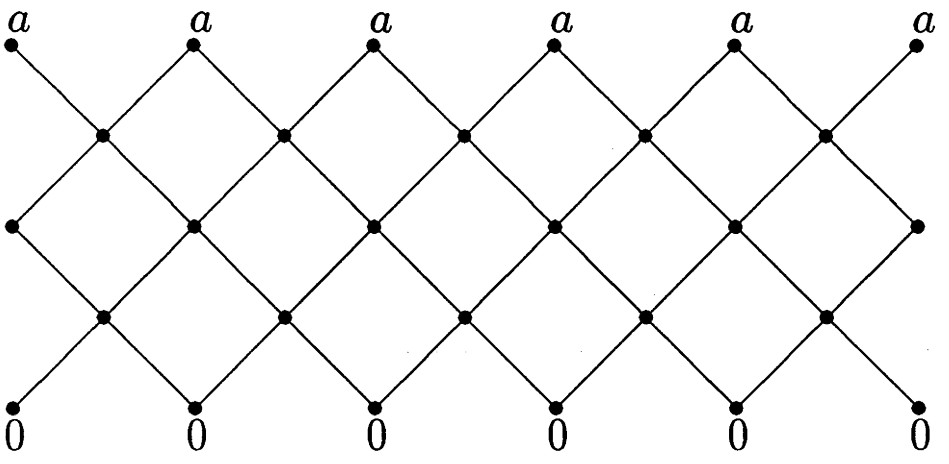

Figure 4.3: The square lattice with periodic boundary conditions horizontally, but with fixed boundary conditions vertically; with all spins being 0 on the bottom row and all spins being a on the top row, where $0 \leq a \leq N-1$.

ary conditions, correlation lengths and interfacial tensions per unit length in both the vertical and horizontal directions, along with the associated critical exponents.

When $k' < 1$, for large L and M, the partition function Z_a should grow as

$$\ln Z_a = -2LMf - 2L(2f_s + s_a) + \cdots$$

where f is the free energy per site, f_s is the surface free energy due to the fixed-spin top and bottom boundary conditions, and s_a is the horizontal interfacial tension between ferromagnetically ordered phases 0 and a. We have omitted an entropic term as well as other terms that are exponentially smaller, and are used to calculate the horizontal and vertical correlation lengths. Expressions for these quantities are given in [26], and we do not reproduce them here. We do remark that the interfacial tensions thus calculated indicate that in this model, wetting becomes favourable when N is sufficiently large. The critical exponents are calculated in [26];

$$\alpha = 1 - 2/N, \quad \alpha_s = 2 - 2/N, \quad \mu_{\rm hor} = \nu_{\rm hor} = 2/N, \quad \mu_{\rm vert} = \nu_{\rm vert} = 1.$$

It is unexpected to find that the critical exponents can depend on direction, as these do; the interfacial tensions and correlation lengths are usually expected to become isotropic in the scaling region. The hyperscaling relation $d\nu = 2 - \alpha$ is violated in this case, and the directional dependence of the exponents can only be a result of

the different boundary conditions in the different directions and the non-positivity of the Boltzmann weights.

4.4.2 Skew-periodic boundary conditions

In [30] the functional relations for the transfer matrices of the chiral Potts model are re-derived for the case of skewed boundary conditions, and the interfacial tension is then calculated in the low temperature limit. This result agrees with the expectation from Z-invariance that the interfacial tensions in the vertical direction should be independent of the vertical rapidities p and p', and also indicates that the physical model should be non-wetting in the $k' \to 0$ limit.

Hence Baxter concludes in [30] that the interfacial tensions of the superintegrable chiral Potts model, with vertical rapidities given by (4.45), should be the same as the interfacial tension of the physical model.

In [32] the partition function is calculated for the lattice with cyclic boundary conditions from top to bottom, and skewed boundaries from left to right, the same boundary conditions as used in [30], and also in our calculation of the physical model [96].

In Reference [32], a set of L largest eigenvalues of $\mathbf{T}_q\hat{\mathbf{T}}_q$ is determined, from which the free energy and interfacial tension are calculated. These eigenvalues are of the form

$$\ln(T_q\hat{T}_q) = -2Lf/k_BT - 2v_r \tag{4.46}$$

where f is the free energy per site of the superintegrable model, and the function v_r is given by

$$v_r = r\ln\mu_q - \ln A(\omega^{-1/2}mt_q) + \tfrac{1}{2}\ln h(\eta m) + m\int_\eta^{1/\eta} \frac{h'(my)}{\pi h(my)}\Psi(\lambda_q, y)dy \tag{4.47}$$

where the functions $A(t)$, $h(t)$ and $\Psi(\lambda, t)$ are

$$A(t) = \prod_{j=1}^{r}\left(1+\omega^{j-(r+1)/2}t\right) \tag{4.48}$$

$$h(t) = A(\omega^{-1/2}t)A(\omega^{1/2}t) \tag{4.49}$$

and

$$\Psi(\lambda,t)=\tan^{-1}\left[\frac{\lambda-1}{\lambda+1}\left(\frac{\eta^{-N}-t^N}{t^N-\eta^N}\right)^{1/2}\right] \tag{4.50}$$

when $\eta < t < \eta^{-1}$. The eigenvalues depend on the complex number $m = s/t_p$, where s is one of the L solutions to

$$\left(\frac{\omega^{r/2}s+1}{\omega^{-r/2}s+1}\right)^L=\omega^{-Qr},$$

different values of s corresponding to different eigenvalues of $\mathbf{T}_q\hat{\mathbf{T}}_q$. The free energy is independent of r, so when L is large one can write

$$Z_r/Z_0=\sum e^{-2Mv_r}$$

where the sum, originally over the N^L eigenvalues of $\mathbf{T}_q\hat{\mathbf{T}}_q$, is approximated exponentially well by restricting the sum to the L largest eigenvalues defined by the L possible values of s. As $L\to\infty$, the values of s form a dense distribution over the positive real axis, so

$$Z_r/Z_0=L\int_0^\infty R(s)e^{-2Mv_r}ds$$

where the distribution function $R(s)$ is independent of L and M. To calculate this integral as $M\to\infty$, one uses the saddle point method, deforming the contour of integration to pass through the saddle point of v_r in the complex s plane, giving for the interfacial tension

$$\epsilon_r/k_BT=2\,(v_r)_{\text{saddle}} \tag{4.51}$$

where by $(v_r)_{\text{saddle}}$ we mean equation (4.47) evaluated at its saddle point in the complex s-plane.

By arguments given in the preceding paragraphs, this is expected to be the interfacial tension not only of the superintegrable chiral Potts model, but also of the physical model. Baxter [30] argues that this formula should be valid all the way up to the order-disorder transition at $k'=1$, even though the superintegrable model seems to have an earlier transition to an incommensurate phase [2, 4, 65]. This is because this result is expected to be valid for sufficiently small k', and there should be no non-analyticities in the result for the physical model as k' approaches the critical value $k'=1$.

4.5 Results and discussion

Our calculation for the chiral Potts model in its physical regime, which makes no such Z-invariance assumptions, is presented in the following chapter. We conclude that the interfacial tension of the physical model is indeed given by equation (4.51). We quote some further results based on this due to Au-Yang and Perk [10]. They write the low-temperature interfacial tension in a new form, and consider the symmetric model, where the interfacial tension simplifies significantly; the symmetric point corresponds to $t_q = \omega^{1/2}$, $(\lambda_q - 1)/(\lambda_q + 1) = \eta^{N/2}$, $t_p = 1$; the saddle point occurs when $s = 1$, and the interfacial tension becomes, from [10],

$$\varepsilon_r/k_BT = \frac{8}{\pi}\int_0^\eta dy \frac{\sin(\pi r/N)}{1 + 2y\cos(\pi r/N) + y^2} \tan^{-1}\left(\frac{\eta^N - y^N}{1 - \eta^N y^N}\right)^{1/2}. \qquad (4.52)$$

In the scaling region, this can be expanded as a series of beta functions [10,32]

$$\begin{aligned}\varepsilon_r/k_BT &= \frac{8B(1/N,1/2)}{\pi(N+2)}\sin(\pi r/N)\eta^{N/2+1} \\ &- \frac{8B(2/N,1/2)}{\pi(N+4)}\sin(2\pi r/N)\eta^{N/2+2} + O(\eta^{N/2+3}),\end{aligned}$$

and so the interfacial tension scales as

$$\varepsilon_r \sim |t|^{1/2+1/N} S(|t|^{1/N})$$

which implies that the critical exponent is

$$\mu = \frac{1}{2} + \frac{1}{N}.$$

The crossover exponent was calculated by Au-Yang and Perk [10]. It is defined by the scaling law in equation (4.1) for the $N = 3$ model; for general N, it is assumed that there is a single relevant chiral field Δ_1, and then in the scaling region of the integrable model, for k small, we have $t \sim k^2$ and $t \sim \Delta_1^2$ for small Δ_1, which implies that the crossover exponent is

$$\phi = \frac{1}{2} - \frac{1}{N}.$$

The crossover exponent is therefore positive when $N > 2$, and the chiral symmetry breaking field in the three state chiral clock model is relevant, with crossover exponent $\phi = 1/6$, which is consistent with Huse et al. [63].

Finally, in both the low-temperature and scaling limits, the interfacial tensions satisfy the inequality $\epsilon_j < \epsilon_k + \epsilon_l$ where $j = k + l \bmod N$. Hence in both of these limits the system is non-wetting, and is presumably so in the entire sub-critical region $0 < k' < 1$.

4.5.1 Excitations in the spectrum of $\mathbf{T}_q$

Excitations of the chiral Potts transfer matrix have been considered by McCoy and Roan [75, 91, 92], in terms of the excitations of the associated quantum spin chain. This is a quantum mechanical model which has a Hamiltonian which commutes with the chiral Potts transfer matrix.

McCoy [92] and McCoy and Roan [91] calculate the ground state and excitations of this spin chain Hamiltonian, in the thermodynamic limit, by solving the corresponding classical lattice model, and then finding the eigenvalues of $\mathcal{H}$, which are related to the eigenvalues of the transfer matrix of the classical lattice model $T(x_q, y_q)$ by

$$E = 2Nkt_p^{N/2}\lambda_p \frac{\partial}{\partial \lambda} \ln \left(T(x_q, y_q)/f_{pq}^L \right) \Big|_{\lambda=\lambda_p} + \text{const.}$$

The additive constant is the same for all eigenvalues.

McCoy and Roan find the eigenvalues of the transfer matrix are of the form (4.46), i.e.

$$\ln T_q = v_{m_p} + \text{ground state terms}$$

where the bulk terms are given in References [91, 92], and the excitations depend on the function

$$\begin{aligned} v_{m_p} &= \zeta_p' - m_p \ln \mu_q - \ln f(-\omega^{-1/2} t_q) \\ &\quad - \frac{1}{4\pi i} \oint_{\mathcal{C}_\lambda} \frac{d\lambda'}{\lambda'} \frac{\lambda' + \lambda_q^{-1}}{\lambda' - \lambda_q^{-1}} \ln \left[f(-\omega^{1/2} t') f(-\omega^{-1/2} t') \right] \end{aligned} \tag{4.53}$$

where the contour $\mathcal{C}_\lambda$ traverses the unit circle in the positive (anti-clockwise) direction, ζ_p' is a q-independent normalisation constant, and $f(t)$ is the polynomial

$$f(t) = \prod_{j=1}^{m_p} (1 + t v_j),$$

and the numbers v_j can be expressed as solutions to a set of Bethe ansatz-type equations.

The function v_{m_p} is very similar to our function v_r. In fact, analytically continuing our result to the region $|\lambda_q| < 1$ (which we describe in Subection 5.5.1 of the following chapter), we find that our band of L largest eigenvalues agrees with McCoy's excitations exactly when $m_p = r$.

This comparison is interesting because McCoy and Roan's result is based on an assumption of the dominant behaviour of the polynomials $\tau_2(t_q)$ corresponding to excitations of the transfer matrix, writing

$$\tau_2(t_q) = h^+(t_q)\frac{f(\omega^{\gamma-1}t_q)}{f(\omega^{\gamma}t_q)} + \omega^Q h^-(\omega t_q)\frac{f(\omega^{\gamma+1}t_q)}{f(\omega^{\gamma}t_q)} \tag{4.54}$$

where $h^+(t)$ and $h^-(t)$ are known functions (expressed as integral formulae) given in [92]. For the superintegrable model, this expression is explicitly a polynomial, but for the more interesting Hermitian and physical cases, it is not. McCoy and Roan assert without justifiaction that this form for $\tau_2(t_q)$ is still correct for these cases in the limit $L \to \infty$, and that for finite L the expression is correct up to subdominant terms, which make the expression for $\tau_2(t_q)$ explicitly a polynomial, and which vanish sufficiently fast as $L \to \infty$.

CHAPTER 5

Calculation of the interfacial tension of the chiral Potts model

In this chapter, we present our calculation of the free energy and interfacial tension of the chiral Potts model. All of our results have been presented in the previous chapter, and in this chapter we include many details that were omitted from the calculation published in Reference [96].

The format is as follows. In Sections 5.1 and 5.2, we define the low temperature limit that we consider, and then review the work of Baxter in References [30, 31]. We then consider the functional relations for the periodic boundary conditions, and determine the polynomials $\tau_j(t_q)$ which correspond to the maximum eigenvalue of the transfer matrix. Subsection 5.3.4 considers the effect of skewing the boundary conditions, and the results for the low temperature limit are summarised at the end of Subsection 5.3.7, before an expression for the desired eigenvalues of the matrix $\boldsymbol{\tau}_2(t_q)$ is derived for arbitrary sub-critical temperatures, equations (5.25) and (5.28).

In the following sections, the required eigenvalues of the matrix $\hat{\mathbf{S}}(\lambda_q)$ are derived, given by equations (5.36) and (5.37), after first considering the low-temperature limit.

Then in the final section, the free energy and interfacial tension, which we have presented in the previous chapter, are derived.

5.1 The low-temperature limit

The low-temperature limit of the chiral Potts model has been considered in References [28–31]. We consider the same low temperature limit as that used in References [30] and [31], and note that this is different from the limit considered in

References [28] and [29].

When we take the limit $k' \to 0$, from equations (4.5), provided that $|\lambda_p|$ and $|\lambda_{p'}|$ are both larger than k', then x_p^N and $x_{p'}^N \to 1$ as $k' \to 0$, so we can choose $x_p, x_{p'} \to 1$ as $k' \to 0$. Further, if $|\lambda_p|$ and $|\lambda_{p'}|$ are smaller than $1/k'$, certainly if they are smaller than unity, we have y_p^N and $y_{p'}^N \to 1$ as $k' \to 0$, so we can also choose $y_p, y_{p'} \to 1$, and hence $t_p, t_{p'} \to 1$. Correspondingly, if $|\lambda_q|$ is greater than k', we can choose $x_q \to 1$ as $k' \to 0$, and if $|\lambda_q|$ is sufficiently greater than unity, then we can keep y_q different from unity, i.e. as a free variable. We then have $t_q = y_q$, and are free to choose $0 < \arg(t_q) < 2\pi/N$.

In summary; we take $k' \to 0$, with $x_p, x_{p'}, x_q, y_p, y_{p'} \to 1$, while $t_q = y_q$ is a variable. For a physical model, we are interested in t_q on the unit circle, $t_q = e^{2iu_q}$, where $0 < u_q < \pi/N$. We also have $k' < |\lambda_p|, |\lambda_{p'}| < 1$, and $1 \ll |\lambda_q| < 1/k'$.

With these choices, in the zero temperature limit the Boltzmann weights (4.3) become

$$W_{pq}(n) = (\mu_p/\mu_q)^n \prod_{j=1}^{n} \frac{t_q - \omega^j}{1 - \omega^j} \quad \text{and} \quad \bar{W}_{pq}(n) = (\mu_p \mu_q)^n \prod_{j=1}^{n} \frac{\omega - \omega^j}{t_q - \omega^j}. \tag{5.1}$$

5.2 The Bethe ansatz calculation

We first review the work on the low-temperature limit that was reported by Baxter in References [30] and [31].

The limit $k' \to 0$ was considered, with μ_p and $\mu_{p'}$ order unity, and $\mu_q = O(k'^{-1/N})$, while the Boltzmann weights $W_{pq}(n)$ and $\bar{W}_{pq}(-n)$ are both $O(k'^{n/N})$. Let $\beta = \omega^{1/2} \mu_p \mu_{p'}$.

Consider the sets of spins $\boldsymbol{\sigma}$ and $\boldsymbol{\sigma}'$ which determine the elements of $\mathbf{T}$; elements of $\mathbf{T}$ will be order $k'^{r/N}$ when the sequence of spins $\sigma_1, \sigma_1', \sigma_2, \ldots, \sigma_L', \sigma_{L+1}$ is monotonic and non-increasing, with all the other elements of $\mathbf{T}$ being of higher order in k'.

The transfer matrices can then be "truncated," retaining only elements corresponding to such spin configurations, and neglecting all configurations which give smaller matrix elements. Doing this, the lattice splits into domains of equal spins, separated by r interfaces, as indicated in Figure 5.1. These interfaces run approximately vertically down the lattice. The interfaces may coalesce, but not cross, and each interface will pass through each row exactly once.

For $r = 0$, the only allowed configuration is the N-fold degenerate ground state,

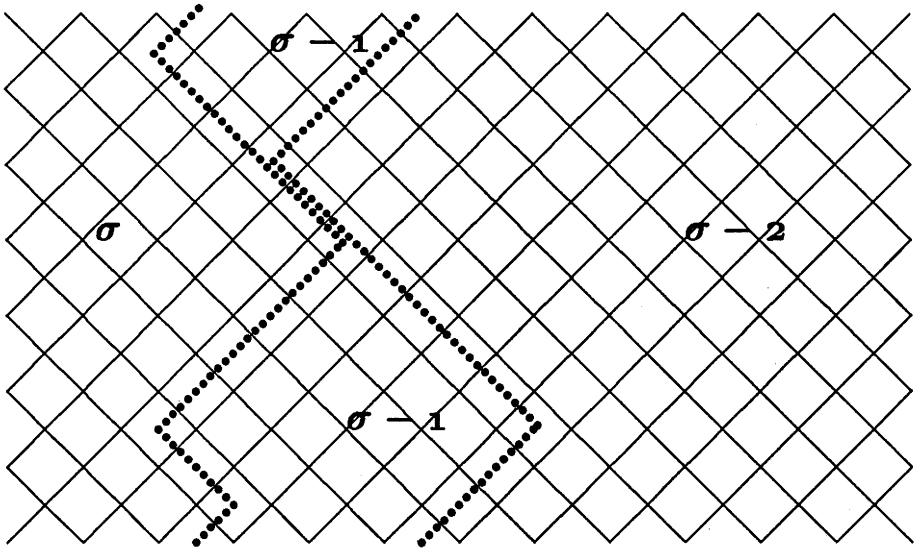

Figure 5.1: The lattice in the $k' \to 0$ limit with skewed boundary conditions. The r interfaces (for $r = 2$) are indicated by the broken lines. In this limit, the interfaces must move monotonically up the lattice, and each interface passes through each row exactly once. The interfaces may coalesce but not cross.

in which all spins in the row are equal to some common value σ, so the truncated transfer matrix $\mathbf{T}_q$ is simply the $N \times N$ identity matrix.

For r non-zero, the transfer matrices will be of dimension $\binom{L}{r} = L!/r!(L-r)!$, and there is a conserved quantity, the number r of interfaces in each row. The problem is amenable to a Bethe ansatz calculation, which Baxter performs explicitly for $r = 0, 1, 2$ and then generalises to arbitrary r in References [30] and [31].

The Bethe ansatz equations of the low-temperature chiral Potts model are very closely related to those of the six-vertex model in a horizontal field [57, 84], the field vanishing when $\beta = 1$. Baxter notes that this is another manifestation of the connection between the chiral Potts model and the six-vertex model [35].

The eigenvalues of $\mathbf{T}_q\hat{\mathbf{T}}_q$ are found to be

$$T_q\hat{T}_q = \prod_{j=1}^{r} \frac{\sin^2(u_q - \alpha_j)}{\eta_q^2 \sin\alpha_j \sin(\alpha_j - \lambda)},$$

where $\eta_q = e^{\pi i/2N}\mu_q$, and the α_j are given by the Bethe ansatz equations

$$\left(\frac{\sin(\alpha_j - \lambda)}{\sin\alpha_j}\right)^L = (-)^{r-1}\beta^{-L}\omega^{-Q} \prod_{l=1}^{r} \frac{\sin(\lambda - \alpha_l - \alpha_j)}{\sin(\lambda - \alpha_j - \alpha_l)}.$$

From this, one can calculate the interfacial tensions ε_r. Baxter explicitly calculates ε_1, and shows that

$$\varepsilon_1 < 2\varepsilon_2$$

in the $k' \to 0$ limit. This means that phase 1 will not wet the phase 0 — phase 2 interface, but rather that it is energetically favourable for the system to jump straight from phase 2 to phase 0. This result is true for $0 < u_q < \pi/N$, in the limit $k' \to 0$.

Further, it is noted that in the $r = 2$ case, there are two types of eigenvectors, "plane waves" and "bound states," with the fully bound states giving the greater contribution to the partition function. Baxter then suggests that for arbitrary r, the dominant contribution to the partition function comes from states with the interfaces bound together, intermediate phases not wetting the interfaces. For L large, the bound states correspond to

$$|\beta^r \sin(\alpha_1 - r\pi/N)/\sin\alpha_1| = 1 \quad \text{and} \quad \alpha_j = \alpha_1 + (1-j)\pi/N. \tag{5.2}$$

The band of largest eigenvalues is calculated and the interfacial tension is expressed as a contour integral over this band of eigenvalues. The integral can be evaluated by the saddle-point method, and the location of this saddle point is discussed.

In this limit, the only dependence of the transfer matrix elements on p and p' is through β. The interfacial tensions are independent of β, and hence are independent of the vertical rapidities p and p', as is expected from Z-invariance.

We consider the functional relations in the low-temperature limit, and derive expressions for the polynomials $\tau_2(t_Q)$ and $\hat{S}(\lambda_q)$ which correspond to the maximum eigenvalues of $\mathbf{T}_q\hat{\mathbf{T}}_q$.

5.3 The polynomial $\tau_2(t_q)$

5.3.1 Periodic boundary conditions

First, we consider the low-temperature limit for periodic (unskewed) boundary conditions. This is considered in [29], but in a different low temperature limit. The work with periodic boundary conditions serves as a framework for the subsequent work with the skewed boundaries.

When we impose periodic boundary conditions onto the lattice, the ground state of the row will be the ferromagnetically ordered state with all of the spins taking

on the same value σ. The transfer matrix will have a unique largest eigenvalue, and from equation (5.1), the maximum eigenvalue of $\mathbf{T}_q$, will be order unity. The functional relation (4.33) simplifies significantly in this limit, and we see that the eigenvalue of the matrix $\tau_2(t_q)$ corresponding to the largest eigenvalue of $\mathbf{T}_q$ is

$$\tau_2(t_q) = c\varepsilon^L(1-t_q)^L + (1-\omega t_q)^L \tag{5.3}$$

where $c = \omega^{Q+L}$, and $\varepsilon = |\mu_p \mu_{p'}|$ (where $\varepsilon > k'^{2/N}$).

5.3.2 The limit $\varepsilon \to 0$

This is a very simple polynomial, and we are particularly interested in the location of its zeros.

First, consider the limit $\varepsilon \to 0$; then (5.3) becomes

$$\tau_2(t_q) = (1-\omega t_q)^L. \tag{5.4}$$

This is a polynomial in t_q with degree L, and a zero of multiplicity L at the point ω^{-1}. Now consider ε small, (we always consider $|\lambda_p|$ and $|\lambda_{p'}|$ smaller than unity) but non-zero; $\tau_2(t_q)$ is given by (5.3), a polynomial in t_q of degree L, which has zeros at the L points (to lowest order in ε)

$$\omega^{-1} + \text{const} \cdot \varepsilon\, e^{2\pi i \ell/L}, \quad \ell = 0, 1, \ldots, L-1,$$

where the constant is order unity. Therefore the zeros of $\tau_2(t_q)$ lie evenly spaced around a circle centered at the point ω^{-1}, and with a radius which is proportional to ε.

Note that changing ε from zero shifted the zeros of the polynomial from a root of unity to a small circle surrounding ω^{-1}. We find similar behaviour in the polynomials $\tau_j(t_q)$, $j = 3, \ldots, N$ which we consider next.

These polynomials are defined by the recurrence relations (4.30) and (4.31). We consider the $\varepsilon \to 0$ limit first; when $\varepsilon = 0$, relation (4.31) reduces to

$$\tau_{j+1}(t_q) = \tau_j(\omega t_q)\, \tau_2(t_q)$$

whereupon

$$\tau_j(t_q) = \prod_{k=1}^{j-1} \tau_2(\omega^{k-1} t_q) = \prod_{k=1}^{j-1} (1-\omega^k t_q)^L. \tag{5.5}$$

Thus the polynomials $\tau_j(t_q)$, $j = 2, \ldots, N$ are polynomials in t_q with degree $(j-1)L$, and have L zeros lying exactly at the points $\omega^{-1}, \omega^{-2}, \ldots, \omega^{-j+1}$. We emphasise that all of the polynomials $\tau_2(t_q), \ldots, \tau_N(t_q)$ are non-zero at and in a neighbourhood of $t_q = 1$.

5.3.3 Location of the zeros for ε non-zero

For ε non-zero, the functional relation (4.31) becomes

$$\tau_{j+1}(t_q) = \tau_j(\omega t_q)\,\tau_2(t_q) - c\varepsilon^L\,(1-\omega t_q)^{2L}\,\tau_{j-1}(\omega^2 t_q),$$

with $\tau_0(t_q) = 0$ and $\tau_1(t_q) = 1$, and c an unimportant order unity constant. The solution to this is

$$\tau_j(t_q) = \sum_{k=0}^{j-1} \frac{c^k \varepsilon^{kL}}{(1-\omega^k t_q)^L} \prod_{l=0}^{j-1} (1-\omega^l t_q)^L, \tag{5.6}$$

a polynomial in t_q of degree $(j-1)L$; this is an exact expression for the polynomial $\tau_j(t_q)$ in the $k' \to 0$ limit. We wish to describe the polynomial $\tau_j(t_q)$ by locating its zeros; we do this as before, setting ε to zero, and then considering ε small but different from zero. We consider $j = 3$ first to demonstrate the method; then from equation (5.6)

$$\begin{aligned}\tau_3(t_q) &= (1-\omega t_q)^L\,(1-\omega^2 t_q)^L + c\varepsilon^L\,(1-t_q)^L\,(1-\omega^2 t_q)^L \\ &+ c^2\,\varepsilon^2\,(1-t_q)^L\,(1-\omega t_q)^L.\end{aligned}$$

When $\varepsilon = 0$, $\tau_3(t_q)$ has L-fold zeros at ω^{-1} and ω^{-2}. For ε non-zero, we expect to find L zeros "close to" both of these points, lying on small circles surrounding them.

Let $\omega^{-1} l_1$ be a zero of $\tau_3(t_q)$ lying "near" ω^{-1}, so l_1 itself must lie in some neighbourhood of unity. We find an equation for l_1 by substituting $\omega^{-1} l_1$ for t_q; the left hand side vanishes, and we have

$$\begin{aligned}0 &= (1-l_1)^L\,(1-\omega l_1)^L + c\varepsilon^L\,(1-\omega^{-1} l_1)^L\,(1-\omega l_1)^L \\ &+ c^2\,\varepsilon^{2L}\,(1-\omega^{-1} l_1)^L\,(1-l_1)^L.\end{aligned} \tag{5.7}$$

This is a polynomial equation in l_1 with degree $2L$, and so it has $2L$ solutions, rather than the L we are seeking. However, only L of these should lie in a neighbourhood of unity, at least for ε sufficiently small. Note that the terms $(1-\omega l_1)$ and $(1-\omega^{-1} l_1)$ are order unity when l_1 lies in a neighbourhood of unity, and that the first two terms on the right hand side of (5.7) will clearly be the largest of the three. Hence we can approximate this equation exponentially well by discarding the third term. Doing so, we obtain

$$0 = (1-l_1)^L + c\epsilon^L,$$

an equation for l_1 which has the L solutions $l_1 = 1+O(\varepsilon)\, e^{2\pi i\ell/L}$, $\ell = 0, 1, \ldots, L-1$, which implies that $\tau_3(t_q)$ has L zeros lying on a small circle centered at ω^{-1} with a radius proportional to ϵ, i.e.

$$\omega^{-1} + \text{const} \cdot \varepsilon\, e^{2\pi i\ell/L}, \quad \ell = 0, 1, \ldots, L-1.$$

By substituting back into (5.7), we see that our assumption regarding which of the three terms were dominant is indeed consistent. To locate the other L zeros of $\tau_3(t_q)$, let $\omega^{-2}l_2$ be a zero that lies "near" ω^{-2}, where l_2 lies in some neighbourhood of unity. Then l_2 satisfies the equation

$$\begin{aligned} 0 &= (1-l_2)^L (1-\omega^{-1}l_2)^L + c\varepsilon^L (1-\omega^{-2}l_2)^L (1-l_2)^L \\ &+ c^2 \varepsilon^{2L} (1-\omega^{-2}l_2)^L (1-\omega^{-1}l_2), \end{aligned}$$

which again should have only L solutions which lie in a neighbourhood of unity, and indeed when this is the case, the factors $(1-\omega^{-1}l_2)$ and $(1-\omega^{-2}l_2)$ are order unity. We need to discard one of these terms, as we did in the equation for l_1. If we assume that the second term is the smallest, i.e. that $(1-l_2)^L < \varepsilon^L$, then we can approximate the equation exponentially well by

$$0 = (1-l_2)^L + O(\varepsilon^{2L})$$

which has solutions $l_2 = 1 + O(\varepsilon^2)\, e^{2\pi i\ell/L}$, $\ell = 0, 1, \ldots, L-1$. Hence the corresponding zeros of $\tau_3(t_q)$ are at the points

$$\omega^{-2} + \text{const} \cdot \varepsilon^2\, e^{2\pi i\ell/L}, \quad \ell = 0, 1, \ldots, L-1,$$

and once more we confirm that the assumption we made is consistent by substitution. These are all of the zeros of $\tau_3(t_q)$ for $r = 0$ and ϵ small.

Next consider the zeros of the polynomial $\tau_j(t_q)$. When $\varepsilon = 0$ we know that zeros of multiplicity L lie at the points ω^{-p}, $p = 1, \ldots, j-1$. When ε is non-zero, we expect that the zeros lie on small circles surrounding these roots of unity, which we confirm next.

Let $\omega^{-p}l_p$ be a zero of $\tau_j(t_q)$ which lies near ω^{-p}, where l_p lies in some neighbourhood of unity. For $j = 3$, for the zeros lying near ω^{-1} we approximated the equation for l_1 by keeping the first and second terms, and for the zeros near ω^{-2}, we approximated the equation for l_2 by keeping the first and third terms. We might expect that for the polynomial $\tau_j(t_q)$, the equation for l_p determining the zeros

around ω^{-p} can be approximated exponentially well by keeping only the first and $p+1$-th terms. We find that this is so.

To determine an equation for l_p, substitute $t_q = \omega^{-p} l_p$ into equation (5.6); the left hand side vanishes, and we have

$$0 = \sum_{k=0}^{j-1} \frac{c^k \varepsilon^{kL}}{(1-\omega^{k-p} l_p)^L} \prod_{l=0}^{j-1} (1-\omega^{l-p} l_p)^L, \quad p = 1, \ldots, j-1.$$

If we write the right hand side of this out in full, we see that it is a sum of j terms, each consisting of a power of ε^L multiplied by an uninteresting constant which is order unity, multiplied by $j-1$ factors $(1-\omega^n l_p)^L$, where n is a positive integer. The terms in the sum corresponding to $k=0$ and $k=p$ appear to be the largest; the former does not have a power of ε^L, and the latter does not contain the factor $(1-l_p)^L$; the other $j-1$ terms contain both of these "small" terms. Hence the equation for l_p can be approximated exponentially well by discarding the smaller terms, giving

$$(1-l_p)^L + \text{const} \cdot \varepsilon^{pL} = 0$$

where the constant is order unity. (We are implicitly assuming that $(1-l_p)^L < \varepsilon^{(p-1)L}$.) The L solutions of this are $l_p = 1 + \text{const} \cdot \varepsilon^p e^{2\pi i \ell / L}$, $\ell = 0, \ldots, L-1$, for $p = 1, \ldots, j-1$ which is consistent with the assumption we made. There are $p-1$ such equations, for $p = 1, \ldots, j-1$, and the $(j-1)L$ zeros of $\tau_j(t_q)$ are therefore

$$\omega^{-p} + \text{const} \cdot \varepsilon^p e^{2\pi i \ell / L}, \quad \ell = 0, \ldots, L-1, \quad p = 1, 2, \ldots, j-1.$$

They do indeed lie on circles surrounding various roots of unity, as expected.

We re-do this working to determine and consider the effect of the skewed boundary conditions.

5.3.4 Maximum eigenvalues for skewed boundary conditions

When we apply the skewed boundaries, the maximum eigenvalue of $\mathbf{T}_q$ is no longer order unity. The lowest energy configuration of a row of the lattice is no longer the completely ordered ferromagnetic ground state, instead, the spins must configure to match the new boundary condition.

In Section 5.2, we mentioned that the maximum eigenvalue of $\mathbf{T}_q$ corresponds to the sequence $\sigma_1, \sigma_1', \sigma_2, \ldots, \sigma_L', \sigma_{L+1}$ being monotonic non-increasing, with $\sigma_{L+1} = \sigma_1 - r$; when this is so, we have

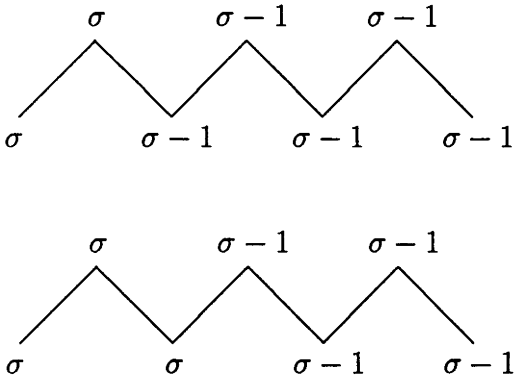

$$\bar{W}(-1) = (\mu_p \mu_q)^{-1} \frac{t_q - 1}{\omega - 1}$$

$$W(1) = (\mu_p / \mu_q) \frac{t_q - \omega}{1 - \omega}$$

Figure 5.2: Two of the $2L$ possible lowest energy states for a row of the lattice with skew parameter $r = 1$. These are generic cases corresponding to the maximum eigenvalues of $\mathbf{T}_q$.

$$\mathbf{T}_q = \mu_q^{-r} \mathbf{F}(t_q) \tag{5.8}$$

where the elements of the matrix $\mathbf{F}(t_q)$ are all polynomials in t_q with degree at most r. The eigenvectors of $\mathbf{T}_q$ are independent of q, so the eigenvalues $F(t_q)$ of $\mathbf{F}(t_q)$ are also polynomials in t_q of degree at most r. In the limit $k' \to 0$, the functional relation (4.33) simplifies

$$\tau_2(t_q) F(\omega t_q) = \omega^{r+Q} \left[\omega \mu_p \mu_{p'} (1 - t_q)\right]^L F(t_q) + (1 - \omega t_q)^L F(\omega^2 t_q) \tag{5.9}$$

which we have written as a relation between the eigenvalues $\tau_2(t_q)$ and $F(t_q)$ of the matrices $\boldsymbol{\tau}_2(t_q)$ and $\mathbf{F}(t_q)$.

We need to determine the largest eigenvalues of $\mathbf{F}(t_q)$, which correspond to the configurations of the row with the largest Boltzmann weights. In the previous section, we considered $r = 0$; we next consider $r = 1$ and $r = 2$.

When $r = 1$ there must be an interface somewhere in the lattice, with a single jump corresponding to the configuration with the lowest energy. The maximum entries of $\mathbf{T}_q$ correspond to the archetypal configurations shown in Figure 5.2, with corresponding weights for the rows indicated in the figure. There are N choices of the spins σ on one side of the interface (which determines the spins on the other side), and a choice of $2L$ locations for the interface. To leading order, the maximum eigenvalue of $\mathbf{T}_q$ will be

$$T_q = c_1 W(1) + c_2 \bar{W}(-1)$$

where c_1 and c_2 are order unity. When we consider the limit $\varepsilon \to 0$, the weight $\bar{W}(-1)$ will clearly dominate, so we have

$$F(t_q) \propto t_q - 1$$

as the maximum eigenvalue of $\mathbf{F}(t_q)$ when $r = 1$. There are L places to put the interface in the $\bar{W}$ direction, giving us a set of L such largest eigenvalues. When ε is small but non-zero, we see that the zero of $F(t_q)$ will shift from unity to another point lying a distance of order ε from unity, as we saw in the previous sections with the zeros of the polynomials $\tau_j(t_q)$.

Taking $r = 2$ is more complicated. Now there are five distinct (in the sense that they have a different Boltzmann weight) possibilities, which are illustrated in Figure 5.3. The first two of these configurations corresponds to the two interfaces lying on the same bond, so phase σ jumps straight to phase $\sigma - 2$, without phase $\sigma - 1$ wetting the interface.

Again consider the limit $\varepsilon \to 0$; then the dominant weights will be $\bar{W}(-2)$ and $\bar{W}(-1)^2$, both being of order ε^{-1}. However, writing $t_q = e^{2iu_q}$, we see that

$$\left|\frac{\bar{W}(-2)}{\bar{W}(-1)^2}\right| = \frac{\sin(u_q + \pi/N)}{2 \sin u_q \cos \pi/N} > 1 \quad \text{for} \quad 0 < u_q < \pi/N$$

so the dominant weight will be $\bar{W}(-2)$. As a result, the maximum eigenvalue of $\mathbf{F}(t_q)$ will be

$$F(t_q) \propto (t_q - 1)(t_q - \omega^{-1}).$$

Thus the maximum eigenvalue in this limit corresponds to the two interfaces being bound together, and the intermediate phase $\sigma - 1$ not wetting the phase σ—phase $\sigma - 2$ interface.

For general r, the maximum eigenvalue in the $\varepsilon \to 0$ limit will correspond to the configuration(s) with the highest power of μ_p in the denominator. For $r = 3$, there are the possibilities $\bar{W}(-3)$, $\bar{W}(-2)\bar{W}(-1)$ and $\bar{W}(-1)^3$, and we can show that $\bar{W}(-3)$ is the dominant configuration for $0 < u_q < \pi/N$, so that

$$F(t_q) = (1 - t_q)(1 - \omega^{-1} t_q)(1 - \omega^{-2} t_q).$$

Looking at larger values of r, we see that in general the maximum eigenvalue corresponds to $\bar{W}(-r)$, and so

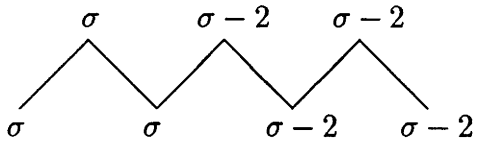

$$W(2) = (\mu_p/\mu_q)^2 \frac{t_q - \omega}{1-\omega} \frac{t_q - \omega^2}{1-\omega^2}$$

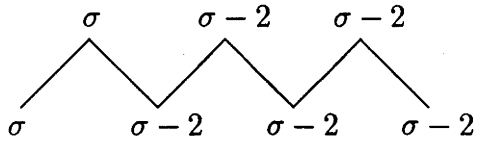

$$\bar{W}(-2) = (\mu_p\mu_q)^{-2} \frac{t_q - 1}{\omega - 1} \frac{t_q - \omega^{-1}}{\omega - \omega^{-1}}$$

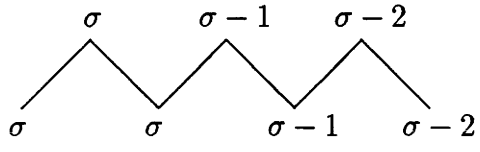

$$W(1)^2 = (\mu_p/\mu_q)^2 \left(\frac{t_q - \omega}{1-\omega}\right)^2$$

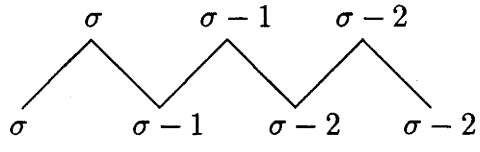

$$\bar{W}(-1)^2 = (\mu_p\mu_q)^{-2} \left(\frac{t_q - 1}{\omega - 1}\right)^2$$

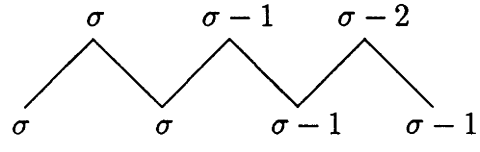

$$W(1)\bar{W}(-1) = \mu_q^{-2} \frac{t_q - 1}{\omega - 1} \frac{t_q - \omega}{1-\omega}$$

Figure 5.3: The five distinct possible lowest energy states for a row of the lattice with skew parameter $r = 2$. These are generic cases corresponding to the maximum eigenvalues of $\mathbf{T}_q$.

$$F(t_q) \propto (1-t_q)(1-\omega^{-1}t_q)\cdots(1-\omega^{-r+1}t_q) \tag{5.10}$$

for $1 < r < N-1$.

This agrees with the maximum eigenvalue of $F(t_q)$ corresponding to the fully bound state eigenvectors mentioned towards the end of Section 5.2. In the limit $\varepsilon \to 0$, the β of that section vanishes, so to maintain the first equality of (5.2) we have to choose $\alpha_1 = 0$, and the other α_j are determined by the second equation of (5.2). This leads to precisely the expression (5.10) for $F(t_q)$.

Having determined the polynomial $F(t_q)$ which is the maximum eigenvalue of the matrix $\mathbf{F}(t_q)$, we can now use the functional relations to determine the corresponding polynomials $\tau_j(t_q)$, $j = 2,\ldots,N$ and $\hat{S}(\lambda_q)$.

First we use equation (5.9) once more to determine the $\tau_j(t_q)$ polynomials. We consider the limit $\varepsilon \to 0$, and then vary ε as in the previous subsection to determine the location of the zeros of the polynomials for ε non-zero.

5.3.5 The limit $\varepsilon \to 0$

Taking the limit $\varepsilon \to 0$, the relation (5.9) becomes

$$\tau_2(t_q)F(\omega t_q) = (1-\omega t_q)^L F(\omega^2 t_q)$$

where $F(t_q)$ is given by (5.10) so it follows that $\tau_2(t_q)$ is given by

$$\tau_2(t_q) = (1-\omega t_q)^{L-1}(1-\omega^{r+1}t_q),$$

a polynomial in t_q with degree L, which has a zero of multiplicity $L-1$ at ω^{-1}, and a simple zero at ω^{-r-1}. This reduces to equation (5.4) when $r = 0$, so the non-zero skew parameter simply shifts one of the zeros of $\tau_2(t_q)$ from ω^{-1} to another root of unity. This is what we find the skew parameter does in general.

We can also calculate the other functions $\tau_j(t_q)$ in this limit. Taking $\varepsilon \to 0$, the functional relation (4.31) becomes

$$\tau_{j+1}(t_q) = \tau_j(\omega t_q)\tau_2(t_q)$$

(because $z(t_q) \to 0$ as $\varepsilon \to 0$), which implies that $\tau_j(t_q)$ is given by

$$\tau_j(t_q) = \prod_{k=1}^{j-1} \tau_2(\omega^{k-1}t_q) = \prod_{k=1}^{j-1}(1-\omega^k t_q)^{L-1}(1-\omega^{r+k}t_q) \tag{5.11}$$

for $j = 2, \ldots, N$. Each $\tau_j(t_q)$ is a polynomial in t_q with degree $(j-1)L$, with zeros of multiplicity 1, $L-1$ or L at the roots of unity ω^{-1}, ω^{-2}, ..., ω^{-r-j-1}. Comparing the expressions (5.5) and (5.11) for $\tau_j(t_q)$, we see that once again the skew parameter has merely shifted some of the zeros of the polynomials. Note in particular that the polynomial $\tau_j(t_q)$ has at most a simple zero at unity itself.

5.3.6 Location of the zeros for ε non-zero

Next we wish to locate the zeros of the polynomials $F(t_q)$ and $\tau_j(t_q)$ when ε has some small but non-zero value. We expect to find that when we increase ε, the zeros will move onto small circles surrounding the roots of unity, rather than lying exactly on the roots of unity themselves.

The zeros of $F(t_q)$ will move, but will still lie within some ε-neighbourhood of the roots of unity $1, \omega^{-1}, \ldots, \omega^{-r-1}$. We accommodate the expected shifting of the zeros by generalising (5.10) to

$$F(t_q) = \prod_{j=1}^{r} (a_j - \omega^{j-1} t_q), \tag{5.12}$$

where the numbers a_j, $j = 1, 2, \ldots, r$ lie within some ε-neighbourhood of unity. When $\varepsilon = 0$, then $a_j = 1$, $j = 1, \ldots, r$. Consider the functional relation (5.9) once more. The left hand side vanishes when $t_q = \omega^{-j} a_j$, so substituting this value for t_q, we get the following Bethe-ansatz type equations for the numbers $a_j, j = 1, \ldots, r$

$$\prod_{k=1}^{r} \frac{a_k - \omega^{k-j+1} a_j}{a_k - \omega^{k-j-1} a_j} = -\omega^{Q+r+L} \varepsilon^L \left(\frac{1 - \omega^{-j} a_j}{1 - \omega^{1-j} a_j} \right)^L, \tag{5.13}$$

where there are r such equations, corresponding to $j = 1, 2, \ldots, r$. We can solve these equations for the a_j to leading order in ε as follows. The a_j are of the form $1 + O(\varepsilon^{\#})$, where $\#$ represents some positive number. We approximate the r equations by collecting all of the factors which are order unity into a "constant" term, and only writing out explicitly factors which are smaller than $O(1)$. Such terms are factors like $(1 - a_j)$ or $(a_i - a_j)$, $1 \leq i, j, \leq r$. Doing so, we get $r - 2$ equations of the form

$$\frac{a_{j-1} - a_j}{a_{j+1} - a_j} = \text{const} \cdot \varepsilon^L, \quad j = 2, \ldots, r-1$$

and two others,

$$\frac{(1 - a_1)^L}{a_2 - a_1} = \text{const} \cdot \varepsilon^L \qquad \text{and} \qquad a_{r-1} - a_r = \text{const} \cdot \varepsilon^L.$$

Multiplying these r equations together gives

$$(1 - a_1)^L = \text{const} \cdot \varepsilon^{rL}$$

which indicates that we have L choices for the parameter a_1, of the form

$$a_1 = 1 + \text{const} \cdot \varepsilon^r e^{2\pi i \ell / L}, \quad \ell = 0, 1, \ldots, L-1, \tag{5.14}$$

corresponding to the L largest eigenvalues of $\mathbf{T}_q$. The other a_j follow, being

$$a_j = a_1 + \text{const} \cdot \varepsilon^{(r-j+1)L} \quad \text{for} \quad j = 2, \ldots, r. \tag{5.15}$$

The zeros of $F(t_q)$ form a "string" of length r in the complex plane, and once the value of a_1 is chosen from the set of L possible values, the other a_j are determined as above. Also, as $L \to \infty$, all of the a_j converge to a_1 (and the zeros of $F(t_q)$ converge to the points $\omega^{1-j} a_1$, $j = 1, \ldots, r$), and so in the thermodynamic limit, there is really only the single parameter, a_1, which is of interest; we let $a = a_1$. We also remark here that we have found a set of L largest eigenvalues of $\mathbf{F}(t_q)$, which are the eigenvalues required to calculate the free energy and the interfacial tension. Thus we are in a similar situation to the one we were in when considering the low-temperature limit of the six-vertex model with either antiperiodic boundary conditions and an even number of columns or periodic boundary conditions and an odd number of columns, in Chapter 3.

5.3.7 Zeros of $\tau_2(t_q)$

We can use this information together with the same functional relation to locate the zeros of $\tau_2(t_q)$ when $k' \to 0$ and ε is small but non-zero. From the result when $\varepsilon = 0$, we would expect to have $L - 1$ of the zeros of $\tau_2(t_q)$ lying in some neighbourhood of the point ω^{-1}, and one zero lying in some neighbourhood of the point ω^{-r-1}.

Once more, we use the functional relation (5.9). Let a zero of $\tau_2(t_q)$ near ω^{-1} be $\omega^{-1} l$, where l lies in some neighbourhood of unity, and $l \to 1$ when $\varepsilon \to 0$. We wish to find some equation for this number l. We consider the cases $r = 1$ and $r > 1$ separately.

When $r = 1$, making our usual approximation (collecting all order unity functions into uninteresting "constants"), the functional relation becomes

$$\tau_2(\omega^{-1} l)(a - l) = c_1 \varepsilon^L + c_2 (1 - l)^L$$

where c_1 and c_2 are order unity "constants." The right hand side is a polynomial in l with degree L; one of its zeros corresponds to the factor $(a-l)$ on the left hand side, and the other $L-1$ zeros correspond to the $L-1$ zeros of $\tau_2(t_q)$ that lie near ω^{-1}. The zeros of the right hand side are at the points

$$l = 1 + \text{const} \cdot \varepsilon\, e^{2\pi i \ell / L}, \quad \ell = 0, 1, \ldots, L-1$$

and one of these must be exactly the point $a = 1 + O(\varepsilon)$, the other $L-1$ being the zeros of $\tau_2(\omega^{-1}l)$, when l is in a neighbourhood of unity. The other zero of $\tau_j(t_q)$ lies near ω^{-2} (remembering that $r = 1$); let this be $\omega^{-2}\alpha$, and substitute this value in for t_q. Then we can approximate the equation by

$$\tau_2(\omega^{-2}\alpha) = c_1\, \varepsilon^L + c_2\,(a - \alpha)$$

so $\alpha = a + O(\varepsilon^L)$, and $\tau_2(t_q)$ has a zero at $\omega^{-2}a + O(\varepsilon^L)$.

Next, when $r > 1$, the functional relation becomes

$$\tau_2(\omega^{-1}l)(a-l) = c_1\, \varepsilon^L\,(a_2 - l) + c_2\,(1-l)^L$$

where c_1 and c_2 are order unity. The right hand side is a polynomial in l of degree L, and the zeros of this polynomial must be the zeros of the left hand side, i.e. the $L-1$ zeros of $\tau_2(\omega^{-1}l)$ that lie near unity (corresponding to the $L-1$ zeros of $\tau_2(t_q)$ that lie near ω^{-1}), and the single zero at $l = a$. We will determine the zeros of the right hand side; first, write $a_2 = a - \varepsilon^{(r-1)L}$, where we will suppress constants which are order unity for the moment. Then the right hand side becomes

$$\varepsilon^L\,(a-l) + \varepsilon^{rL} + (1-l)^L. \tag{5.16}$$

This must contain the factor $(a-l)$, as it is a factor of the left hand side. Using the identity

$$a^n - b^n = (a-b)\sum_{k=0}^{n-1} a^k\, b^{n-k-1}$$

we can write the second and third terms of (5.16) as

$$\varepsilon^{rL} + (1-l)^L = (1 - \varepsilon^r - l)\left(\varepsilon^{r(L-1)} + \cdots + (1-l)^{L-1}\right),$$

but the factor $(1 - \varepsilon^r - l)$ must be exactly $(a-l)$, so the right hand side becomes

$$(a-l)\left(\varepsilon^L + \varepsilon^{r(L-1)} + \cdots + (1-l)^{L-1}\right)$$

which explicitly contains the factor $(a-l)$ as required. Hence

$$\tau_2(\omega^{-1}l) = \varepsilon^L + \varepsilon^{r(L-1)} + \cdots + (1-l)^{L-1}$$

where again we have suppressed all constants which are order unity. We can locate the zeros of this polynomial easily, noting that when $r > 1$ the first and last terms dominate, so the equation can be approximated exponentially well by ignoring all but these two terms. Then the zeros will occur at $l = 1+O(\varepsilon^{L/(L+1)})\, e^{2\pi i\ell/(L-1)}$, $\ell = 1, 2, \ldots, L-1$. We can also locate the other zero of $\tau_2(t_q)$, which we expect will lie in some neighbourhood of the point ω^{-r-1}. Let this zero be $\omega^{-r-1}\alpha$, and substitute this into the functional relation as before. The resulting equation is (suppressing any constants which are order unity)

$$\tau_2(t_q) = \varepsilon^L + a_r - \alpha$$

which implies that $\tau_2(t_q)$ has a further zero at $\omega^{-r-1}a_r + O(\varepsilon^L)$. (In the limit $L \to \infty$, this zero approaches the point $\omega^{-r-1}a$.)

In summary, then, we have shown that the zeros of $\tau_2(t_q)$ are made up of a set of $L-1$ which are distributed around a circle centered at ω^{-1}, with a radius proportional to ε^L when $r = 1$, and to $\varepsilon^{L/(L-1)}$ when $r > 1$; and a single outlier which lies within a distance $O(\varepsilon^L)$ from the point a_r.

The zeros of the polynomials $\tau_j(t_q)$, $j = 2, 3, \ldots, N-1$, were found to lie clustered around the roots of unity $\omega^{-1}, \omega^{-2}, \ldots, \omega^{-N+1}$, and each polynomial has at most a simple zero at or near unity itself.

Hence there exists a domain in the t_q-plane which excludes the roots of unity $\omega^{-1}, \omega^{-2}, \ldots, \omega^{-N+1}$, and also excludes the zeros of all of the polynomials $\tau_j(t_q)$, $j = 2, \ldots, N$ which lie near these roots of unity. We call this domain $\mathcal{D}_t$. The polynomials have at most a simple zero at $t_q = a$ lying inside $\mathcal{D}_t$, and this zero lies in some neighbourhood of unity.

5.3.8 Non-zero, sub-critical temperatures

We can use this information to work out integral formulae for the polynomials $\tau_2(t_q)$, $\tau_3(t_q)$, ..., $\tau_N(t_q)$, in the large-lattice $L \to \infty$ limit, which are valid at non-zero temperatures. We use Cauchy's integral formula to write expressions for the polynomials by surrounding their zeros by contours, and obtain integral expressions which are valid outside the contour.

We have located the zeros in the limit $k' \to 0$, and for ε small but non-zero. We wish to vary k' also, so our results will be useful at arbitrary temperatures, and in particular valid as the system approaches criticality.

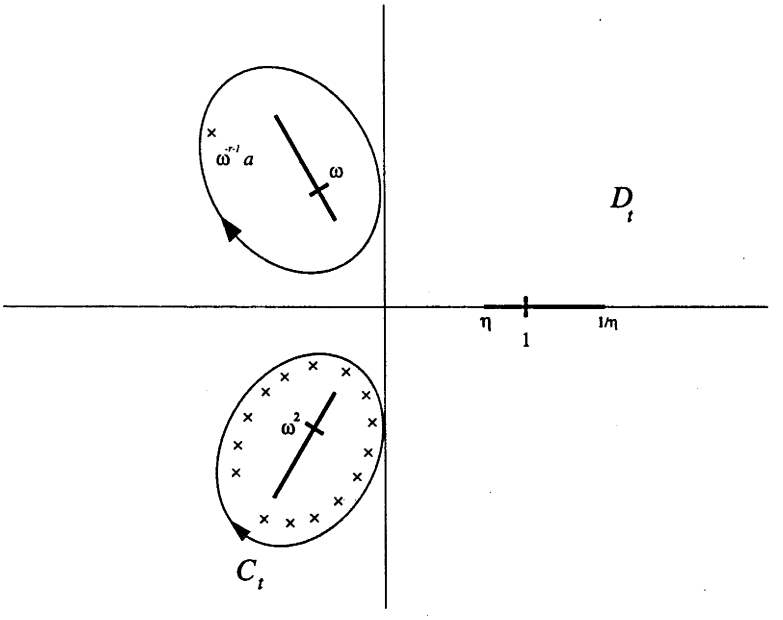

Figure 5.4: The cut complex t_q-plane, with $N = 3$, with the branch cuts for λ_q as a function of t_q indicated by the bold lines. The zeros of $\tau_2(t_q)$ with $r = 1$ are indicated ($\times$), with $L - 1$ of them surrounding ω^2, and one at ωa. The contour C_t, indicated, surrounds all the zeros of $\tau_2(t_q)$ except ωa. The domain $\mathcal{D}_t$ lies outside the two contours.

The zeros of $\tau_2(t_q)$ may move further as k' increases, and the ring they lie on will surround the branch cut for λ_q as a function of t_q. The zeros of $\tau_3(t_q), \ldots, \tau_N(t_q)$ will move likewise as we increase k', but for k' small enough, will still lie in a neighbourhood of their "parent" roots of unity.

The domain $\mathcal{D}_t$ excludes all of the branch cuts for λ_q as a function of t_q, apart from the one between η and $1/\eta$. The domain is illustrated in Figure 5.3.9 for $N = 3$; this lies outside the contours which encircle the roots of unity ω and ω^{-1}, and the polynomials $\tau_j(t_q)$ have at most a simple zero in $\mathcal{D}_t$, at $t_q = a$.

5.3.9 The polynomial $\tau_2(t_q)$

We follow the method of References [29] and [28]. From equations (4.31) and (4.32), we see that

$$\tau_2(t_q)\tau_2(\omega t_q)\cdots\tau_2(\omega^{N-1}t_q) = \alpha_q + \bar{\alpha}_q + \xi \tag{5.17}$$

where ξ represents a sum of products of the polynomials τ_2 and z. The left hand side of (5.17) is a polynomial in t_q^N of degree L, which we will call $M(t_q)$. Let its zeros be the points $a_1^N, \ldots, a_L^N$, so

$$M(t_q) \propto \prod_{j=1}^{L} (a_j^N - t_q^N). \tag{5.18}$$

(In the limits $k', \varepsilon \to 0$, we found $a_j^N = 1$, $j = 1, \ldots, L$; for k' and ε different from zero, we expect the a_j to lie in some neighbourhood of this point.) Following our comments regarding the location of the zeros of $\tau_2(t_q)$ in the $k' \to 0$ limit, we can write

$$\tau_2(t_q) \propto (a_1 - \omega^{r+1} t_q) \prod_{j=2}^{L} (a_j - \omega t_q). \tag{5.19}$$

If we indicate the dependence of the polynomial $\tau_2(t_q)$ on the skew parameter r by the subscript $\tau_2(t_q)_r$, we have

$$\tau_2(t_q)_r = \frac{a_1 - \omega^{r+1} t_q}{a_1 - \omega t_q} \tau_2(t_q)_{r=0} \tag{5.20}$$

and so introducing the skew parameter r once again shifts one of the zeros of the polynomial.

The zeros of $M(t_q)$ will occur in N sets of L points, clustered around the roots of unity $1, \omega, \ldots, \omega^{N-1}$. Let $\mathcal{C}_t$ be a simple closed contour oriented in the positive direction which surrounds all the zeros of $M(t_q)$ that lie near the point ω^{-1}, i.e. $\mathcal{C}_t$ just surrounds the hole in $\mathcal{D}_t$ around ω^{-1}. This contour is also indicated in Figure 5.3.9. Inside $\mathcal{C}_t$ lie the $L-1$ zeros of $\tau_2(t_q)$ that are made up of the L original zeros of the polynomial, less the one that was shifted; and the shifted zero of $\tau_2(\omega^{-r} t_q)$.

Let $a = a_1$, so $\omega^{-1} a$ is the zero of $\tau_2(t_q)$ which gets shifted when the boundary conditions are skewed. Then using Cauchy's integral formula and equation (5.19), and integrating, we can write

$$\ln \left\{ \tau_2(s) \frac{a - \omega s}{a - \omega^{r+1} s} \right\} = \frac{1}{2\pi i} \oint_{\mathcal{C}_t} \ln C(t - s) \frac{d}{dt} \ln M(t)\, dt \tag{5.21}$$

where C is a constant of integration, to be determined. This form of $\tau_2(s)$ is valid whenever s is outside $\mathcal{C}_t$.

Consider the limit $L \to \infty$. From the low-temperature limit, when k' and $\varepsilon \to 0$ with $k' \ll \varepsilon^{N/2}$, we note the following;

$$\bar{\alpha}_q = O(1), \quad \alpha_q = O(\varepsilon^{NL}), \quad z(t_q) = O(\varepsilon^L), \quad \tau_2(t_q) \leq O(1). \tag{5.22}$$

With this in mind, the dominant term in equation (5.17) for $M(t)$ is $\bar{\alpha}_q$, all the other terms decaying exponentially to zero as $L \to \infty$. If we assume that this behaviour persists for general k' and ε, then in the $L \to \infty$ limit, we may replace $M(t_q)$ with $\bar{\alpha}_q$. Substituting this into equation (5.21), we have the exact expression

$$\ln\left\{\tau_2(s)\,\frac{a-\omega s}{a-\omega^{r+1}s}\right\} = \frac{1}{2\pi i}\oint_{\mathcal{C}_t} \ln C(s-t)\,\frac{d}{dt}\ln\bar{\alpha}(\lambda)\,dt \tag{5.23}$$

for L large and s outside $\mathcal{C}_t$. The λ occurring in the integrand is chosen so that $|\lambda| > 1$, to be consistent with the low-temperature limit calculations. This integral is taken around the contour of integration $\mathcal{C}_t$ on the $|\lambda_q| > 1$ sheet of the t_q Riemann surface. However, the integrand of (5.23) is now analytic inside the part of the cut t_q-plane that lies inside $\mathcal{C}_t$ (the function $\bar{\alpha}(\lambda)$ has zeros when $\lambda = \lambda_p$ or $\lambda_{p'}$, but as $|\lambda_p|, |\lambda_{p'}| < 1$, the zeros of $\bar{\alpha}(\lambda)$ lie on the other t_q-plane). We can thus shrink the contour of integration down until it just surrounds the branch cut from $\omega^{-1}\eta$ to $\omega^{-1}\eta^{-1}$.

As t goes around this branch cut in the $t-$plane, λ goes once around the unit circle in the λ-plane in the positive direction. Changing variables from t to λ in the integral, then

$$\ln\left\{\tau_2(s)\,\frac{a-\omega s}{a-\omega^{r+1}s}\right\} = \frac{1}{2\pi i}\oint_{\mathcal{C}_\lambda} \ln C(s-t)\frac{d}{d\lambda}\ln\bar{\alpha}(\lambda)\,d\lambda, \tag{5.24}$$

where $\mathcal{C}_\lambda$ represents the unit circle in the λ plane.

The constant C is evaluated from the $L \to \infty$ limit of (5.17). We make the substitution $\lambda = e^{i\theta}$, so $t = \omega^{-1}\Delta(\theta)$; then replacing s by t_q, we have

$$\ln\left\{\tau_2(t_q)\frac{a-\omega t_q}{a-\omega^{r+1}t_q}\right\} = \frac{L}{4\pi}\int_0^{2\pi}\left(\frac{1+\lambda_p e^{i\theta}}{1-\lambda_p e^{i\theta}} + \frac{1+\lambda_{p'}e^{i\theta}}{1-\lambda_{p'}e^{i\theta}}\right)\ln\left[\Delta(\theta)-\omega t_q\right]d\theta \tag{5.25}$$

as our integral formula for $\tau_2(t_q)$. This agrees with equation (5.20), and is exact subject to our assumptions about the location of the zeros, for t_q outside $\mathcal{C}_t$ and L large.

5.3.10 The polynomials $\tau_j(t_q)$

We can use equations (4.30)–(4.32) together with (5.20) to derive an expression for the functions $\tau_3(t_q), \ldots, \tau_N(t_q)$ in the limit $L \to \infty$. Iterating (4.30)–(4.32), we have

$$\tau_j(t_q) = \tau_2(t_q)\,\tau_2(\omega t_q)\cdots\tau_2(\omega^{j-2}t_q) + \xi' \tag{5.26}$$

where ξ' is a function made up of sums of products of τ_2 and z functions as before. As long as t_q is not a zero of any of the τ_2 functions appearing in this formula (i.e. for t_q in $\mathcal{D}_t$), the z functions will be exponentially smaller than any of the τ_2 functions, and therefore negligible as $L \to \infty$. Therefore, we have

$$\tau_j(t_q) = \prod_{k=1}^{j-1} \tau_2(\omega^{k-1} t_q), \tag{5.27}$$

which is valid for L large and for $t_q \in \mathcal{D}_t$.

5.3.11 Possible values of a

We noted that there were L values a could take in the $k' \to 0$ limit, each one corresponding to a different bound-state eigenvalue of the transfer matrix. For general k' we derive an equation for the possible values of a as follows. Consider the $j = N - r$ case of equation (4.25). In the $k' \to 0$ limit we see from (5.8) and (5.12) that T_q has a zero when $t_q = a$, and we see later that this is true for k' non-zero also (though we do not assume it here). From (5.20) and (5.26), remembering that when $r = 0$ the zeros of $\tau_2(t_q)$ are clustered around ω^{-1}, we can see that the polynomials $\tau_r(\omega^{N-r} t_q)$ and $\tau_{N-r}(t_q)$ are both non-zero at $t_q = a$. If we then substitute $t_q = a$ into (4.25), the relation becomes

$$\bar{H}^{(N-r)}_{p'q} \Big/ H^{(N-r)}_{pq} = -\omega^{jr+Q} \tau_r(\omega^{N-r} a) \Big/ \tau_{N-r}(a)$$

which can be written using (5.27) and (5.25) as

$$\begin{aligned} L \ln \left[(\omega \mu_p \mu_{p'})^r \prod_{j=1}^{r} (t_p - \omega^{-j} a)(t_{p'} - \omega^{-j} a) \right] &= Q \ln \omega \\ &+ \frac{L}{4\pi} \int_0^{2\pi} \left(\frac{1 + \lambda_p e^{i\theta}}{1 - \lambda_p e^{i\theta}} + \frac{1 + \lambda_{p'} e^{i\theta}}{1 - \lambda_{p'} e^{i\theta}} \right) \\ &\times \sum_{j=1}^{r} \ln \left[(\Delta(\theta) - \omega^{-j} a)(\Delta(\theta) - \omega^{-j+1} a) \right] d\theta. \end{aligned} \tag{5.28}$$

This integral equation is exact in the limit $L \to \infty$, and for finite L it is exact up to terms that vanish exponentially with L. We have plotted the various allowed values of a in Figure 4, numerically solving the equation for $L = 60$, and $k' = 0.104$, $t_p = 11/20$, $\mu_p = 1/2$. Note that there are L possible values for a, that they lie on a closed contour surrounding the branch cut for λ_q as a function of t_q, and that they are distributed non-uniformly around this contour. As $L \to \infty$, the solutions to (5.28) become densely spaced on this contour.

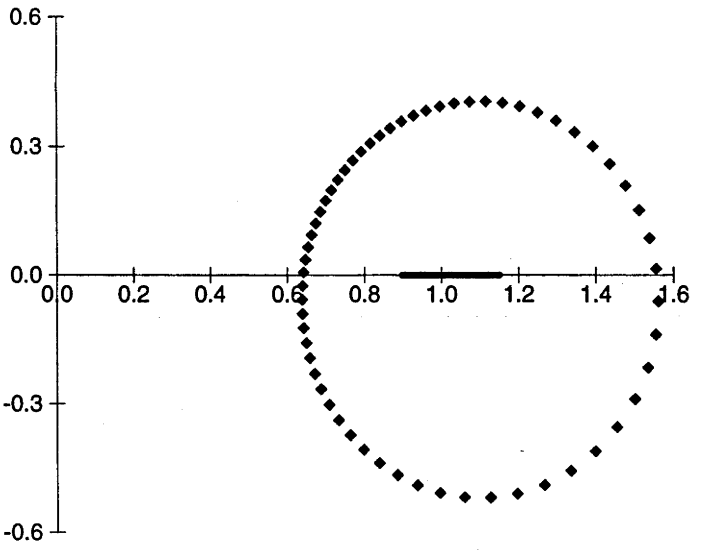

Figure 5.5: Possible values of a for $N = 3$, $r = 1$, $k' = 0.104$, $\lambda_p = 1/8$, $t_p = 11/20$ and $L = 60$. The branch cut for λ_q as a function of t_q is shown in bold, between the branch points η and $1/\eta$.

5.4 The polynomial $\hat{S}(\lambda_q)$

5.4.1 The limit $k' \to 0$ again

We also need to determine the zeros of the polynomial $\hat{S}(\lambda_q)$, which is defined by equation (4.36), in this limit. Call the right hand side of the functional relation (4.25) $r_j(t_q, \lambda_q)$, $j = 0, 1, \ldots, N-1$. The zeros of $r_j(t_q, \lambda_q)$ are zeros of any of the functions on the left hand side of (4.25), i.e. zeros of either T_q, $\hat{T}_{\bar{q}j0}$ or $\Lambda_q^{(j,0)}$.

In the limit $k' \to 0$, equations (4.21),(4.22) and (4.23) become

$$\Lambda_q^{(j,0)} \propto \left(\lambda_q \mu_p^{j-N}\right)^L, \quad H_{pq}^{(j)} \propto \left(\lambda_q \mu_p^{j-N}\right)^L, \quad \bar{H}_{p'q}^{(j)} \propto \left(\mu_{p'}^{N-j}/k'\right)^L,$$

where the proportionality constants are order unity. As we have mentioned, in this limit T_q is order unity so the zeros of $r_j(t_q, \lambda_q)$ in the λ_q-plane are the zeros of $\hat{T}_{\bar{q}j0}$, and hence of $\hat{S}(\lambda_q)$. It is now simply a matter of locating the zeros of the function $r_j(t_q, \lambda_q)$. The polynomials $\tau_j(t_q)$ are order unity also, so the expression for $r_j(t_q, \lambda_q)$ simplifies, becoming

$$r_j(t_q, \lambda_q) \propto c_1\, \varepsilon^{(N-j)L}\, \lambda_q^{-L} + c_2\, k'^L$$

for $j = 1, \ldots, N-1$, where c_1 and c_2 are order unity. The zeros of the functions r_j for $j = 1, \ldots, N-1$ lie on circles centered at the origin and with radii proportional to ε^{N-j}/k', while r_0 is order unity. All $(N-1)L$ of these zeros are contained inside the annulus $1 < |\lambda_q| < 1/k'$, and these make up all the zeros of $\hat{S}(\lambda_q)$.

5.4.2 Skewed boundary conditions

Guided by the results of the last section, we expect that when we apply the skewed boundary conditions, some of the zeros of $\hat{S}(\lambda_q)$ will shift. From equations (5.9), (5.12) and (5.14), we see that when $t_q \in \mathcal{D}_t$, then $T_q \propto (\varepsilon^r - k'\lambda_q)$, with a proportionality constant which is order unity. Also, $\tau_j(t_q)$ and $\tau_{N-j}(\omega^j t_q)$ are order unity unless $0 \le j \le N-r-1$ when $\tau_{N-j}(\omega^j t_q) \propto (\varepsilon^r - k'\lambda_q)$, or $N-r+1 \le j \le N-1$ when $\tau_j(t_q) \propto (\varepsilon^r - k'\lambda_q)$. The functional relation (4.25) becomes

$$r_j(t_q, \lambda_q) \propto c_1\, \varepsilon^{(N-j)L}\, \tau_j(t_q)\, \lambda_q^{-L} + c_2\, k'^L\, \tau_{N-j}(\omega^j t_q) \tag{5.29}$$

where c_1 and c_2 are order unity, and $\tau_j(t_q)$ or $\tau_{N-j}(\omega^j t_q)$ is either order unity or proportional to $(\varepsilon^r - k'\lambda_q)$ depending on the value of j. There are N such equations, with $j = 0, 1, \ldots, N-1$.

The zeros of r_j and $\hat{T}_{\bar{q}j0}$ are as follows; when $j = 0$, then $r_0 \propto (\varepsilon^r - k'\lambda_q)$, and so r_0 has only a single zero, which in fact corresponds to the zero of T_q. Thus $\hat{T}_{\bar{q}00}$ is order unity.

When $1 \le j \le N-r-1$, then r_j has L zeros lying on circles centered at the origin and with radii proportional to $\varepsilon^{N-j-r/L}/k'$, and one outlier at a distance proportional to ε^r/k'. This outlier must belong to T_q, the L zeros lying on each of the circles belonging to $\hat{T}_{\bar{q}j0}$.

When $j = N-r$, the L zeros of r_j lie on a circle centered at the origin and with radius proportional to ε^r/k'. One of these must belong to T_q, and so the zeros of $\hat{T}_{\bar{q}(N-r,0)}$ are the remaining $L-1$ zeros that lie on the circle.

Finally, when $N-r+1 \le j \le N-1$, the zeros of r_j consist of $L-1$ points lying on circles centered at the origin and with radii proportional to $\varepsilon^{(N-j)L/(L-1)}/k'$ and one outlier at a distance proportional to ε^r/k'. The outlier belongs to T_q, the $L-1$ zeros spaced around each of the circles to $\hat{T}_{\bar{q}j0}$.

All the zeros of $\hat{T}_{\bar{q}j0}$, $j = 1, 2, \ldots, N-1$, are zeros of $\hat{S}(\lambda_q)$, and thus we have located $(N-1)L - r$ zeros of $\hat{S}(\lambda_q)$, all of which lie outside the unit circle, in the annulus $1 < |\lambda_q| < 1/k'$.

Let $\hat{S}_j(\lambda_q)$, $j = 1, 2, \ldots, N-1$, be the polynomial in λ_q which has the same zeros as $r_j(t_q, \lambda_q)$ when $t_q \in \mathcal{D}_t$. (The $j = 0$ polynomial is simply a constant.) Then each $\hat{S}_j(\lambda_q)$ is a polynomial of degree $L+1$ if $j = 1, \ldots, N-r-1$, and degree L if $j = N-r, \ldots, N-1$. They all contain the factor $(\lambda_q - \lambda_a)$, where λ_a is the value of λ_q corresponding to $t_q = a$, with $|\lambda_a| > 1$. (This factor belongs to T_q in each case, and not to $\hat{S}(\lambda_q)$.) Otherwise all of their zeros lie on circles centered at the origin and which lie inside the annulus $1 < |\lambda_q| < 1/k'$, and $\hat{S}(\lambda_q)$ contains the factor

$$(\lambda_q - \lambda_a)^{1-N} \prod_{j=1}^{N-1} \hat{S}_j(\lambda_q).$$

However, the polynomial $\hat{S}(\lambda_q)$ must have $(N-1)L$ zeros, so there are r still to locate. We have only found the zeros that lie outside the unit circle, so there must be r zeros inside the unit circle. Consider the polynomial $S(\lambda_q)$ defined by (4.34). The product of the $T(\omega^j x_q, y_q)$ functions becomes a product of $F(\omega^j t_q)$ functions in the $k' \to 0$ limit, so $S(\lambda_q) \propto (a_1 - t_q)(a_2 - t_q) \cdots (a_r - t_q)$, when $t_q \in \mathcal{D}_t$. Denote the corresponding zeros in the λ_q-plane as $\lambda_{a_1}, \lambda_{a_2}, \ldots, \lambda_{a_r}$, where each of the λ_{a_j}, $j = 1, \ldots, r$ are chosen so that $|\lambda_{a_j}| > 1$, so that $\hat{S}(\lambda_q)$ also has the factor

$$\prod_{j=1}^{r} \left(\lambda_q - \lambda_{a_j}^{-1}\right).$$

Hence in the $k' \to 0$ limit, we have located all $(N-1)L$ zeros of $\hat{S}(\lambda_q)$. We have

$$\hat{S}(\lambda_q) \propto \frac{\left(\lambda_q - \lambda_{a_1}^{-1}\right) \ldots \left(\lambda_q - \lambda_{a_r}^{-1}\right)}{(\lambda_q - \lambda_a)^{N-1}} \prod_{j=1}^{N-1} \hat{S}_j(\lambda_q) \tag{5.30}$$

where the proportionality constant is order unity.

Hence the skew parameter has sent r of the zeros of $\hat{S}(\lambda_q)$ inside the unit circle.

5.4.3 The polynomial $\hat{S}(\lambda_q)$ for k' non-zero

We can also work out an integral equation for the polynomial $\hat{S}(\lambda_q)$, when k' is non-zero and L large. As $L \to \infty$, then $a_j \to a$, $j = 1, \ldots, r$, so $\lambda_{a_j} \to \lambda_a$. Hence for L large, $\hat{S}(\lambda_q)$ has a zero of multiplicity r corresponding to the factor $(\lambda_q - \lambda_a^{-1})^r$.

For k' non-zero, we expect that the zeros of $r_j(\lambda_q)$ will still lie in largely the same distribution as they do in the $k' \to 0$ limit, but that perhaps they will shift as k' increases. We still expect $(N-1)L - r$ of the zeros to lie inside the annulus $1 < |\lambda_q| < 1/k'$, and that the r-fold zero at λ_a^{-1} will lie inside the annulus $k' < |\lambda_q| < 1$.

The zeros outside the unit circle can be surrounded by two contours, one lying just outside the unit circle, called $\mathcal{C}_-$, and one lying outside $\mathcal{C}_-$, called $\mathcal{C}_+$, as indicated in Figure 3. Both contours are contained inside the annulus $1 < |\lambda_q| < 1/k'$, and are oriented in the positive direction.

Using Cauchy's integral formula as in the previous section, we have

$$\frac{d}{d\lambda}\ln \hat{S}_j(\lambda) = \frac{1}{2\pi i}\oint_{\mathcal{C}_+} \frac{d\lambda'}{\lambda-\lambda'}\frac{d}{d\lambda'}\ln r_j(\lambda') - \frac{1}{2\pi i}\oint_{\mathcal{C}_-} \frac{d\lambda'}{\lambda-\lambda'}\frac{d}{d\lambda'}\ln r_j(\lambda'),$$

$j = 1,\ldots,N-1$, which is valid when either λ is inside $\mathcal{C}_-$ or outside $\mathcal{C}_+$. This expression is exact for finite L, and it simplifies in the limit $L \to \infty$. From the $k' \to 0$ limit, we see that on $\mathcal{C}_+$ the second term of (4.25) dominates, while on $\mathcal{C}_-$, the first does. Define the polynomial $\xi(\lambda)$ by

$$\xi(\lambda) = \prod_{j=1}^{N-1} \hat{S}_j(\lambda). \tag{5.31}$$

Then integrating with respect to λ, we have for λ outside $\mathcal{C}_+$ and $t' \in \mathcal{D}_t$

$$\begin{aligned}\ln\xi(\lambda) &= c_1 + \frac{1}{2\pi i}\oint_{\mathcal{C}_+} d\lambda' \ln(\lambda-\lambda')\frac{d}{d\lambda'}\ln\left[\prod_{j=1}^{N-1} H_{pq}^{(j)}\,\tau_{N-j}(\omega^j t')\right] \\ &\quad - \frac{1}{2\pi i}\oint_{\mathcal{C}_-} d\lambda' \ln(\lambda-\lambda')\frac{d}{d\lambda'}\ln\left[\prod_{j=1}^{N-1} \bar{H}_{p'q}^{(j)}\,\tau_j(t')\right]\end{aligned} \tag{5.32}$$

where c_1 is a q-independent constant of integration.

As the functions $H_{pq}^{(j)}$ and $\bar{H}_{pq}^{(j)}$ appear as logarithmic derivatives in the integrands, we can neglect any factors they possess that are independent of the q-variables (as these do not contribute to the integrals); we have

$$\begin{aligned}\prod_{j=1}^{N-1} H_{pq}^{(j)} &\propto (\lambda'-\lambda_p)^{L(N-1)}\prod_{j=1}^{N-1}\left(t_p-\omega^j t'\right)^{-jL}, \\ \prod_{j=1}^{N-1} \bar{H}_{p'q}^{(j)} &\propto [\lambda'/(\lambda'-\lambda_{p'})]^{(N-1)L}\prod_{j=1}^{N-1}\left(t_{p'}-\omega^j t'\right)^{jL}.\end{aligned} \tag{5.33}$$

Substituting these and (5.32) into (5.31) and expressing the integrands in terms of t' and λ' only (rather than x', y' etc.), and evaluating the integrals that contain only λ', we get

$$\begin{aligned}\ln\xi(\lambda) &= c_2 + (N-1)\ln\bar{\alpha}_q \\ &\quad + \frac{1}{2\pi i}\oint_{\mathcal{C}_+} d\lambda' \ln(\lambda-\lambda')\frac{d}{d\lambda'}\ln\left[\prod_{j=1}^{N-1}\frac{\tau_{N-j}(\omega^j t')}{(t_p-\omega^j t')^{jL}}\right] \\ &\quad - \frac{1}{2\pi i}\oint_{\mathcal{C}_-} d\lambda' \ln(\lambda-\lambda')\frac{d}{d\lambda'}\ln\left[\prod_{j=1}^{N-1}\tau_j(t')(t_{p'}-\omega^j t')^{jL}\right]\end{aligned} \tag{5.34}$$

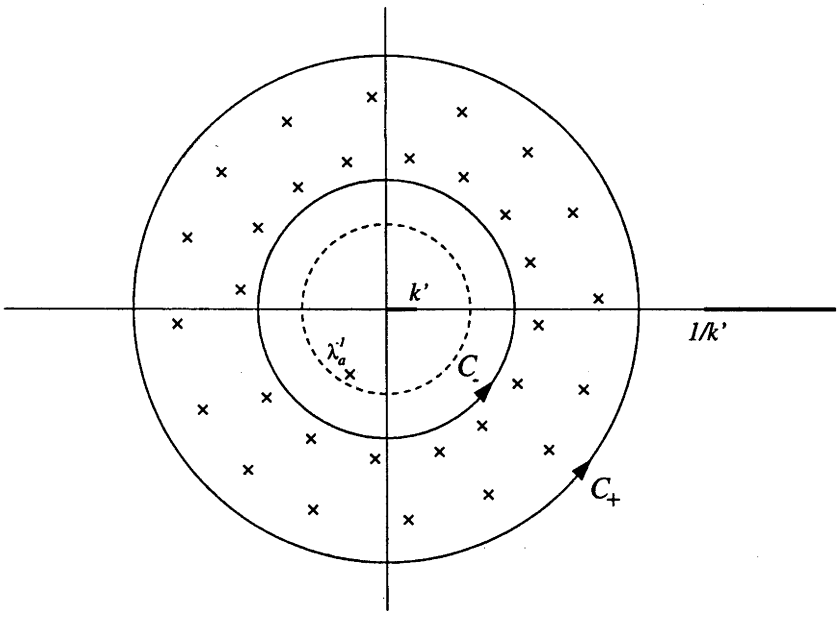

Figure 5.6: The cut λ_q-plane, showing the branch cuts for t_q as a function of λ_q. The zeros of the polynomial $\hat{S}(\lambda_q)$ are indicated ($\times$), with $(N-1)L-r$ of them lying between the contours $\mathcal{C}_+$ and $\mathcal{C}_-$, and r lying inside the unit circle (the broken line), where we indicate the case $r=1$.

(where c_2 is a new q-independent constant of integration). The next step, following [28] and [29] would be to integrate this expression by parts. However the integrands have branch points when the factor $(a-t)$ occurs in the argument of the logarithm in the integrands, corresponding to branch points at $0, \lambda_a^{-1}, \lambda_a$ and ∞ in the λ_q-plane. We use (5.20) and (5.27) to manifest the factors $(a-t)$ explicitly, writing them as $a^N - t^N$, which is an analytic function of λ. Once these factors are removed, the functions remaining in the integrands contain no branch points, so the integrals are then single-valued around their respective contours, and hence we can perform an integration by parts. In fact, the resulting integrands have no zeros at all between the contours $\mathcal{C}_+$ and $\mathcal{C}_-$, so both of these contours can be shifted to the unit circle, and the integrals combined, to give

$$\begin{aligned}\ln \xi(\lambda) &= c_1 + (N-1)\ln \bar{\alpha}_q + (N-r-1)\ln(\lambda-\lambda_a) \\ &+ (N-2r)\ln\left[(\lambda-\lambda_a^{-1})/\lambda\right] \\ &+ \frac{N}{2\pi i}\oint \frac{d\lambda'}{\lambda-\lambda'}\ln g(t') - \frac{1}{2\pi i}\oint \frac{d\lambda'}{\lambda-\lambda'}U[t']\end{aligned}$$

where

$$g(t) = \prod_{j=1}^{r-1}(a-\omega^j t) \Big/ \prod_{j=r+1}^{N-1}(a-\omega^j t) \tag{5.35}$$

and

$$\begin{aligned} U[t] &= \sum_{j=1}^{N-1} \ln\left[(t_p-\omega^j t)^{jL}(t_{p'}-\omega^j t)^{jL}\tau_j(t)_{r=0}\Big/\tau_{N-j}(\omega^j t)_{r=0}\right] \\ &= \sum_{j=1}^{N-1}\left\{jL\ln\left[(t_p-\omega^j t)(t_{p'}-\omega^j t)\right] + (N-2j)\ln\tau_2(\omega^{j-1}t)_{r=0}\right\}. \end{aligned}$$

The polynomial $\hat{S}(\lambda_q)$, is related to $\xi(\lambda_q)$ by (5.30) and (5.31), so we get

$$\begin{aligned} \ln\hat{S}(\lambda_q) &= c_3 + (N-1)\ln\bar{\alpha}_q + (N-r)\ln(\lambda_q-\lambda_a^{-1}) - r\ln(\lambda_q-\lambda_a) \\ &- (N-2r)\ln\lambda_q + \frac{N}{2\pi i}\oint\frac{d\lambda'}{\lambda_q-\lambda'}\ln g(t') - \frac{1}{2\pi i}\oint\frac{d\lambda'}{\lambda_q-\lambda'}U[t']. \end{aligned}$$

(where c_3 is independent of q) for $|\lambda_q|>1$. Finally, we can replace $1/(\lambda_q-\lambda')$ with $(\lambda_q+\lambda')/[2\lambda'(\lambda_q-\lambda')]$ while only adding on a q-independent constant, so if we let $\lambda'=e^{i\theta}$, and $t'=\Delta(\theta)$, we get

$$\begin{aligned} \ln\hat{S}(\lambda_q) &= c_4 + (N-1)\ln\bar{\alpha}_q - N\,I(\lambda_q) \\ &- \tfrac{1}{2}\left[A(\lambda_q^{-1},t_p) + A(\lambda_q^{-1},t_{p'}) + B(\lambda_p,\lambda_q^{-1}) + B(\lambda_{p'},\lambda_q^{-1})\right] \\ &+ (N-r)\ln(\lambda_q-\lambda_a^{-1}) - r\ln(\lambda_q-\lambda_a) - (N-2r)\ln\lambda_q \end{aligned} \tag{5.36}$$

where

$$I(\lambda_q) = \frac{1}{4\pi i}\oint\frac{d\lambda'}{\lambda'}\frac{\lambda_q+\lambda'}{\lambda_q-\lambda'}\ln g(t') \tag{5.37}$$

when $|\lambda_q|<1$.

5.5 The free energy and interfacial tension

Consider once again equation (4.25), taking $k=j$, $l=0$. From the limit $k'\to 0$, we see that when $|\lambda_q|>1$ and L is large, the second term of the right hand side exponentially dominates the first. Thus in the $L\to\infty$ limit, we have

$$T_q\,\Lambda_q^{(j,0)}\,\hat{T}_{\bar{q}j0} = H_{pq}^{(j)}\,\tau_{N-j}(\omega^j t_q) + \text{an exponentially smaller term.} \tag{5.38}$$

We take the product of this equation over j running from 0 to $N-1$, and ignore the second term which is negligible for large L. From equations (4.21) and (4.22) we have

$$\prod_{j=0}^{N-1} \Lambda_q^{(j,0)} = \left[\frac{(\omega\mu_p)^{N(N-1)/2}}{N^N (y_p - x_q)^N} \prod_{j=1}^{N-1} (y_{p'} - \omega^j y_q)^j (x_p - \omega^{N-j-1} y_q)^j \right]^L$$

and

$$\prod_{j=0}^{N-1} H_{pq}^{(j)} = \left[\frac{(\omega\mu_p)^{N(N-1)/2}}{(y_p^N - x_q^N)^N} \prod_{j=1}^{N-1} \left(t_p - \omega^{N-j-1} t_q\right)^j \right]^L ,$$

so using these and equations (4.36) and (4.15) we derive an expression for the eigenvalues $T_q\hat{T}_q$:

$$\begin{aligned} \left(T_q\hat{T}_q\right)^N \hat{S}(\lambda_q)^2 &= e^{-\pi i L(N-1)(N-2)/3} \left(\lambda_q^2 \big/ \lambda_p \lambda_{p'}^3\right)^{(N-1)L/2} (\bar{\alpha}_q)^{2(N-1)} \\ &\times (g_{pq} g_{p'q})^{NL} D^N \prod_{j=0}^{N-1} \tau_{N-j}(\omega^j t_q)^2 \\ &\times \prod_{j=1}^{N-1} \left[\left(t_q - \omega^j t_p\right)\left(t_q - \omega^j t_{p'}\right)\right]^{-2(N-j)L} . \end{aligned} \tag{5.39}$$

We take logarithms, substitute in the expression for $\hat{S}(\lambda_q)$ from the previous section, and also note that

$$\begin{aligned} \sum_{j=0}^{N-1} \ln \tau_{N-j}(\omega^j t_q) &= \tfrac{1}{2}\left[C(\lambda_p, t_q) + C(\lambda_{p'}, t_q)\right] + L\pi i(N-1)(2N-1)/6 \\ &- r \ln(a^N - t_q^N) + N \sum_{j=0}^{r-1} \ln(a - \omega^j t_q). \end{aligned}$$

Equation (5.39) contains an unknown multiplicative term, the matrix D^N, which is independent of q. Because there is already an unknown term (the integration constant appearing in (5.36)), we can in fact write all terms which are independent of q as a single constant, $m_{pp'}$, which will be determined shortly. We write (5.39) as

$$N \ln\left(T_q\hat{T}_q\right) = m_{pp'} + E_{pq} + E_{p'q} + 2NF_q. \tag{5.40}$$

The function E_{pq}, which is proportional to L, and therefore contributes to the bulk part of the partition function was given in equation (4.43), and the function F_q, which is independent of L, is given by

$$F_q = -r \ln \mu_q - \ln\left[(\lambda_q - \lambda_a^{-1})/\lambda_q\right] + \sum_{j=0}^{r-1} \ln(a - \omega^j t_q) - I(\lambda_q).$$

This depends on p and p' only through a (and also λ_a), and contributes to the interfacial tension.

The constant $m_{pp'}$ is calculated as follows. Consider the $j = N-1$ case of equation (5.38); ignoring the exponentially small corrections (i.e. assuming L is large), the right hand side is an exactly known function (the τ_{N-j} function in this case being unity). Applying the automorphism R to both sides, we find

$$T_{Rq}\hat{T}_q = (g_{pq}g_{qp})^L \quad \text{and} \quad T_q\hat{T}_{Rq} = (g_{p'q}g_{qp'})^L . \tag{5.41}$$

From (5.40), we see that the constant $m_{pp'}$ is therefore given by

$$2m_{pp'} = \ell_p + \ell_{p'} - 2N(F_q + F_{Rq})$$

where

$$\ell_p = NL\ln(g_{pq}g_{qp}) - E_{pq} - E_{p,Rq}.$$

The function $E_{p,Rq}$ is defined by the analytic continuation formulae and and we find that $\ell_p + \ell_{p'} = 0$. The function F_{Rq} is defined in terms of the analytic continuation of $I(\lambda_q)$ to $|\lambda_q| < 1$, and we find that $I(\lambda_q)$ defined by (5.37) has the analytical continuation formula

$$I_{\rm ac}(\lambda_q) + I(1/\lambda_q) = \ln g(t_q) \tag{5.42}$$

when $|\lambda_q| < 1$, and where $g(t_q)$ is given by (5.35). Hence we find that

$$m_{pp'} \;=\; -N\,(F_q + F_{Rq}) \;=\; -N\ln(-\lambda_a k'/k^2).$$

Let $2v_r = 2F_q + m_{pp'}$, so

$$\begin{aligned} v_r \;&=\; r\ln\mu_q - \sum_{j=0}^{r-1}\ln(a-\omega^j t_q) + \ln\left[(\lambda_q - \lambda_a^{-1})/\lambda_q\right] \\ &+\; \tfrac{1}{2}\ln(-k'\lambda_a/k^2) + I(\lambda_q). \end{aligned} \tag{5.43}$$

We can re-write (5.43) so that it depends only on a, rather than on both a and λ_a. The contour of integration of $I(\lambda_q)$ as defined by (5.37) is around the unit circle in the λ'-plane; if we change the variable of integration to t', where t' and λ' are related by (4.8) then we integrate around the branch cut between η and $1/\eta$ in the t'-plane. Writing this as a line integral along one side of the cut, we can rewrite $I(\lambda_q)$ as

$$\begin{aligned} I(\lambda_q) \;&=\; \frac{1}{\pi}\int_\eta^{1/\eta} dt'\Psi(\lambda_q,t')\frac{d}{dt'}\ln h(-\omega^{r/2}t'/a) + r\ln a - \ln\left[(\lambda_q-\lambda_a^{-1})/\lambda_q\right] \\ &-\; \tfrac{1}{2}\ln(-\lambda_a k'/k^2) + \tfrac{1}{2}\ln h(-\omega^{r/2}/a) \end{aligned}$$

where the functions $A(t)$, $h(t)$ and $\Psi(\lambda,t)$ are defined by (4.37), (4.49) and (4.50) respectively. Letting $m=-\omega^{r/2}/a$, we find that v_r is given by (4.47).

The variable a can take on any of the L values allowed by equation (5.28). Thus we have the following expression for the L largest eigenvalues of the transfer matrix;

$$N\ln\left(T_q\hat{T}_q\right)=L(E_{pq}+E_{p'q})-2v_r. \tag{5.44}$$

To calculate the partition function, for large L, the sum will be dominated by these L bound-state eigenvalues. As $L\to\infty$, the sum becomes an integral over the allowed values of a, so we write

$$Z_r=\oint\rho(a)\left(T_q\hat{T}_q\right)^M da,$$

where $\rho(a)$ is some distribution function which is independent of M and L. Noting that E_{pq} is independent of a, then the free energy is

$$-N\psi/k_BT=\tfrac{1}{2}\left(E_{pq}+E_{p'q}\right)$$

(which reduces to the analytical continuation of the ground state eigenvalue of the system calculated in [29] when $p=p'$). Thus the interfacial tension is given by

$$e^{-M\epsilon_r/k_BT}=\oint\rho(a)e^{-2Mv_r}da. \tag{5.45}$$

For M large, this integral can be evaluated by the saddle-point method; the integral is dominated by the contribution from its saddle point, and so as $M\to\infty$ the integral is given by the value of its integrand at its saddle point, together with some multiplicative factors with which we are unconcerned.

We can now follow the arguments of References [30] and [32] regarding the location of the saddle point. In [32] it was demonstrated that in the limit $k'\to 0$, the function v_r possesses a saddle point which is independent of p and p', and hence the integral can be evaluated by deforming the contour of integration to pass through this saddle point. Assuming that this holds for general k', then we arrive at equation (4.51) for the interfacial tension. As expected, this depends on q but not on p or p'.

Further comments are included in Section 4.5 of Chapter 4.

5.5.1 Continuation to $|\lambda_q|<1$

To compare this to the work of McCoy and Roan mentioned in Section 4.5.1, we have to analytically continue our band of eigenvalues back to the region $|\lambda_q|<1$.

When $|\lambda_q| > 1$ and $0 < \arg t_q < 2\pi/N$, the eigenvalues are given by equation (5.44), where v_r is given by equation (4.47) when we choose $m = -\omega^{r/2}/a$, or equivalently, by equation (5.43). We consider the latter expression.

To analytically continue this to $|\lambda_q| < 1$ and $-2\pi/N < \arg t_q < 0$, we use the analytical continuation formula (5.42) for $I(\lambda_q)$ for $|\lambda_q| < 1$.

Re-writing equation (5.35) defining the function $g(t)$ as $g(r, a, t)$, to exhibit its dependence on a and r explicitly, we have the relation

$$g(r, a, t) = \frac{\omega^{r(1-r)}}{g(N-r, \omega^{-r}a, t)},$$

so if we write $v_r = v(r, a, t_q, \lambda_q)$ when $|\lambda_q| > 1$ and $0 < \arg t_q < 2\pi/N$, and the analytic continuation of the function to the region $|\lambda_q| < 1$, $-2\pi/N < \arg t_q < 0$ as $v_{\rm ac}(r, a, t_q, \lambda_q)$, we have

$$v_{\rm ac}(N-r, \omega^{-r}a, t_q, \lambda_q) = v(r, a, \omega t_q, \lambda_q^{-1})$$

when $|\lambda_q| < 1$ and $-2\pi/N < \arg t_q < 0$. Hence applying the rotation R, which changes t_q to ωt_q and λ_q to $1/\lambda_q$, has the effect of changing r to $N-r$ and a to $\omega^{-r}a$.

Hence for $|\lambda_q| < 1$, we can write

$$v_r^{\rm ac} = -r \ln \mu_q - \sum_{j=1}^{r} \ln(a - \omega^j t_q) - \frac{1}{4\pi i} \oint_{C_\lambda} \frac{d\lambda'}{\lambda'} \frac{\lambda' + \lambda_q^{-1}}{\lambda' - \lambda_q^{-1}} \ln j(t')$$

where $j(t) = (a-t)(a-\omega t)^2 \cdots (a-\omega^{r-1}t)^2(a-\omega^r t)$. This is identical to equation (4.53) if we take $m_p = r$, and

$$v_j = \omega^{j-1/2}/a, \qquad j = 1, \cdots, r$$

and also replace our t_q by $\omega^{-1}t_q$ (due to the different convention adopted concerning which values of t_q correspond to which choice of λ_q).

Part III

The Potts model

CHAPTER 6

The Potts model

Generalisations of the Ising model to higher-state spins have been introduced by a number of authors. Notable have been the Ashkin-Teller model, a generalisation to four-state spins, introduced in 1943 [6], and the Potts and clock models, which were introduced by Potts in 1952 [102], and independently studied by Kihiara et al. in 1954 [76]. Potts located the critical temperature of the model for all values of N using a duality relation similar to that introduced by Kramers and Wannier for the Ising model [78].

For the Potts model, spins $\sigma = 0, 1, \ldots, N-1$ sit on the sites of the lattice and interact with a delta-function interaction energy $-J\delta(\sigma, \sigma')$ or $-\bar{J}\delta(\sigma, \sigma')$, and the total energy is given by

$$-\mathcal{H}(s) = -J \sum_{\text{horiz.}} \delta(\sigma, \sigma') - \bar{J} \sum_{\text{vert.}} \delta(\sigma, \sigma').$$

The partition function is defined as usual, and we are interested in the partition functions of the model on finite lattices with skewed boundary conditions.

For an $L \times M$ lattice with toroidal boundary conditions, we identify the first and last spins in each row and the top and bottom spins in each column. If we skew the boundary conditions, we instead identify $\sigma_1 = \sigma_{L+1} + h$, $\sigma_i^{(1)} = \sigma_i^{(M+1)} + v$, where h and v are the horizontal and vertical skewing parameters, and σ_1, σ_{L+1} are the first and last spins in a horizontal row, and $\sigma_i^{(1)}, \sigma_i^{(M+1)}$ are the bottom and top spins in column i. We shall denote the partition function of the model on the $L \times M$ lattice with skewing parameters h and v as Z_{LM}^{hv}. For a $\mathbf{Z}_N$ invariant model, we can restrict the skew parameters h and v to take the values $0, 1, \ldots, N-1$ without loss of generality.

The two-dimensional Potts model is related to a number of other problems in statistical mechanics and graph theory, which are discussed in for example References [19, 88, 118] and references contained therein.

Among other subjects discussed in Reference [118], some duality relations for the Potts models are given. These relate partition functions in the high and low temperature phases, and can be used to determine information about the phase diagram of a model, and especially to locate its critical point. We mention one duality relation here for the N-state models which is not mentioned in Reference [118], but which can be derived easily by following the derivation of the duality relation of the superintegrable chiral Potts model in Reference [26],

$$\sum_{h=0}^{N-1}\sum_{v=0}^{N-1} \omega^{lh+mv} Z^{hv} = N Z^{m,-l}. \tag{6.1}$$

For $N > 2$ the Potts model is exactly solvable only at criticality [15]. The solution was obtained by Baxter in 1973, by relating the Potts model to a staggered six-vertex model on a related lattice. The staggered vertex model has different Boltzmann weights on the two sub-lattices, and is in general not exactly solvable. However, when the weights on the two sub-lattices become equal, it reduces to the usual homogeneous six-vertex model, which can be solved exactly in the thermodynamic limit. This corresponds to the Potts model being critical, and also to the model being self-dual [19]. As well as calculating the free energy per site, Baxter also deduced that the Potts model has a continuous transition when $N \leq 4$ and a transition of the first order when $N > 4$.

The Potts model is critical (self-dual) when its interaction coefficients satisfy

$$(e^{J/k_BT} - 1)(e^{\bar{J}/k_BT} - 1) = N,$$

and the free energy per site of the critical Potts model can be written in terms of the free energy of the six-vertex model, which was given in Chapter 2.

As well as the free energy per site in the thermodynamic limit, we are also interested in exact solutions on finite lattices. The partition function of the Ising model has been calculated explicitly and exactly for an $L \times M$ lattice of finite but arbitrary extent, with toroidal boundaries imposed. This was achieved by Onsager's student Kaufman in 1949 [72], wherein the partition function is expressed as a sum of four terms which are finite products of elementary functions. The only other two-dimensional lattice model whose partition function has been calculated exactly and explicitly on a finite lattice is the superintegrable chiral Potts model, by Baxter in 1989 [25, 26]. **The partition function on a lattice with** cylindrical boundary conditions was calculated as a single product of a finite number of terms. Also, the partition functions of other models such as the six- and eight-vertex models

can be calculated on finite lattices, but only in terms of the solution of sets of transcendental equations.

We consider the solution of the critical three-state Potts model on finite lattices, and attempt to generalise a result of the Ising model to the Potts model. Given that the three-state Potts model is such a simple generalisation of the Ising model, and that the critical model is integrable, we might hope that this is possible, but unfortunately this does not seem to be the case.

A large part of our investigations involve calculating exactly the partition functions of the critical Potts models on finite lattices with toroidal boundary conditions skewed in both the horizontal and vertical directions. The partition functions are expressed as polynomials in a particular variable, and we analyse the zeros of the polynomials and of certain linear combinations of the partition functions, and attempt to find simple contours on which they lie.

There have been many studies of the zeros of the partition function of lattice models since Lee and Yang's famous circle theorem in 1952 [79], and studies for the Potts models have been carried out in for example References [21,86–88].

Baxter has studied the zeros of the partition function of the zero-temperature anti-ferromagnetic N-state Potts model on the triangular lattice, expressing the partition function Z as a polynomial in the variable N. Martin et al. consider the three-state Potts model on triangular and square lattices in two and three dimensions, expressing the partition functions as polynomials in a temperature-like variable. Here we study the square-lattice models at criticality, expressing Z as a polynomial in a variable z related to the anisotropy (often called the spectral parameter) of the model.

We also use our results to investigate the finite-size corrections of the three state Potts model at criticality. There has been a large amount of theoretical work done on finite-size corrections for critical lattice models in recent years, and we present a brief summary. The finite-size corrections of a model with toroidal boundaries are characterised by the so-called modular invariant partition function, $Z(q)$, where q is the modular parameter, which is related to the dimensions and anisotropy of the lattice. For a lattice with $\mathcal{N}$ sites, the partition function $Z_{\mathcal{N}}$ is related to the free energy per site of the infinite system f by

$$\ln Z_{\mathcal{N}} = -\mathcal{N} f / k_B T + \ln Z(q) + \text{correction terms}, \tag{6.2}$$

where the correction terms should vanish as $\mathcal{N} \to \infty$.

Given the relatively small sizes of the lattices considered, we find this relation to hold to a remarkable degree accuracy. In particular, for a spatially isotropic model on a square $L \times L$ lattice, for which $\ln Z(q) \sim 1$, the correction terms seem to approach zero as $1/L$, with a small (~ 0.04) numerical coefficient.

Our results have been published in Reference [95].

6.1 The Pfaffian solution of the Ising model

An alternative solution to the Ising model was discovered in 1963 by Kasteleyn [71]. This combinatorial solution was based on the solution of the dimer problem, which was found independently and simultaneously in 1961 by Kasteleyn [70] and Temperley and Fisher [110].

The partition functions of the zero-field Ising model on finite square lattices with a variety of boundary conditions can be related to the Pfaffians of certain anti-symmetric matrices. For lattices with free boundary conditions in both directions, or with cylindrical boundaries (periodic in one direction and free in the other), anti-symmetric matrices A_f and A_c can be found such that the partition functions can be written as the Pfaffian of the corresponding matrix, $\mathrm{Pf}\, A_f$ and $\mathrm{Pf}\, A_c$. Unfortunately, while the elements of the matrices are known, the structure of the matrices is such that their determinants have never been evaluated explicitly.

However, for lattices wound onto a torus, the partition function can be expressed as a linear combination of the Pfaffians of four matrices A_i, $i = 1, 2, 3, 4$;

$$Z = \tfrac{1}{2}\left[-\mathrm{Pf}\, A_1 + \mathrm{Pf}\, A_2 + \mathrm{Pf}\, A_3 + \mathrm{Pf}\, A_4\right], \tag{6.3}$$

and the Pfaffians of the matrices A_i can be written out explicitly. Defining

$$z_1 = \tanh E_1/k_BT, \qquad z_2 = \tanh E_2/k_BT.$$

they have determinant

$$\det A_i = \prod_{\theta_1,\theta_2} \left[(1+z_1^2)(1+z_2^2) - 2z_1(1-z_2^2)\cos\theta_1 - 2z_2(1-z_1^2)\cos\theta_2\right] \tag{6.4}$$

where the product $\prod_{\theta_1}$ is over $\theta_1 = 2\pi l/L$ if $i = 1, 2$, and is over $\theta_1 = \pi(2l-1)/L$ if $i = 3, 4$ ($l = 1, 2, \ldots, L$); the product $\prod_{\theta_2}$ is over $\theta_2 = 2\pi m/M$ if $i = 1, 3$, and is over $\theta_2 = \pi(2m-1)/M$ if $i = 2, 4$ ($m = 1, 2, \ldots, M$).

The Pfaffian is related to the determinant of the anti-symmetric matrix by

$$\det A = \left(\mathrm{Pf}\, A\right)^2,$$

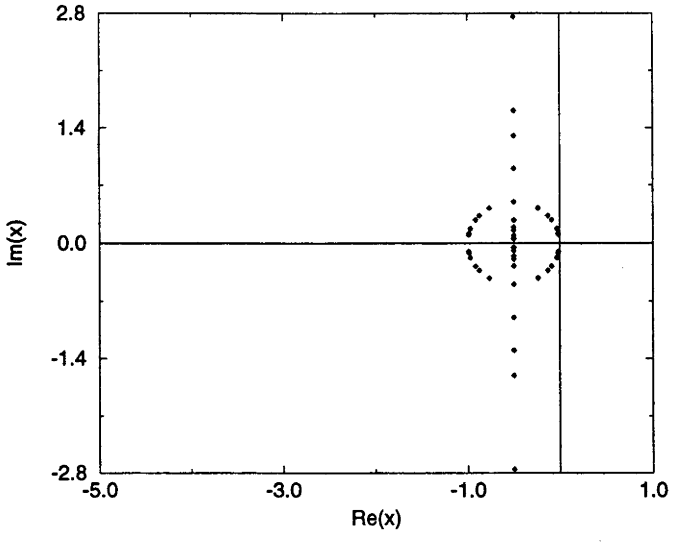

Figure 6.1: The zeros of the Pfaffian Pf A_4 for $L = M = 4$.

and hence given the determinants, we only know the Pfaffians in equation (6.3) up to a choice of $\pm$ signs. These must be determined, and this can be done by considering high and low temperature limits, as in Reference [89], where the signs are found to depend both on the temperature, and whether or not the model has an interface in its low-temperature configuration.

We consider only the critical model on finite lattices. The Ising model is critical when $k = 1$, with k given by equation (1.2), which corresponds to $|z_1 z_2| + |z_1| + |z_2| = 1$. We write $z_1 = 1/(1+2x)$ and $z_2 = x/(1+x)$, so that the Boltzmann weights of the critical model become

$$W(0) = \frac{1+x}{x}, \qquad \bar{W}(0) = 1 + 2x. \tag{6.5}$$

The expression for the determinants becomes

$$\begin{aligned} \det A_i &= [(1+x)(1+2x)]^{-2LM} \\ &\quad \times \prod_{\theta_1} \prod_{\theta_2} \left[(1+2x+2x^2)^2 - 4x^2(1+x)^2 \cos\theta_1 - (1+2x)^2 \cos\theta_2 \right], \end{aligned}$$

so at criticality, $\det A_1 = 0$.

We denote the partition function of the Ising model on a toroidal lattice with periodic boundaries in both the horizontal and vertical directions by Z_{LM}^{++}, with

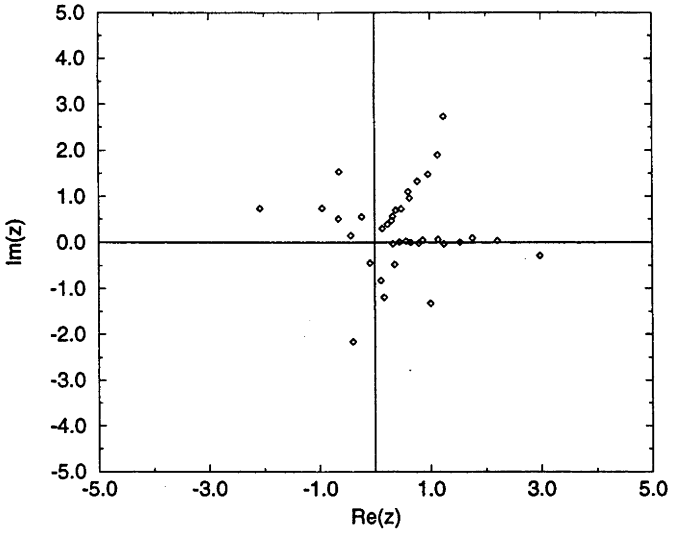

Figure 6.2: The zeros of the partition function of the three-state self-dual Potts model on a 3×3 lattice with toroidal boundary conditions, in the complex z-plane.

anti-periodic boundaries in the horizontal direction by Z_{LM}^{-+}, in the vertical by Z_{LM}^{+-}, and in both directions by Z_{LM}^{--}. From Chapter V of [89], we have, for the critical model,

$$\begin{aligned}
Z_{LM}^{++}(x) &= \tfrac{1}{2}\rho(x)\left[(\det A_2)^{1/2} + (\det A_3)^{1/2} + (\det A_4)^{1/2}\right] \\
Z_{LM}^{+-}(x) &= \tfrac{1}{2}\rho(x)\left[-(\det A_2)^{1/2} + (\det A_3)^{1/2} + (\det A_4)^{1/2}\right] \\
Z_{LM}^{-+}(x) &= \tfrac{1}{2}\rho(x)\left[(\det A_2)^{1/2} - (\det A_3)^{1/2} + (\det A_4)^{1/2}\right] \\
Z_{LM}^{--}(x) &= \tfrac{1}{2}\rho(x)\left[(\det A_2)^{1/2} + (\det A_3)^{1/2} - (\det A_4)^{1/2}\right]
\end{aligned}$$

where

$$\rho(x) = [(1+x)(1+2x)]^{-ML}$$

and the square roots are chosen to be positive. Thus the partition functions of the critical models depend non-trivially on the Pfaffians of only three matrices, and we have the self-duality relation

$$Z_{LM}^{++}(x) = Z_{LM}^{+-}(x) + Z_{LM}^{-+}(x) + Z_{LM}^{--}(x).$$

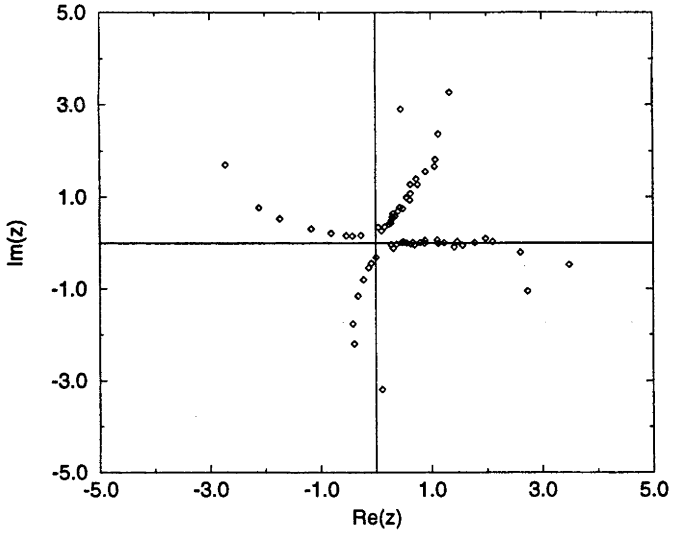

Figure 6.3: The zeros of the partition function of the three-state self-dual Potts model on a 4 × 4 lattice with toroidal boundary conditions, in the complex z-plane.

These linear relations can be inverted, to give the following;

$$2\rho(x)(\det A_2)^{1/2} = Z_{LM}^{-+}(x) + Z_{LM}^{--}(x)$$
$$2\rho(x)(\det A_3)^{1/2} = Z_{LM}^{+-}(x) + Z_{LM}^{-+}(x)$$
$$2\rho(x)(\det A_4)^{1/2} = Z_{LM}^{+-}(x) + Z_{LM}^{--}(x)$$

which demonstrates that particular linear combinations of the skewed-boundary partition functions are equal to single Pfaffians.

The zeros of the various partition functions are very complicated, and only asymptote to lie on simple contours as the thermodynamic limit is approached. In contrast, the zeros of the Pfaffians formed by taking the above linear combinations of the partition functions are extremely simple, and lie exactly on simple contours for finite L and M. As an example of this, we have plotted the zeros of the Pfaffian $\mathrm{Pf}\, A_4$ for $L = M = 4$ in Figure 6.1. The zeros lie exactly on the circle $|x+1/2| = 1/2$ and the line $\mathrm{Re}(x) + 1/2 = 0$, for finite L and M, in contrast to the zeros of the partition functions, which are much more complicated.

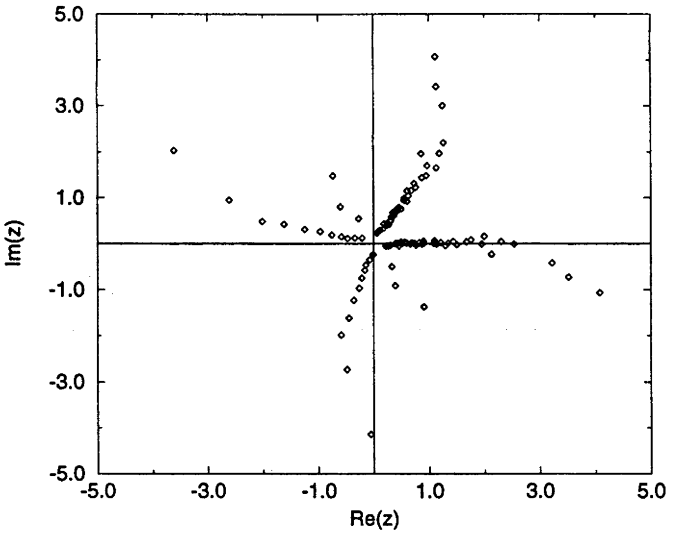

Figure 6.4: The zeros of the partition function of the three-state self-dual Potts model on a 5 × 5 lattice with toroidal boundary conditions, in the complex z-plane.

6.2 The critical three-state Potts model

The Boltzmann weights of the $N = 3$ self-dual Potts model can be parameterised as

$$W(0) = (1 + x)/x, \quad W(1) = W(2) = 1 \tag{6.6}$$

$$\bar{W}(0) = 1 + 3x, \quad \bar{W}(1) = \bar{W}(2) = 1. \tag{6.7}$$

This parameterisation is an obvious generalisation of that used for the Ising model in the previous section (6.5). The variable x is related to the spatial anisotropy of the lattice, with $x = \pm 1/\sqrt{3}$ corresponding to an isotropic lattice. The partition function will be a Laurent polynomial in the variable x whose coefficients are positive integers; it can be written as x^{-2ML} multiplied by a polynomial in x with degree at most $4ML$.

Replacing x by $1/3x$ interchanges $W(0)$ and $\bar{W}(0)$, which corresponds to rotating the lattice through 90 degrees and interchanging L and M. When unskewed toroidal boundary conditions are imposed onto the lattice, this substitution leaves the partition function invariant, and so Z in this case can be expressed as a polynomial in the variable $y = x + 1/3x$, with degree at most $2ML$.

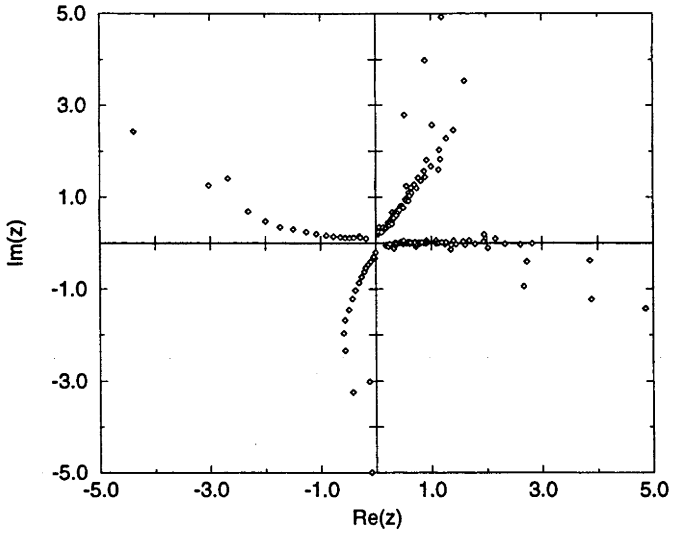

Figure 6.5: The zeros of the partition function of the three-state self-dual Potts model on a 6×6 lattice with toroidal boundary conditions, in the complex z-plane.

6.2.1 Toroidal and skew-toroidal boundary conditions

In general we expect nine partition functions with the different skewed boundary conditions. Using obvious symmetries, these nine functions reduce to five, and only four for a square lattice. Reflecting the lattice horizontally or vertically, we have

$$Z_{LM}^{h,v}(x) = Z_{LM}^{-h,v}\left(\frac{1}{3x}\right) = Z_{LM}^{h,-v}\left(\frac{1}{3x}\right) = Z_{LM}^{-h,-v}(x),$$

and so we are just left with the following five partition functions:

$$Z_{LM}^{00}(x) = Z_{LM}(x), \qquad Z_{LM}^{01}(x) = Z_{LM}^{02}(x), \qquad Z_{LM}^{10}(x) = Z_{LM}^{20}(x)$$

$$Z_{LM}^{11}(x) = Z_{LM}^{22}(x), \qquad Z_{LM}^{12}(x) = Z_{LM}^{21}(x).$$

Rotating the lattice through 90 degrees is equivalent to interchanging $W(n)$ with $\bar{W}(n)$ and L with M. This gives the symmetry relation

$$Z_{LM}^{h,v}(x) = Z_{ML}^{-v,h}\left(\frac{1}{3x}\right),$$

so on a square $L \times L$ lattice, we also have the relation

$$Z_{LL}^{01}(x) = Z_{LL}^{10}(x)$$

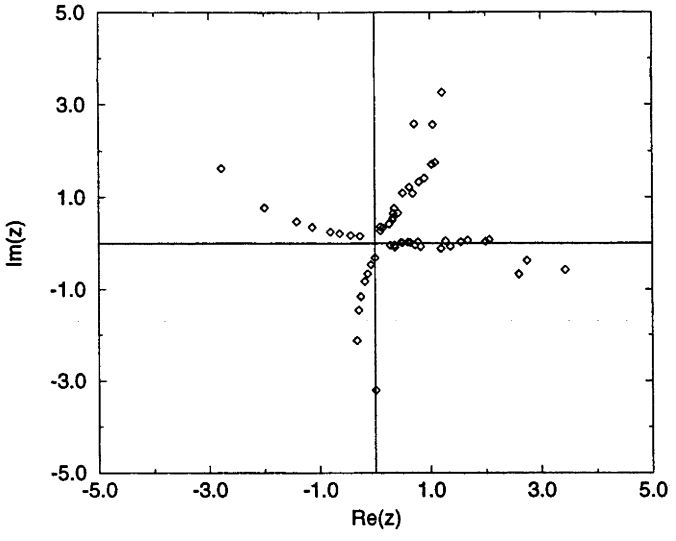

Figure 6.6: The zeros of the partition function $Z_{44}^{01}(z)$ on a 4×4 lattice with the skew-toroidal boundary conditions $h = 0$, $v = 1$.

so there are only four different partition functions on a square lattice.

Finally, we observed the self duality relation (6.1)

$$Z_{LM}^{00}(x) = Z_{LM}^{01}(x) + Z_{LM}^{10}(x) + Z_{LM}^{11}(x) + Z_{LM}^{12}(x).$$

6.2.2 Large-lattice free energy

To end this section, we include the results for the Potts model free energy per site in the thermodynamic limit. The exact solution indicates the analytic properties of the free energy per site f, and this in turn tells us the contours towards which the zeros of the finite-lattice partition functions will asymptote as the lattice size increases. Guided by the results of the Ising model, we hoped to be able to find linear combinations of the skewed-boundary partition functions which would have zeros lying exactly on these contours. The exact free energy per site is used in a later section, when we consider the finite-size corrections of the model in the context of the modular invariant partition function.

The free energy of the Potts model at criticality can be found either by its Temperley-Lieb equivalence to an ice-type model as in [15,19], or by the inversion relation method [20]. We reproduce some of the details of the latter method here,

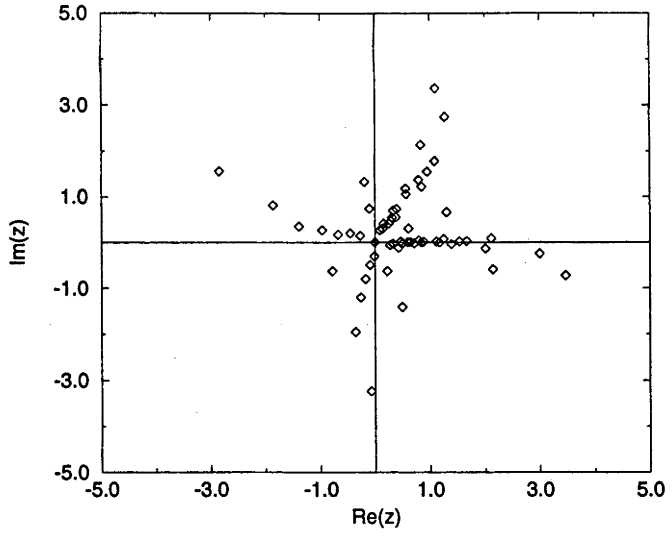

Figure 6.7: The zeros of the partition function $Z_{44}^{11}(x)$ on a 4×4 lattice with the skew-toroidal boundary conditions $h = 1$, $v = 1$.

along with the exact solution.

Following [20], we use the variable μ, where $2\cos\mu = \sqrt{N}$, so $\mu = \pi/6$ for the $N = 3$ model. We then re-parameterise the anisotropy x in terms of the spectral parameter v,

$$x = \frac{1}{\sqrt{3}} \frac{\sin(\mu - v)}{\sin v},$$

and the Boltzmann weights become

$$W(0) = \frac{\sin(\mu + v)}{\sin(\mu - v)}, \quad \bar{W}(0) = \frac{\sin(2\mu - v)}{\sin v}, \tag{6.8}$$

the others remaining unity. Regarding v as a variable, we denote the partition function per site for a finite lattice as $\kappa_{LM}(v) = (Z_{LM})^{1/2LM}$, and for the infinite lattice

$$\kappa(v) = \lim_{L,M\to\infty} \kappa_{LM}(v),$$

where the limit is taken through large values of both L and M.

In Reference [20] a number of relations for $\kappa(v)$ are given, including the inversion, periodicity and crossing symmetry relations. The latter two are

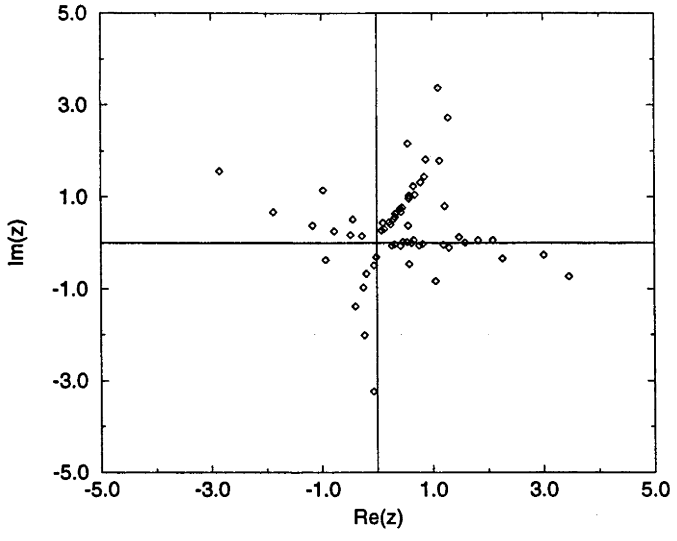

Figure 6.8: The zeros of the partition function $Z^{12}_{44}(x)$ on a 4×4 lattice with the skew-toroidal boundary conditions $h = 1$, $v = 2$.

$$\kappa(v) = \kappa(\pi + v), \qquad \kappa(v) = \kappa(\mu - v). \tag{6.9}$$

To match the normalisation of the weights (6.8) with those used in [20], we should take the constant ρ_0 therein to be

$$\rho_0 = \frac{\sin\mu \sin 2\mu}{\sin v \sin(\mu - v)}.$$

The inversion relations for $\kappa(v)$ then read, from Reference [20]

$$\kappa(v)\kappa_{ac}(-v) = \rho_0^2 \sin(\mu + v)\sin(\mu - v)/\sin^2\mu \tag{6.10}$$

$$\kappa(v)\kappa_{ac}(2\mu - v) = \rho_0^2 \sin v \sin(2\mu - v)/\sin^2\mu \tag{6.11}$$

$$\kappa(v)\kappa_{ac}(\pi - v) = -\rho_0^2 \sin(\mu - v)\sin(\mu + v)/\sin^2\mu \tag{6.12}$$

$$\kappa(v)\kappa_{ac}(\pi + 2\mu - v) = -\rho_0^2 \sin v \sin(2\mu - v)/\sin^2\mu \tag{6.13}$$

where $\kappa_{ac}(v)$ is the analytic continuation of $\kappa(v)$ through the point $v = 0$, defined in [20]. To get the free energy from the inversion relations, one uses equations (6.10) and (6.11) when $\mathbf{0 < \mathrm{Re}(v) < \mu}$, **(6.11) and (6.12)** when $\mu < \mathrm{Re}(v) < \pi/2$, (6.12) and (6.13) when $\pi/2 < \mathrm{Re}(v) < \mu + \pi/2$, and equations (6.13), (6.10) and (6.9) for $\mu + \pi/2 < \mathrm{Re}(v) < \pi$.

This divides the complex v-plane into four regions, in each of which $\kappa(v)$ has a different analytical form. The physical regime is when $0 < \mathrm{Re}(v) < \mu$, where all the Boltzmann weights are real and positive. The expressions for $\kappa(v)$ in each of the regions can be found from the appropriate inversion relations together with some analyticity assumptions [20] on $\kappa(v)$, and the results are presented here for completeness.

(i) For $0 < \mathrm{Re}(v) < \mu$:

$$\ln \kappa(v) = \ln \rho_0 + 2 \int_{-\infty}^{\infty} \frac{\cosh(\pi - 2\mu)\, t \sinh v\, t \sinh(\mu - v)\, t}{t \sinh \pi\, t \cosh \mu\, t}\, dt \tag{6.14}$$

(ii) $\mu < \mathrm{Re}(v) < \frac{1}{2}\pi$:

$$\ln \kappa(v) = \ln \rho_0 + 2 \int_{-\infty}^{\infty} \frac{\sinh(v - \mu)\, t\, \phi(v)}{t \sinh \pi\, t \sinh(\pi - 2\mu)\, t}\, dt$$

where

$$\phi(v) = \sinh(\pi - \mu)\, t \sinh(\pi - 2\mu - v)\, t + \sinh \mu\, t \sinh(v - 2\mu)\, t$$

(iii) $\frac{1}{2}\pi < \mathrm{Re}(v) < \mu + \frac{1}{2}\pi$:

$$\ln \kappa(v) = \ln \rho_0 + \int_{-\infty}^{\infty} \frac{\cosh \mu t \cosh(\pi - 2\mu)\, t - \cosh 2\mu t \cosh(2v - \pi - \mu)\, t}{t \sinh \pi t \cosh \mu t} dt$$

(iv) $\mu + \frac{1}{2}\pi < \mathrm{Re}(v) < \pi$:

$$\ln \kappa(v) = \ln \rho_0 + 2 \int_{-\infty}^{\infty} \frac{\sinh(\pi - v)\, t \phi(\pi - v + \mu)}{t \sinh \pi t \sinh(\pi - 2\mu)\, t} dt.$$

Equation (6.9) is used to find $\ln \kappa(v)$ outside the range $0 < v < \pi$. Since $\mu = \pi/6$ is a rational fraction of π, we can reduce these integrals to infinite series. For the physical regime, equation (6.14) thus gives

$$\begin{aligned} \ln \kappa(v) \;=\; & \frac{1}{2} \ln 3 + \frac{4}{3\pi} \sum_{n=1}^{\infty} \frac{\sin 6v(2n-1)}{(2n-1)^2} + \frac{2}{\pi}(\mu - 2v) \ln \cot 3v \\ & + \ln \frac{\sin(\mu + v) \sin(2\mu - v)}{\sin(\mu - v) \sin v} + \frac{1}{3} \ln[\tan v \tan(\mu - v)]. \end{aligned} \tag{6.15}$$

6.3 Results

We calculated the partition functions for the lattices using edge transfer matrices, Reference [19, 20], to build up the lattice one edge at a time, calculating the coefficients of the polynomials using FORTRAN and modular arithmetic [77]. The length of the largest coefficient in the polynomials seemed to increase exponentially with the size of the lattice, and for the 6×6 lattice, the longest coefficient was already an integer of order 10^{66}. Expressed as a function of $y = x + 1/3x$, the longest coefficient of the polynomials was approximately halved, which made the polynomials significantly easier to handle. The partition functions for the 1×1 through 6×6 square lattices have been included in appendix A. It is important that the polynomials be computed exactly, as the location of the zeros of the polynomials can be very sensitive to small errors in the coefficients.

In the thermodynamic limit, we expect the zeros of the partition function to lie on the boundaries between the different phases, which is when $\mathrm{Re}(v) = 0$, μ, $\pi/2$ or $\mu + \pi/2$.

We actually plotted the graphs in terms of the variable

$$z = e^{2iv} = \frac{(1-\omega^2)x - \omega^2}{(1-\omega^2)x + 1},$$

so the boundaries between the phases are the rays $\arg(z) = 0, \pi/3, \pi$, and $4\pi/3$ (which correspond to the line $\mathrm{Re}(x) = -1/2$ and the circle $|x + 1/3| = 1/3$).

The zeros in the z-plane for the 3×3, 4×4, 5×5 and 6×6 lattices are shown in Figures 6.2, 6.3, 6.4, and 6.5. They are beginning to fall on the expected rays, with some scatter at the ends of each ray. Also note the line of zeros for the 3×3 and 5×5 lattices, with arguments of approximately $\pm 2\pi/3$. For the lattices we looked at, (1×1 through 6×6), these occured when L and M were both odd.

Also, in Figures 6.6, 6.7 and 6.8, we plot the zeros of the partition functions $Z_{44}^{01}(z)$, $Z_{44}^{11}(z)$ and $Z_{44}^{12}(z)$ in the z-plane, to demonstrate the effect of skewing the boundary conditions. We see that the zeros are distributed in much the sane pattern, but are shifted slightly.

As well as this, we also attempted to find linear combinations of the partition functions with various boundary conditions which have particularly simple zeros, reminiscent of the zeros of the Pfaffians mentioned at the start of this chapter, but were unable to find any convincing combinations.

As a side-note, we can verify the calculation in [20] of the density of zeros lying

		L								
		1	2	3	4	5	6	7	8	9
	1	0.0341	0.0852	0.1580	0.2342	0.3078	0.3781	0.4458	0.5119	0.5771
	2	0.0852	0.0194	0.0251	0.0360	0.0479	0.0603	0.0728	0.0852	0.0974
	3	0.1580	0.0251	0.0132	0.0140	0.0170	0.0206	0.0242	0.0279	0.0317
	4	0.2342	0.0360	0.0140	0.0099	0.0098	0.0110	0.0124	0.0139	0.0154
M	5	0.3078	0.0479	0.0170	0.0098	0.0079	0.0077	0.0082	0.0089	0.0096
	6	0.3781	0.0603	0.0206	0.0110	0.0077	0.0066	0.0064	0.0066	0.0070
	7	0.4458	0.0728	0.0242	0.0124	0.0082	0.0064	0.0057	0.0055	0.0056
	8	0.5119	0.0852	0.0279	0.0139	0.0088	0.0066	0.0055	0.0050	0.0049
	9	0.5771	0.0974	0.0317	0.0154	0.0096	0.0070	0.0056	0.0049	0.0045

Table 6.1: Correction terms C_{LM} for the isotropic model

on each contour of the phase diagram. According to equations (5.15) of [20], one would expect to find for an $L \times M$ lattice the fraction $(\pi - 3\mu)/(\pi - 2\mu) = 3/4$ of the zeros on the rays $\arg z = 0$ and $\pi/3$, and the other $\mu/(\pi - 2\mu) = 1/4$ of the zeros on the rays $\arg z = \pi$ and $4\pi/3$. That this is the case can be verified simply by counting the zeros which are "on" each of the rays in the included graphs, Figures 6.2, 6.3, 6.4, and 6.5.

6.4 Finite Size Corrections

6.4.1 Conformal and Modular Invariance

The partition functions we have calculated can be used to test the predictions of finite-size corrections due to conformal and modular invariance. Many reviews of these subjects exist including [39–41, 66, 99], and only a summary of the necessary results will be presented here.

At criticality, various observables of a statistical mechanical system are believed to be invariant under scaling and conformal transformations. This assumption, which originally led to predictions of relationships between the critical exponents [69] has been later developed into a classification of universality classes of the critical behaviour for two-dimensional systems (determined by a parameter c, the central charge of the Virasoro algebra associated with the model) [36], and more recently to a classification of the modular invariant partition functions on a torus [38].

It was shown in [54] that for a statistical mechanical system with an hermitian transfer matrix, corresponding to a unitary conformal field theory, if $c < 1$ then c is restricted to take on the values

		L							
		1	2	3	4	5	6	7	8	9
	1	0.0256	0.0266	0.0385	0.0505	0.0625	0.0746	0.0867	0.0988	0.1111
	2	0.0266	-0.0090	0.0141	0.0109	0.0116	0.0115	0.0110	0.0103	0.0095
	3	0.0385	0.0141	-0.0042	0.0085	0.0086	0.0077	0.0076	0.0074	0.0069
	4	0.0505	0.0109	0.0085	0.0001	0.0057	0.0070	0.0065	0.0062	0.0060
M	5	0.0625	0.0116	0.0086	0.0057	0.0021	0.0045	0.0057	0.0056	0.0053
	6	0.0746	0.0115	0.0077	0.0070	0.0045	0.0028	0.0039	0.0047	0.0048
	7	0.0867	0.0110	0.0076	0.0065	0.0056	0.0039	0.0029	0.0035	0.0040
	8	0.0988	0.0103	0.0074	0.0062	0.0056	0.0047	0.0035	0.0029	0.0031
	9	0.1111	0.0095	0.0070	0.0060	0.0053	0.0048	0.0040	0.0031	0.0028

Table 6.2: Correction terms C_{LM} for the anisotropic model

$$c = 1 - \frac{6}{h(h-1)}$$

where $h = 4, 5, 6, \ldots$.

Modular invariance predicts the leading corrections to the partition function should take the form of equation (6.2), with $\mathcal{N} = 2LM$, and f is the free energy per site in the thermodynamic limit. The modular invariant partition function, $Z(q)$, describes the leading finite-size corrections in the limit of L, M large, with the ratio L/M fixed. Here q is the modular parameter, given by [99]

$$q = e^{2\pi i \tau}, \quad \tau = e^{i(\pi-\theta)} L/M, \tag{6.16}$$

where $\theta = 6v$, where v is the spectral parameter.

One requires $Z(q)$ to be invariant under the action of the modular group, which maps a torus formed by identifying sides of a parallelogram in the complex plane with edges 0, 1, τ, and $1 + \tau$ onto itself. The modular group acts through the generators T and S, where

$$\begin{aligned} T : \tau &\rightarrow 1 + \tau \\ S : \tau &\rightarrow -\tau^{-1}. \end{aligned}$$

Note that the rotational symmetry $x \rightarrow 1/3x$ of Z_{LM} corresponds to the latter of these.

These requirements place very stringent constraints on the form of $Z(q)$, and in fact lead to a complete classification of all possible modular invariant partition functions for $c < 1$ theories, which are labeled by the A, D and E Lie algebras [38].

The three state Potts model is related to the D_4 minimal conformal field theory [38] with $c = 4/5$, $h = 6$ [48]. The corresponding modular invariant partition function reads

$$Z(q) = |\chi_{1,1}(q) + \chi_{4,1}(q)|^2 + |\chi_{2,1}(q) + \chi_{3,1}(q)|^2 + 2|\chi_{3,3}(q)|^2 + 2|\chi_{4,3}(q)|^2 \tag{6.17}$$

where $\chi_{r,s}$ is the character of the representation of the Virasoro algebra, given by

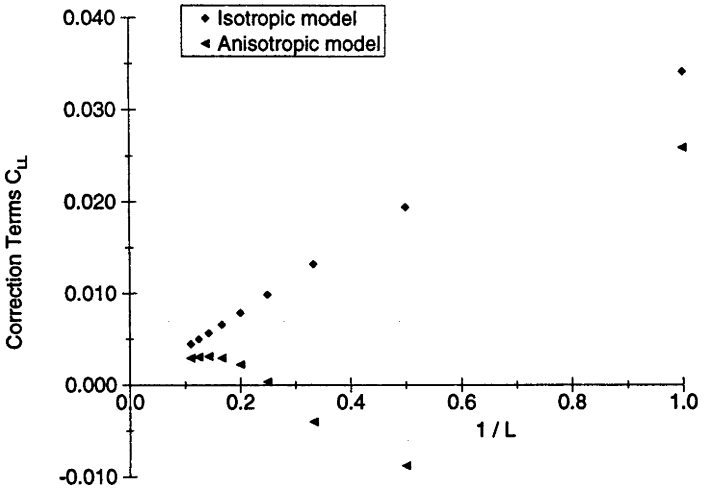

Figure 6.9: Next-order corrections to the modular invariant partition function. Top: isotropic model; below; anisotropic model.

$$\chi_{r,s} = q^{-c/24} \prod_{n=1}^{\infty} (1-q^n)^{-1} \sum_{n=-\infty}^{\infty} \left\{ q^{\frac{[2h(h-1)n+hr-(h-1)s]^2-1}{4h(h-1)}} - q^{\frac{[2h(h-1)n+hr+(h-1)s]^2-1}{4h(h-1)}} \right\}$$

6.4.2 Numerical Results

In this section, we shall verify the predictions of modular invariance by numerically evaluating the correction terms in (6.2) for various lattice sizes and demonstrating that they vanish as the lattice size increases. Writing the correction terms as C_{LM}, we can write (6.2) as

$$\ln Z_{LM}(v) = -2LMf/kT + \ln Z(q) + C_{LM}, \tag{6.18}$$

and we expect that

$$C_{LM} \to 0 \text{ as } L,\ M \to \infty. \tag{6.19}$$

It is computationally easier to evaluate the partition function Z_{LM} numerically for a particular value of x than it is to evaluate the entire polynomial, and so for these calculations we are able to use larger lattice sizes than before. Here, we present results on up to 9×9 lattices.

For the numerical studies, we considered an isotropic ($\theta = \pi/2$) and a particular anisotropic ($\theta = \pi/4$) case of the model. From (6.15) and (6.16) we have

(i) $\theta = \pi/2, \quad q = e^{-2\pi L/M}, \quad f/kT = 2.0702$

(ii) $\theta = \pi/4, \quad q = e^{-\sqrt{2}\pi(1+i)L/M}, \quad f/kT = 2.3150,$

where (i) and (ii) correspond to the isotropic and anisotropic cases respectively. Using these and the numerical values of Z_{LM}, we calculated C_{LM}. They are given in tables 1 and 2 for all $L \times M$ lattices with $1 \leq L, M \leq 9$. The correction terms are close to zero as expected, and vanish as the lattice size increases in both directions.

We next restricted our attention to just the square $L \times L$ lattices. In this case, we have for the isotropic model (i)$\ln Z(q) = 1.0479$ and for the anisotropic model (ii)$\ln Z(q) = 1.0535$. Figure 6.9 plots C_{LL} against $1/L$ for the square lattice models. Both of the curves are clearly converging towards zero as expected. For the isotropic model, the curve is approximately linear, with equation

$$C_{LL} = 0.04\, L^{-1}.$$

The results are less clear for the anisotropic model, but still compatible with (6.19).

APPENDIX A

The partition functions for the three-state self-dual Potts model

We have calculated the partition functions from Chapter 6 for all values of L and M in the range $1 \leq L, M \leq 6$, and all values of h and v. Here we present only the square lattice non-skewed partition functions for $L = 1, \ldots, 6$. It is convenient to divide each of them by a factor of 3^L and (using our earlier remarks) to exhibit them as polynomials in $y = 3x + 3 + 1/x$, so we actually present

$$P_{LL}(y) = 3^{-L} Z_{LL}(y);$$

$$P_{11}(y) = 3 + 2y + y^2$$

$$P_{22}(y) = 243 + 648y + 324y^2 - 72y^3 + 534y^4 - 184y^5 + 92y^6 - 8y^7 + y^8$$

$$\begin{aligned} P_{33}(y) = {} & 177147 + 1062882y + 2302911y^2 + 2047032y^3 + 1377810y^4 \\ & +2913084y^5 + 3158028y^6 + 664848y^7 + 103518y^8 + 930852y^9 + 306666y^{10} \\ & -270864y^{11} + 220374y^{12} - 62532y^{13} + 16956y^{14} - 2160y^{15} + 297y^{16} - 18y^{17} + y^{18} \end{aligned}$$

$$\begin{aligned} P_{44}(y) = {} & 1162261467 + 12397455648y + 55788550416y^2 + 136372012128y^3 \\ & +214315274952y^4 + 324629671968y^5 + 582654906288y^6 + 750632777568y^7 \\ & +607521384972y^8 + 795120766560y^9 + 965737104624y^{10} + 130605470496y^{11} \\ & +322442584488y^{12} + 916063289568y^{13} - 526868886960y^{14} + 147997956384y^{15} \\ & +596145500838y^{16} - 737714208096y^{17} + 610533631440y^{18} - 343154709792y^{19} \\ & +156664410984y^{20} - 55836596448y^{21} + 16860264048y^{22} - 4098594336y^{23} \\ & +856735500y^{24} - 143074912y^{25} + 20606608y^{26} - 2274208y^{27} + 217560y^{28} \\ & -14816y^{29} + 880y^{30} - 32y^{31} + y^{32} \end{aligned}$$

$$P_{55}(y) = 68630377364883 + 1143839622748050y + 8578797170610375y^2$$

$$+38127987424935000\,y^3 + 114511055566221450\,y^4 + 268776892687508460\,y^5$$
$$+589388078205374850\,y^6 + 1246116772225702800\,y^7$$
$$+2209159127195440650\,y^8 + 3194839081210230900\,y^9$$
$$+4647346048981897830\,y^{10} + 7079557052341783800\,y^{11}$$
$$+8225530257835830150\,y^{12} + 7279248720513503700\,y^{13}$$
$$+9357732890461402200\,y^{14} + 11647930212445937760\,y^{15}$$
$$+5762094309484412175\,y^{16} + 3517524430230368250\,y^{17}$$
$$+9571985653589609175\,y^{18} + 4023612873756685800\,y^{19}$$
$$-2229800910702224940\,y^{20} + 4898159054026700400\,y^{21}$$
$$+2681786734169855850\,y^{22} - 3147689863270981800\,y^{23}$$
$$+2051627825339895150\,y^{24} + 1388963485815183972\,y^{25}$$
$$-2128929001082085150\,y^{26} + 1331521145545374000\,y^{27}$$
$$+57684225191190300\,y^{28} - 746264103632814600\,y^{29} + 794712829019154840\,y^{30}$$
$$-530326171478212200\,y^{31} + 272216641223522475\,y^{32} - 112688467988737950\,y^{33}$$
$$+39181982508236025\,y^{34} - 11549532336644520\,y^{35} + 2939341744610550\,y^{36}$$
$$-645489038603700\,y^{37} + 123764044894650\,y^{38} - 20572630471200\,y^{39}$$
$$+2994872555520\,y^{40} - 376168331200\,y^{41} + 41274998450\,y^{42} - 3850715800\,y^{43}$$
$$+311887300\,y^{44} - 20890960\,y^{45} + 1201800\,y^{46} - 54000\,y^{47} + 2025\,y^{48} - 50\,y^{49} + y^{50}$$

$$P_{66}(y) = 36472996377170786403 + 875351913052098873672\,y$$
$$+9774763029081770756004\,y^2 + 67337256422563309652472\,y^3$$
$$+323677580071625634445290\,y^4 + 1190511022192078620004056\,y^5$$
$$+3687722524516725255571236\,y^6 + 10401597851065757493067944\,y^7$$
$$+26959565969402691459552399\,y^8 + 61845999495375641704282080\,y^9$$
$$+125647098622601501820237264\,y^{10} + 240022887437101067312705280\,y^{11}$$
$$+441519613264037985882669180\,y^{12} + 733107095097853745341073520\,y^{13}$$
$$+1080397799595306894464550936\,y^{14} + 1583729683005096563042792880\,y^{15}$$
$$+2328323646550484968888509486\,y^{16} + 2838504538453872771496776528\,y^{17}$$
$$+2998311552325305734846468616\,y^{18} + 3991877767098756951115949136\,y^{19}$$
$$+4841333866013199882396682320\,y^{20} + 3196379048673075802526844288\,y^{21}$$
$$+3459976739860325500668722256\,y^{22} + 6426702369613569850064037792\,y^{23}$$
$$+1939688548729838668685318472\,y^{24} - 4575519452446624402343504 64\,y^{25}$$
$$+8182886135467873465543625568\,y^{26} + 6471555414842003993150866 56\,y^{27}$$
$$-6305992509148856315800268364\,y^{28} + 1116466753276179873623238 3792\,y^{29}$$
$$-1150370452169839095281894232\,y^{30} - 1017082070574212709879935 1120\,y^{31}$$
$$+1508006634348751169002176 5802\,y^{32} - 6545462183956141046776619856\,y^{33}$$
$$-6614535334864417091310887640\,y^{34} + 1496183999185601493363667 9152\,y^{35}$$

$$-1328744652591824313350238 6732\,y^{36} + 5052764542237547744805308208\,y^{37}$$
$$+3710788464236653463646633048\,y^{38} - 8724170242510213586259010896\,y^{39}$$
$$+9453474078656450703547435326\,y^{40} - 7536505183924558142291909184\,y^{41}$$
$$+4912333469209503026020498320\,y^{42} - 2732858726369737791501547488\,y^{43}$$
$$+1328953157744139878205736584\,y^{44} - 5730030332286244899518658 24\,y^{45}$$
$$+2212658938968739721932560 48\,y^{46} - 7704246334216308253524604 8\,y^{47}$$
$$+2431666227639554027297127 0\,y^{48} - 6982429693990831900853904\,y^{49}$$
$$+1829455359148989531820728\,y^{50} - 4381425919603306873982 88\,y^{51}$$
$$+9605617135738783216855 2\,y^{52} - 1928494155716609299977 6\,y^{53}$$
$$+3546892729335283210944\,y^{54} - 5971045193919768251 52\,y^{55}$$
$$+9195729194336208375 6\,y^{56} - 1292850832462824038 4\,y^{57}$$
$$+1657229052282802272\,y^{58} - 192992758661806560\,y^{59} + 20382424207664976\,y^{60}$$
$$-1941330716173728\,y^{61} + 166448903581008\,y^{62} - 12734381143296\,y^{63}$$
$$+868496151105\,y^{64} - 52033203144\,y^{65} + 2742705468\,y^{66} - 123785496\,y^{67}$$
$$+4816638\,y^{68} - 152280\,y^{69} + 3996\,y^{70} - 72\,y^{71} + y^{72}$$

Bibliography

[1] G. Albertini, B. M. McCoy, J. H. H. Perk and S. Tang, *Nucl. Phys. B* **314** (1989) 741

[2] G. Albertini, B. M. McCoy and J. H. H. Perk, *Phys. Lett. A* **135** (1989) 159

[3] G. Albertini, B. M. McCoy and J. H. H. Perk, *Adv. Stud. Pure Math.* **19** (1989) 1

[4] G. Albertini, B. M. McCoy and J. H. H. Perk, *Phys. Lett. A* **139** (1989) 204

[5] G. Albertini, S. Dasmahapatra, and B. M. McCoy, *Int. Jour. Mod. Phys. A* **7** *Suppl. 1A* (1992) 1

[6] J. Ashkin and Teller, *Phys. Rev.* **64** (1943) 178

[7] H. Au-Yang, B. M. McCoy, J. H. H. Perk, S. Tang and M. L. Yan, *Phys. Lett. A* **123** (1987) 219

[8] H. Au-Yang, B. M. McCoy, J. H. H. Perk and S. Tang, in *Algebraic Analysis*, Vol. 1, M. Kashiwara and T. Kawai, eds. (Academic Press, San Diego, 1988), p. 29

[9] H. Au-Yang and J. H. H. Perk, in *Advanced Studies in Pure Mathematics*, Vol. 19 (Kinokuniya-Academic, Tokyo, 1989), p. 57

[10] H. Au-Yang and J. H. H. Perk, *J. Stat. Phys.* **78** (1995) 17

[11] M. T. Batchelor, R. J. Baxter, M. J. O'Rourke and C. M. Yung, *J. Phys. A.* **28** (1995) 2759

[12] R. J. Baxter, *Stud. Appl. Math.* **50** (1971) 51

[13] R. J. Baxter, *Phys. Rev. Lett.* **26** (1971) 832

[14] R. J. Baxter, *Ann. Phys.* **70** (1972) 193

[15] R. J. Baxter, *J. Phys. C* **6** (1973) L445

[16] R. J. Baxter, *J. Stat. Phys.* **8** (1973) 25

[17] R. J. Baxter and I. G. Enting, *J. Phys. A* **11** (1978) 2463

[18] R. J. Baxter, *Phil. Trans. Roy. Soc. Lond. A* **289** (1978) 315

[19] R. J. Baxter, *Exactly Solved Models in Statistical Mechanics* (London: Academic, 1982)

[20] R. J. Baxter, *J. Stat. Phys.* **28** (1982) 1

[21] R. J. Baxter, *J. Phys. A* **20** (1987) 5241

[22] R. J. Baxter, J. H. H. Perk and H. Au-Yang, *Phys. Lett. A* **128** (1988) 138

[23] R. J. Baxter, *Phys. Lett. A* **133** (1988) 185

[24] R. J. Baxter, *J. Stat. Phys.* **52** (1988) 639

[25] R. J. Baxter, in *Advanced Studies in Pure Mathematics*, Vol. 19 (Kinokuniya-Academic, Tokyo, 1989), p. 95

[26] R. J. Baxter, *J. Stat. Phys.* **57** (1989) 1

[27] R. J. Baxter, V. V. Bazhanov and J. H. H. Perk, *Int. J. Mod. Phys. B* **4** (1990) 803

[28] R. J. Baxter, *Phys. Lett. A.* **146** (1990) 110

[29] R. J. Baxter, in *Proc. Fourth Asia-Pacific Physics Conference*, eds. S. H. Ahn, Il-T. Cheon, S. H. Choh and C. Lee (World Scientific, Singapore), Vol. 1 (1991) 42

[30] R. J. Baxter, *J. Stat. Phys.* **73** (1993) 461

[31] R. J. Baxter, *Rev. Math. Phys. (Special Issue)* **6** (1994) 869

[32] R. J. Baxter, *J. Phys. A* **27** (1994) 1837

[33] R. J. Baxter, *J. Stat. Phys.* **78** (1995) 7

[34] R. J. Baxter, *J. Stat. Phys.* **82** (1996) 1235

[35] V. V. Bazhanov and Yu. G. Stroganov, *J. Stat. Phys.* **59** (1990) 799

[36] A. A. Belavin, A. M. Polyakov, and A. B. Zamolodchikov, *Nucl. Phys. B* **241** (1984) 333

[37] H. A. Bethe, *Z. Phyzik.* **71** (1931) 205

[38] A. Cappelli, C. Itzykson and J.-B. Zuber, *Nucl. Phys. B* **280** (1987) 445

[39] J. L. Cardy, in *Phase Transitions and Critical Phenomena,* Vol. 11, C. Domb and J. L. Lebowitz, eds. (Academic Press, London, 1987).

[40] J. L. Cardy, *Conformal Invariance and Statistical Mechanics*, in *Les Houches, Session XLIV, Fields, Strings and Critical Phenomena*, E. Brézin and J. Zinn-Justin eds. (1989)

[41] P. Christe and M. Henkel, *Introduction to Conformal Invariance and Its Applications to Critical Phenomena* (Springer-Verlag, Berlin Heidelberg, 1993).

[42] E. T. Copson, *An Introduction to the Theory of Functions of a Complex Variable* (Oxford University Press, London) 1935

[43] P. Curie, *Ann. Chem. Phys.* **5** (1895) 289; *J. de Phys.* **4** (1895) 263

[44] S. Dasmahapatara, R. Kedem and B. M. McCoy, *Nucl. Phys. B* **396** (1993) 506

[45] H. J. de Vega and F. Woynarovich, *Nucl. Phys. B* **25** (1985) 439

[46] L. Dolan and M. Grady, *Phys. Rev. D* **25** (1982) 1587

[47] C. Domb, *The Curie Point* in *Statistical mechanics at the turn of the decade*, E. G. D. Cohen ed. (Marcel Dekker, Inc, 1971) p. 81

[48] Vl. S. Dotsenko, *Nucl. Phys. B.* **235** (1984) 54

[49] C. Fan and F. Y. Wu, *Phys. Rev. B* **2** (1970) 723

[50] V. A. Fateev and A. B. Zamolodchikov, *Phys. Lett. A* **92** (1982) 37

[51] M. E. Fisher, *Phys. Rev.* **124** (1961) 1664

[52] M. E. Fisher and A. E. Ferdinand, *Phys. Rev. Lett.* **19** (1967) 169

[53] M. E. Fisher, *J. Phys. Soc. Japan (Suppl.)* **26** (1967) 87

[54] D. Friedan, Z. Qiu, S. Shenker, *Phys. Rev. Lett.* **52**:1575-1578 (1984) and in *Vertex Operators in Mathematics and Physics*, ed. J. Lepowsky, S. Mandelstam and I. Singer (Springer, NY, 1985).

[55] G. Galavotti and A. Martin-Löf, *Commun. Math. Phys.* **25** (1971) 87

[56] J. W. Gibbs, "Elementary Principles in Statistical Mechanics," (1902). Reprinted by Dover, New York, 1960.

[57] M. Gaudin, *La Fonction d'Onde de Bethe* (Masson, Paris, 1983)

[58] G. von Gehlen and V. Rittenberg, *Nucl. Phys. B* **257** [FS14] (1985) 351

[59] W. Gilbert, *Die Magnete Magneticisque Corporibus et de Magno Magnete Tellure Physilogia Nova* (Translated by P. F. Mottelby, New York 1893, and for the Gilbert Club, London, 1900) (1600) 66

[60] S. Howes, L. P. Kadanoff and M. den Nijs, *Nucl. Phys.* **B215** [FS7] (1983) 169

[61] D. A. Huse, *Phys. Rev. B* **24** (1981) 5180

[62] D. A. Huse, and M. E. Fisher, *Phys. Rev. Lett.* **49** (1982) 793

[63] D. A. Huse, A. M. Szpilka and M. E. Fisher, *Physica A* **121** (1983) 363

[64] E. Ising, *Z. Physik* **31** (1925) 253

[65] H. Itoyama, B. M. McCoy, and J. H. H. Perk, *Int. J. Mod. Phys. B* **4** (1989) 995

[66] C. Itzykson, in *Proc. First Asia Pacific Workshop on High Energy Physics*, B. E. Baaquie, C. K. Chew, C. H. Oh, K. K. Phua, eds. (World Scientific, Singapore, 1987).

[67] J. D. Johnson, S. Krinsky and B. M. McCoy, *Phys. Rev. Lett.* **29** (1972) 492

[68] J. D. Johnson, S. Krinsky and B. M. McCoy, *Phys. Rev. A* **8** (1973) 2526

[69] L. P. Kadanoff, W. Goetze, D. Hamblen, R. Hecht, E. A. S. Lewis, V. V. Palciauskas, M. Rayl, J. Swift, *Rev. Mod. Phys* **39** (1967) 395

[70] P. W. Kasteleyn, *Physica* **27** (1961) 1209

[71] P. W. Kasteleyn, *J. Math. Phys.* **4** (1963) 287

[72] B. Kaufman, *Phys. Rev.* **76** (1949) 1232

[73] B. Kaufman and L. Onsager, *Phys. Rev.* **76** (1949) 1244

[74] R. Kedem and B. M. McCoy, *J. Stat. Phys.* **71** (1993) 865

[75] R. Kedem and B. M. McCoy, *Int. J. Mod. Phys. B* **8** (1994) 3601

[76] T. Kihiara, Y. Midzuno and J. Shizume, *J. Phys. Soc. Jpn* **9** (1954) 681

[77] D. E. Knuth, *The Art of Computer Programming Vol. 2—Semi-Numerical Algorithms* (Addison-Wesley, 1969).

[78] H. A. Kramers and G. H. Wannier, *Phys. Rev.* **60** (1941) 252, 263

[79] T. D. Lee and C. N. Yang, *Phys. Rev.* **87** (1952) 404, 410

[80] E. H. Lieb, *Phys. Rev.* **162** (1967) 162

[81] E. H. Lieb, *Phys. Rev. Lett.* **18** (1967) 692

[82] E. H. Lieb, *Phys. Rev. Lett.* **18** (1967) 1046

[83] E. H. Lieb, *Phys. Rev. Lett.* **19** (1967) 108

[84] E. H. Lieb and F. Y. Wu, in *Phase transitions and critical phenomena* Vol. 1, C. Domb and M. S. Green eds. (Academic Press, New York) p. 321

[85] V. B. Matveev and A. O. Smirnov, *Lett. Math. Phys.* **19** (1990) 1

[86] P. P. Martin and J. M. Maillard, *J. Phys. A* **19** (1986) L547

[87] P. P. Martin, *Nucl. Phys. B* **225** (1983) 497

[88] P. Martin, *Potts Models and Related Problems in Statistical Mechanics* (World Scientific, Singapore, 1991).

[89] B. M. McCoy and T. T. Wu, *The Two-Dimensional Ising Model* (Harvard University Press, Cambridge, Mass, 1973).

[90] B. M. McCoy, J. H. H. Perk, S. Tang and C. H. Sah, *Phys. Lett. A* **125** (1987) 9

[91] B. M. McCoy and S. Roan, *Phys. Lett. A* **150** (1990) 347

[92] B. M. McCoy, in *ICM-90 Satellite Conference Proceedings "Special Functions" (Lecture Notes in Mathematics)* M. Kashiwara and T. Miwa eds (Springer) (1991) 245

[93] L. Onsager, *Phys. Rev.* **65** (1944) 117

[94] L. Onsager, in *Critical Phenomena in Alloys, Magnets and Superconductors,* eds. R. E. Mills, E. Ascher and R. I. Jaffee (McGraw-Hill, N. Y., 1971)

[95] M. J. O'Rourke, R. J. Baxter and V. V. Bazhanov, *J. Stat. Phys.* **78** (1995) 665

[96] M. J. O'Rourke and R. J. Baxter, *J. Stat. Phys.* **82** (1996) 1

[97] S. Ostlund, *Phys. Rev. B* **24** (1981) 398

[98] L. Pauling, *J. Am. Chem. Soc.* **57** (1935) 2680

[99] P. A. Pearce, *Int. Jour. Mod. Phys. B* **4** (1990) 715

[100] J. H. H. Perk, in *Theta Functions Bowdoin 1987* (American Mathematical Society, Providence, Rhode Island, 1989)

[101] R. Peierls, *Proc. Camb. Phil. Soc.* **32** (1936) 477

[102] R. B. Potts, *Proc. Camb. Phil. Soc.* **48** (1952) 106

[103] J. S. Rowlinson, *Nature* **224** (1969) 541 duscussing T. Andrews' Bakerian Lecture of 1869, "On the continuity of the gaseous and liquid states of matter"

[104] J. S. Rowlinson and B. Widom, *Molecular theory of capillarity*, International series of monographs on chemistry Vol. 8, (Oxford University Press, New York) 1982

[105] F. Rys, *Helv. Phys. Acta* **36** (1963) 537

[106] J. C. Slater, *J. Chem. Phys.* **9** (1941) 16

[107] B. Sutherland, *Phys. Rev. Lett.* **19** (1967) 103

[108] B. Sutherland, C. P. Yang and C. N. Yang, *Phys. Rev. Lett.* **19** (1967) 588

[109] B. Sutherland, *J. Math. Phys.* **11** (1970) 3183

[110] H. N. V. Temperley and M. E. Fisher, *Phil. Mag.* **6** (1961) 1061

[111] K. G. Wilson, *Phys. Rev. B* **4** (1971) 3174

[112] K. G. Wilson and J. Kogut, *Phys. Rep.* **12C** (1974) 75

[113] F. Y. Wu, *Phys. Rev. Lett.* **18** (1967) 605

[114] F. Y. Wu, *Phys. Rev.* **168** (1968) 539

[115] F. Y. Wu, *Phys. Rev.* **183** (1969) 604

[116] F. Y. Wu, *Phys. Rev. Lett.* **22** (1969) 560

[117] F. Y. Wu, *Phys. Rev. Lett.* **22** (1969) 1174

[118] F. Y. Wu, *Rev. Mod. Phys.* **54** (1982) 235

[119] C. N. Yang, *Phys. Rev.* **150** (1952) 808

[120] C. P. Yang, *Phys. Rev. Lett.* **19** (1967) 586